Passive Positioning Using Linear Multilateration

Eric R. Widdison

A dissertation submitted to the faculty of
Brigham Young University
in partial fulfillment of the requirements for the degree of

Doctor of Philosophy

David G. Long, Chair
Willie Harrison
Cammy Peterson
Karl Warnick

Department of Electrical and Computer Engineering

Brigham Young University

Copyright © 2023 Eric R. Widdison

All Rights Reserved

Passive Positioning Using Linear Multilateration

Eric R. Widdison
Department of Electrical and Computer Engineering
Doctor of Philosophy

BYU Engineering

Abstract

Passive localization of aircraft in flight using signal time of arrival (TOA) poses some unique challenges. The sensors must be deployed in an approximately coplanar configuration, which produces significant vertical uncertainty in the estimated position. This dissertation examines the traditional algorithms used in passive localization. It presents general forms of linear TOA, time difference of arrival (TDOA), angle of arrival (AOA), and frequency difference of arrival (FDOA) equations from the literature and explains how to apply an intuitive geometric interpretation of these equations. It presents two novel algorithms for passive localization. One uses a one dimensional AOA (1AOA) to improve the vertical estimate. The other employs an *a priori* estimate to approximate the non-linear localization problem as a linear problem and produce a high quality position estimate. A comprehensive survey of the literature is presented. This dissertation provides a summary and classification of passive localization algorithms from the literature with simple descriptions of how the form of the equations relate to their numerical stability. It presents two novel algorithms for passive localization. The hybrid multilateration and triangulation algorithm improves wide area multilateration by using vertical 1AOA to constrain the vertical position. The multilateration with *a priori* estimates algorithm provides a linear localization method that utilizes previous location estimates.

Keywords: multilateration, TOA, TDOA, AOA, FDOA, multistatic radar, literature review

Acknowledgments

My degree was funded by the US Department of Defense Science, Mathematics, and Research for Transformation (SMART) program. It would not have happened without the approval and support of the Air Force Lifecycle Management Center Aerospace Dominance Enablers Division (AFLCMC/HBZCD) engineering leadership, especially Lynn Silver and Britton Hayden. I owe a great deal to my coworkers who carried extra burdens and were exceptionally patient and supportive, including Jeremy Larsen, Tabitha Hyer, Tony Lewis, Charlie Lovatt, Eric Fink, and especially Joe Myers. I am so fortunate to be involved in such engaging work with such talented and dedicated people.

The opinions expressed in this dissertation are the author's own and do not reflect the view of the US Air Force, the Department of Defense, or the United States government.

To Henry, Katherine, Megan, and Sarah, you are what make everything worthwhile. Thank you for your patience with my physical absences as I work on becoming an absent-minded professor, and for coming to me for help on your homework. You helped me more than you know. I am so proud of you.

None of this would have happened without the prompting, support, and encouragement of my long-term editor, friend, companion, and wife, Becky. Thank you for believing in me and pushing me to take this journey. You brighten my life and fill me with joy. I am forever in your debt.

Table of Contents

List of Figures

List of Tables

Nomenclature

1AOA	Single angle of arrival
2AOA	Two angles of arrival (azimuth and elevation)
ACAS	Airborne Collision Avoidance System
ADS-B	Automatic Dependent Surveillance-Broadcast
AOA	Angle of Arrival
CERN	European Organization for Nuclear Research (Conseil européen pour la Recherche nucléaire)
CRLB	Cramér-Rao Lower Bound
DAB	Digital Audio Broadcasting
DOA	Direction of Arrival
DVB-T	Digital Video Broadcasting-Terrestrial
E-911	Enhanced 911
EW	Electronic Warfare
FDOA	Frequency Difference of Arrival
GNSS	Global Navigation Satellite System
GPS	Global Positioning System
GROA	Gain Ratio of Arrival
HM	Hybrid Multilateration and Triangulation
LDCAS	L-band Digital Aeronautical Communication System
LOP	Line of Position
LOS	Line of Sight
LS	Least Squares
MIMO	Multiple Input and Multiple Output
ML	Maximum Likelihood
ML	Multilateration
NLOS	Non-Line of Sight
PDF	Probability Density Function
PSO	Particle Swarm Optimization
RSS	Received Signal Strength

RWR	Radar Warning Receiver
TDOA	Time Difference of Arrival
TOA	Time of Arrival
UAV	Unmanned Aerial Vehicle
WLS	Weighted Least Squares

1 Introduction

1.1 History and Motivation

Since shortly before World War II, aircraft have been employed to attack targets far behind enemy lines and radars have been employed to detect those attacks so that defenders can respond quickly and decisively. These two developments, made independently at roughly the same time, have changed the face of warfare, setting off the field of electronic warfare (EW), also dubbed the radar game [1], a back-and-forth of escalating technologies for detecting aircraft and evading detection.

The radar game largely stabilized towards the end of the Cold War. Radar technology reached a plateau of capability, and aircraft developed a standard suite of EW capabilities that were reasonably effective, including jammers and radar warning receivers (RWRs), which alerted pilots to enemy radar systems and allowed them to take appropriate actions. The end of the Cold War saw the introduction of stealth aircraft, such as the F-117 Nighthawk and B-2 Spirit. Stealth aircraft changed the radar game, and it would take radars well over a decade to respond. The proliferation of stealth aircraft has progressed, with the development of the F-117, B-2, F-22, F-35 (see Fig. 1.1), Su-57, Su-75, J-20, and FC-31 aircraft.

More recently, the development of unmanned aerial vehicles (UAVs) once again shows potential to radically change the state of air power. In particular, swarms of powerful and expendable UAVs can be every bit as deadly as modern fighter and bomber aircraft while also being as difficult to target as flies in a swarm or birds in a flock. This poses a significant challenge for radars, most of which have a beam width that is far too wide to enable the resolution of individual targets within a swarm.

One key weapon in an aircraft's EW arsenal is the RWR. This device detects the signals emitted by a radar and identifies the type of system that emitted the signals. In many cases the RWR can determine whether the radar is searching, tracking the aircraft, or providing guidance to a surface-to-air missile that is aimed at the aircraft. If the radar is deemed to be a sufficient threat, the RWR notifies the pilot[a] so that they can take evasive action.

In playing the radar game, both the aircraft and radar benefit from stealth. For the radar, one way to achieve this is to operate in a passive mode. If the radar is not emitting any energy, then the aircraft has no way of knowing that it is being observed. This is passive detection or passive

[a] This behavior is frequently depicted in films. A slowly beeping RWR indicates a radar in search mode. Faster beeping indicates tracking mode, making target updates up to several times per second. A steady tone is consistent with the radar providing constant or near-constant target illumination to help guide a missile in flight.

Figure 1.1: Maj. Kristin Wolfe, F-35A Lightning II Demonstration Team commander, performs an aerial maneuver during the Reno Air Races in Reno, Nevada, 19 Sep. 2021. Photo from US Air Force, photographed by TSgt. Nicolas Myers.

localization. In passive localization, a target is located by detecting and analyzing signals that it emits. A key application, which contributed to the surge in passive localization research in the 1990s, is locating cellular telephones that call for emergency services.

1.2 Contributions

The work in this dissertation is inspired by the problems of locating stealth aircraft and individual objects in a UAV swarm[b]. These are very difficult problems which this dissertation does not attempt to fully solve. In this dissertation, I explore passive localization where signals transmitted from an aircraft are detected and used to determine the position of the aircraft. In particular, I look at the algorithms used to calculate position based on the time of arrival (TOA) or time difference of arrival (TDOA) and angle of arrival (AOA) of the signals and develop two new algorithms that can help improve the speed and accuracy of localization.

[b]Given that a typical UAV is smaller than a manned aircraft, these two problems are not mutually exclusive.

TOA and TDOA localization, also known as multilateration, is a well-known problem. TDOA localization, with mutliple transmitters and a single receiver, is how the global navigation satellite systems (GNSS) such as the global positioning system (GPS) function. In the aircraft localization problem this is reversed, with one transmitter at an unknown location and many receivers at known locations.

This effort produced three technical papers that have been submitted to peer reviewed journals. Two papers have been published [2, 3] and one is currently in review [4].

My work includes a review of passive localization techniques, algorithms, and applications. This involves identifying the common equations used across multiple localization algorithms and presenting a simple form of these equations. These simplified, noise-free equations are useful for identifying the shared techniques used across papers. They also make it possible to intuitively understand the geometry of the problem and its solution. Building an intuitive understanding of the problem enables the identification of numerically unstable scenarios without having to perform an exhaustive numerical analysis. This simplified interpretation of linear localization equations is unique in the literature. Most papers start with statistical models which are wrestled into submission in a flurry of symbols, substitution, and abstraction. This approach obfuscates the way that the resulting equations relate to the original problem. Papers rarely even identify the point where they present the solution to the localization problem.

The literature review in Ch. 2 provides an extensive list of applications where localization algorithms are employed. This includes, among others, locating cellular and wireless devices, tracking aircraft and satellites, and acoustic localization. It also provides a brief review of some TOA-based bistatic radar applications. Passive bistatic radar, using emitters of opportunity such as radio or television stations, is a very popular topic, with hundreds of papers produced every year. This literature review and functional analysis has been submitted for peer review [4].

TOA localization of aircraft faces a significant obstacle due to the geometric requirements and constraints. The receivers must cover a large area, and must also be mounted on or near the ground. This produces a receiver constellation that is nearly coplanar. For most TOA-based localization algorithms, the coplanar sensors produce numerically unstable equations, where vertical position (i.e. perpendicular to the plane approximated by the receivers) is difficult to calculate accurately. One way to resolve the vertical uncertainty is by measuring the elevation angle of each of the arriving signals. This constrains the calculated vertical position, greatly improving the accuracy of the estimate. I develop an algorithm that removes the z dimension from the multilateration equations, instead calculating it with triangulation using TOA and AOA. This algorithm out-performs the standard linear TDOA algorithm in total accuracy, particularly when the receivers are nearly coplanar. This algorithm has been published in a peer reviewed journal [2].

One issue common with linear multilateration algorithms is that they do not incorporate any *a priori* information about the target location. Such information could be used to either improve the accuracy of the estimate. It could also be used to track objects in a formation or swarm. I develop a multilateration algorithm that incorporates an *a priori* estimate to produce a planar approximation of the spheres implied by the TDOA measurements. The intersection of those planes is a straightforward linear problem. This works well when the target is close enough to the initial estimate. I present a method for improving the accuracy of the algorithm when the initial estimate is not close enough to the true

position, as described in Sec. 4.3.3. This algorithm is well-suited for use in a Kalman filter or a swarm tracking algorithm. This algorithm has been published in a peer reviewed journal [3].

1.3 Outline

Chapter 2 provides a history of multilateration algorithms, with particular focus on linear multilateration algorithms. Linear localization equations make it possible to combine multiple measurements, including measurements of different types, into a single system of equations that provide a single solution to the localization problem. They are much faster to compute than iterative algorithms and much easier to expand and adapt than quadratic algorithms. The chapter presents simplified forms of linear TOA, TDOA, AOA, frequency difference of arrival (FDOA), and multistatic radar equations that are found in the literature. It examines how these forms of the equations constrain the solution, which can help to identify when the algorithms are numerically unstable. It also includes a review of the literature employing TOA, TDOA, and AOA algorithms.

This chapter is supplemented by Appendix A, which derives a single generalized system of TOA and TDOA equations. These equations can be simplified to produce the most common TOA equations, or in a different way to produce the most common TDOA equations. This shows how the two algorithms are related.

Chapter 3 presents a wide area hybrid multilateration and triangulation algorithm where the TOA measurements are paired with AOA measurements to reduce the vertical error. In the algorithm, multilateration is used for the horizontal directions and triangulation is used for the vertical direction. The algorithm performs well against the standard linear TDOA algorithm except in a few cases where it is numerically unstable, which are identified and modeled.

Chapter 4 presents a linear multilateration algorithm that uses an *a priori* estimate of a target position to approximate the non-linear geometry of the localization problem as a simple set of linear equations. When the initial estimate is sufficiently close to the true value, it meets or exceeds the performance of other linear localization algorithms. It also includes an iterative version that is able to correct for poor estimates of the target position. This algorithm can be used to update the position of a target that is being tracked, or to calculate the position of a UAV in a swarm relative to a central point within the swarm.

Chapter 5 summarizes the work of this dissertation. It offers possible avenues to extend the research presented here.

2 *A Review of Linear Multilateration Techniques and Applications*

This chapter is composed from a paper entitled "A Review of Linear Multilateration Techniques and Applications" that is in review at the journal *IEEE Access* [4]. I hereby confirm that the use of this article is compliant with all publishing agreements.

2.1 Introduction

Multilateration is a localization approach that uses distances from several known points to an unknown point to determine the location of that unknown point. This is typically done by using the propagation time, measured from a signal time of arrival (TOA), to calculate the distance or relative distance between two points. This is the foundation of how many modern location services function, such as the Global Positioning System (GPS), work. It can also be used to determine the position of a radio frequency (RF) source at an unknown location. This has been an active area of research since at least the 1960s, with big pushes made in the 1970s with the development of GPS, in the 1990s with the proliferation of cellular telephones and the need to locate callers to emergency services [5], and in the 21st century with focus on passive localization and multistatic radar.

Over time, three families of methods have been developed for solving the time of arrival positioning problem. The earliest approaches used iterative methods, which are a relatively easy way to approach solving non-linear equations, but which can take longer to compute and may not converge to the correct solution. These were followed in the 1980s by methods which manipulate the system of equations to produce a single quadratic equation of one variable, which then produces two solutions, one of which is correct. The mid-1990s saw the introduction of linear methods for solving the system of equations. These provide a single, closed form solution, which comes at the expense of requiring at least one more measurement than the non-linear methods.

One of the strengths of linear equations is that they can be easily expanded to include additional measurements. The additional measurements can be more TOA measurements, or any other measurements that can be related to the problem using linear equations. This flexibility

has allowed for the development of localization algorithms employing angle of arrival (AOA), frequency difference of arrival (FDOA), received signal strength (RSS), and direction of arrival[a] (DOA). The introduction of linear methods of solving the positioning equations has also led to a proliferation of algorithms. Amid this proliferation, many papers derive their own versions of the linear multilateration algorithms.

[a]DOA differs from AOA in that DOA assumes that the signal source is far enough from the receivers that the AOA is the same for all receivers. In other words, the receivers form an antenna array, and the signal source lies in the far field of that array. In AOA, the source is close enough to the recievers that the AOA measurements are distinct enough to be used for triangulation.

Each of these algorithms has advantages and disadvantages. These often arise from how the equations they employ are derived. Most derivations start with a noisy measurement model and attempt to derive a maximum likelihood estimator from that. In doing so, the solutions usually correspond to one of a handful of solutions to the noise-free localization problem. The connection to the simple solution is generally lost in a sea of symbols, sometimes buried under many layers of substitutions, to the point that the solution no longer has a clear connection to the underlying physical problem, nor to the other algorithms that use similar equations.

This paper presents an analysis and survey of the linear equations employed in algorithms to solve localization problems using TOA multilateration. There are a number of other survey papers on the subject, addressing general and specific applications of TOA localization. Iliev [6] provides a broad survey of the applications of multilateration. Gao [7] explores localization methods as applied to small-scale applications, such as inside a single room or building. Yang [8] also surveys indoor multilateration, with particular attention to neural network approaches. Tahat [9] provides a review of the performance of multilateration and triangulation algorithms, addressing the relative strengths and weaknesses of each approach. Zhang [10] provides a very high-level overview of the current work with passive bistatic radar[b], along with potential applications and areas for further development.

[b]Passive bistatic radar can be geometrically and algorithmically similar to multilateration. The linear versions of the multistatic radar equations, which are presented in Sec. 2.2.1, are nearly identical to time difference of arrival (TDOA) multilateration equations.

This paper presents a brief history of some common algorithms used to solve multilateration problems. It provides a simple description of common linear solutions to the noise-free localization problem, including straightforward derivations and an intuitive interpretation of how these equations project measurement error onto the physical geometry of the problem. It also includes a review of examples from the literature that employ algorithms that use the equations presented in this paper.

2.2 Multilateration algorithms

There are three primary approaches to solving the multilateration problem that have been known for decades, which we classify as iterative, algebraic or quadratic, and linear. The most cited papers for each of these methods date back to the 1970s, 80s, and 90s, respectively.

The iterative method seeks to minimize the error in an estimated solution to the location equations, which are generally non-linear. Typical methods include steepest descent [11], or the multivariable Newton-Raphson method or Taylor series approximation [12][13, pp. 229-249], typically using the Jacobian of an error function. Of these, Foy [12]

is the one most often cited in positioning papers, likely because Foy was applying this method to a localization problem, as opposed to a more general optimization problem. Most iterative approaches can incorporate an arbitrary number of data points and can be extended to include more measurements such as AOA measurements, as long as it can be incorporated into a cost function. Iterative methods generally have two weaknesses. The biggest problem with iterative methods is that they usually have more than one basin of convergence, meaning that a given initial estimate may iterate to a locally optimal solution rather than to the globally optimal solution, and the boundaries between these regions can become fractals [14]. Iterative algorithms also take longer to compute than direct, closed-form methods.

An alternate iterative approach is a genetic algorithm called particle swarm optimization (PSO) [15–17]. It includes a number of random estimates that are iteratively updated to seek out the optimal solution, akin to a swarm of birds or insects. It is a potentially powerful tool which is more likely to converge to an optimal solution than the traditional single-path iteration approaches. It is significantly slower than any of the other methods presented in this paper, and its convergence accuracy is limited by the final step size of the algorithm.

Bancroft [18] proposed an algebraic approach to exactly solving multilateration equations in 1985. His approach determines two vectors that, together, describe a quadratic function with two roots that are possible solutions. These two solutions are similar to the basins of convergence of the iterative methods[c]. A key advantage of a quadratic solution is that both of these roots are produced directly, making it possible to evaluate both and choose the better one. Bancroft's method incorporates an arbitrary number of linear equations and scales to accommodate an arbitrary number of points. Another quadratic method, developed by Bucher [19], is written to solve the multilateration problem for four points. Bucher's approach is intended for implementation on a programmable chip, and as such it does not scale to include more than four measurements nor to incorporate more data.

[c] In our experience, iterative multilateration problems have two basins of convergence, which correspond to the two roots of the quadratic approach.

Iterative and quadratic approaches have been the standard methods for solving multilateration and bistatic radar problems and have been used extensively in the literature. While they are less common in more recent papers, they are still used regularly, in part because it is more intuitive to employ non-linear methods to solve localization problems that are defined in a non-linear manner.

A linear solution to the multilateration problem has been sought since the problem was first posed in the 1960s. Early methods sought to find D linear equations that could be used to directly solve the D-dimensional multilateration problem [20, 21], which meant that the linear position equations depended on one or more unknown, non-linear terms. The key to most modern linear algorithms is to include an extra variable, along with one or more extra measurements, to address these unknowns.

The first fully linear solution to the multilateration problem was developed by Chan [22] in 1995. Their approach employs $N + 1$ measurements

to generate N non-linear multilateration equations, which each includes an unknown transmit clock offset, then subtracts one of these equations from each of the others. The non-linear unknown terms are the same for each equation, so this subtraction cancels out the non-linear unknown terms, leaving only linear equations. Chan's method is described as "hyperbolic" because the difference equations describe a single branch of a four-dimensional hyperboloid. While this is true, the equations themselves are linear, though there has been some confusion about this in the literature [23]. These equations, which we call time difference of arrival (TDOA) equations, are derived and explored further in Sec. 2.2.1.

The second standard linear approach deals with the non-linear terms by simply replacing them with an extra variable. This variable, as defined, represents the square of the distance from the origin to the target. The earliest version that we have seen of this method was presented by Chen in 2002 [24], with a clearer derivation given by Norrdine[d] [26, 27]. This new variable nominally preserves the radii of the multilateration spheres, but as an independent variable it not bound by that constraint. This approach requires just $D + 1$ measurements to produce $D + 1$ equations, which is better than the $D + 2$ measurements required by Chan's method. While the two methods look quite different, they can be derived from the same equations, as shown in Appendix A. The equations for Norrdine's algorithm, which we call time of arrival (TOA) equations, are derived and explored further in Sec. 2.2.1.

[d] Similar equations have been around for a long time. In 1969, Gaarder [25] gave a nearly linear form of the localization equations that was quite similar to Norrdine's. These near misses can be found throughout the literature, with early papers coming close to producing linear equations without actually eliminating all of the non-linear terms.

While many papers derive their localization equations from first principles, it is rare to find papers that employ functionally different multilateration equations from those of Chan or Norrdine. When distinct equations are produced, they can usually be derived from Chan's [28] or Norrdine's [29] equations. It is common to find papers that attempt to produce new approaches and instead re-derive Chan's or Norrdine's methods exactly [30], although this is often buried under layers of convoluted notation[e] [33].

[e] One danger of independently deriving localization equations is that the equations may gather too much data, such as [31], which measures AOA on three axes even though that adds no information above a two-axis (azimuth/elevation) approach. It is also possible to under-utilize the data, such as [32], which pairs M TOA measurements to produce $M/2$ TDOA measurements, rather than producing $M - 1$ independent equations.

Linear equations offer a number of advantages over non-linear algorithms. Unlike iterative methods, they do not require an initial guess and they they do not have convergence problems[f], and are much faster to compute. Unlike quadratic methods, they can readily be expanded by adding more linear equations to include more and different measurements. This comes at a cost of requiring at least 1-2 more measurements than are required for non-linear methods.

[f] This refers to the fact that iterative methods typically have 2 or more regions of convergence. Depending on the initial value, an iterative algorithm may not converge to the optimal solution. This is distinct from numerical stability, which affects most of the algorithms discussed in this paper, with PSO as the notable exception.

The use of linear equations to solve the positioning problem has enabled a wide range of approaches. Any data that can be related to the problem by linear equations can be added to a linear algorithm by (relatively) straightforward matrix concatenation [34–36]. This has led to a boom in multilateration techniques that employ AOA or other information.

In over-determined systems of linear equations, each equation can be weighted to change how much it contributes to or dominates the solution to the total problem. Most of the papers employing linear localization equations devote considerable effort to statistical analysis to

determine an optimal weighting matrix. We note that the current paper is only interested in the linear equations used and does not address the weighting matrices and associated statistical analyses. Those analyses and weighting matrices are important parts of their respective algorithms, especially when it comes to optimizing the performance of the algorithms on noisy measurements and achieving the Cramér-Rao lower bound (CRLB).

2.2.1 The Geometry of Linear Localization Equations

Localization is a physical problem. If one or more equations provide a correct solution to that problem then there should be a geometric interpretation of the equations that physically describes how the equations produce a valid solution. This geometrical understanding is rarely the motivation for deriving the solution[g] to the localization equations, but finding it helps in understanding the equations and their solutions, including giving a more intuitive sense of when they become numerically unstable. This section presents a general approach to understanding the geometry of linear positioning equations. It also presents simple, intuitive derivations of the noise-free positioning equations. This can aid the reader in understanding the linear positioning equations used throughout the literature.

[g] A notable exception to this is a paper by Lee [37], which provides an intuitive geometric derivation of a far less intuitive result from his earlier papers [38, 39]. Lee's papers analyze the geometric stability of the multilateration problem without providing an algorithm for solving it.

For the equations presented in this paper, we consider a transmitter at a point $\mathbf{u}$ that emits a signal at time t_u that is received at N different points $\mathbf{p}_i$, $i = 1, \ldots, N$ at times t_i. These times are converted to a pseudodistance $d_i = vt_i$ where v is the propagation speed of the signal, which is normally the speed of light c. These time of arrival values, along with the time that the signal was transmitted, describe spheres centered on the receivers. Two-dimensional examples of these spheres are shown as circles in Figs. 2.1 and 2.2 The transmitter $\mathbf{u}$ lies at the intersection of those spheres.

Finding that intersection is a fundamentally non-linear problem. If t_u is known then it is the TOA problem, which requires finding the intersection of spheres. If t_u is unknown then the solution lies at the intersection of 4-dimensional hyperboloids, each with its foci at the locations of a pair of receivers. Methods for converting this non-linear problem into linear equations are presented in Secs. 2.2.1 and 2.2.1.

To understand the geometry of a linear equation, consider the generic linear equation

$$ax + by + cz = d. \tag{2.1}$$

The solution to this equation is a plane that is perpendicular to the vector $[a, b, c]^{\mathrm{T}}$, intersecting that vector at a distance from the origin of $d/\sqrt{a^2 + b^2 + c^2}$. The specific location of this intercept is not as important as understanding the relative shape and orientation of these solution surfaces. Combining linear equations for multiple measurements produces a system of linear equations, each one contributing to a set of solution planes. If the solution planes are roughly perpendicular to each other

then the problem is well-conditioned. If they are nearly parallel then the problem is ill-conditioned.

In this section we consider linear equations in 4 dimensions, with the fourth dimension describing some non-spatial parameter, such as transmission time, or some other nuisance variable employed to help linearize the equations. The general form of this 4-dimensional equation is

$$\begin{bmatrix} \mathbf{a}^{\mathrm{T}} & e \end{bmatrix} \begin{bmatrix} \mathbf{x} \\ w \end{bmatrix} = d \tag{2.2}$$

where w is a nuisance variable[h]. This equation describes a 3-dimensional subspace that is perpendicular to the vector $\begin{bmatrix} \mathbf{a}^{\mathrm{T}} & e \end{bmatrix}^{\mathrm{T}}$. Because it is much harder to mentally visualize higher dimensional spaces, we consider the projection of this subspace onto the familiar xyz space. This means considering (2.2) as

$$\mathbf{a}^{\mathrm{T}}\mathbf{x} = d - ew \tag{2.3}$$

which is a plane perpendicular to $\mathbf{a}$, but where the its intersection point now depends on the value of w. This means that, as w changes, the solution planes for each equation moves along that vector. The solution to the equations is then the point where, as these solution planes translate along the vectors, they become closest to intersecting at a single point.

[h]In this context, a nuisance variable is any unknown value that is not a spatial coordinate of the unknown transmitter. While it may describe some attribute of the transmitter, such as its transmit time or distance from the origin, it is not typically of interest and is discarded after the position is calculated.

The remainder of this section presents the noise-free equations of a number of common linear localization equations, including a straightforward derivation of each equation and an intuitive description of the underlying geometry. The methods we derive are

- Time of arrival (TOA),
- Time difference of arrival (TDOA),
- Azimuth-only angle of arrival (AOA),
- Azimuth and elevation angle of arrival (2AOA),
- Arbitrarily oriented single angle of arrival (1AOA),
- Vertical-only angle of arrival with multilateration (vertical AOA),
- Frequency difference of arrival (FDOA), and
- TDOA-based bistatic radar (bistatic TDOA).

Time of arrival (TOA)

The single receiver non-linear multilateration equations in 3 dimensions are

$$d_i - d_u = \sqrt{(x_i - x_u)^2 + (y_i - y_u)^2 + (z_i - z_u)^2} \tag{2.4}$$

$$x_i^2 + y_i^2 + z_i^2 - d_i^2 = 2x_i x_u + 2y_i y_u + 2z_i z_u - 2d_i d_u - x_u^2 - y_u^2 - z_u^2 + d_u^2 \tag{2.5}$$

where $\mathbf{p}_i = [x_i, y_i, z_i]^{\mathrm{T}}$ is the location of a known point where time of arrival pseudodistance measurement d_i is taken, and $\mathbf{u} = [x_u, y_u, z_u]^{\mathrm{T}}$ is the location where a signal was transmitted at the time corresponding to pseudodistance d_u.

There are two common approaches to dealing with the quadratic terms in Eq. 2.5 that produce purely linear equations. The method we consider in this section [26, 27] uses a dummy variable K which is nominally equal to $x_u^2 + y_u^2 + z_u^2 - d_u^2$, to replace those terms. This approach assumes that the unknown transmit time $d_u = 0$. The more general form of these equations is derived in Appendix A. Because K does not replace the $d_i d_u$ term, this approach is only accurate when d_u can be accurately approximated[i].

[i]The accuracy of the estimate of d_u must be at least equal to the measurement accuracy in order to avoid adding significant error to the calculated position. While this cannot be done in all cases, in some applications, such as tracking aircraft based on ADS-B or beacon transmissions, this kind of estimate is possible.

The corresponding linear TOA equations are of the form

$$x_i x_u + y_i y_u + z_i z_u + K = \frac{x_i^2 + y_i^2 + z_i^2 - d_i^2}{2}. \tag{2.6}$$

The equation describes a plane perpendicular to the vector $\mathbf{p}_i = [x_i, y_i, z_i]^{\mathrm{T}}$, as shown in Fig. 2.1. The K variable, while nominally equal or related to $x_u^2 + y_u^2 + z_u^2$, is actually free to vary independently from the other unknowns[j]. The practical effect is that $\mathbf{u}$ can lie on a larger or smaller sphere than K implies.

[j]The independence of K from the position estimate is addressed in [40] which attempts to constrain the 2-dimensional solution so that $x_u^2 + y_u^2 \approx K$.

By considering the orientation of these planes, we can intuitively understand that this method provides a numerically stable solution when the points $\mathbf{p}_i$ are distributed around the origin. When they are all very far from the origin in the same direction, the planes are nearly parallel and the system of equations may be ill-conditioned. This method is used frequently in the literature [24, 41–58].

Time difference of arrival (TDOA)

In TDOA multilateration, the non-linear terms in Eq. 2.5 are eliminated by taking the difference between the equations for two different points [22]. Since the non-linear unknown terms are equal in each equation, they cancel out, leaving only linear terms. The resulting equation is of the form

$$(x_i - x_j)x_u + (y_i - y_j)y_u + (z_i - z_j)z_u - (d_i - d_j)d_u = \frac{1}{2}\left(x_i^2 + y_i^2 + z_i^2 - x_j^2 - y_j^2 - z_j^2 - d_i^2 + d_j^2\right). \tag{2.7}$$

This approach is also used frequently in the literature [2, 11, 16, 30, 33–35, 49, 50, 52, 55, 59–72]. Many of these papers independently derive Eq. 2.7. This is sometimes done explicitly, such as the maximum likelihood (ML) derivation given in [30].

Eq. 2.7 describes a plane that is perpendicular to the line between $\mathbf{p}_i$ and $\mathbf{p}_j$. In multilateration, the unknown point lies at the intersection of spheres centered on the known points. The intersection of two spheres is a circle or a point. The plane described by this equation is the plane

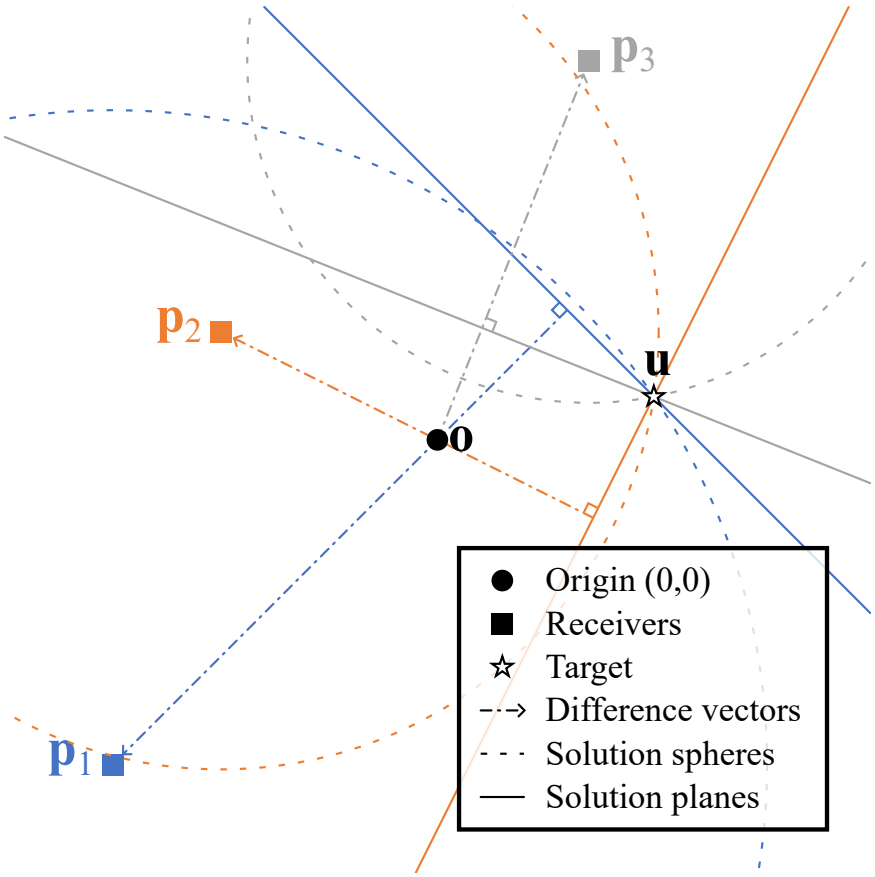

Figure 2.1: Illustration of the linearization of the TOA localization equations in 2 dimensions. The solution lies at the intersection of planes (or lines, in 2 dimensions) that are perpendicular to the position vectors for the receivers.

containing the circle of intersection for the spheres centered at $\mathbf{p}_i, \mathbf{p}_j$, as shown in Fig. 2.2.

The fact that this gives the plane, rather than the circle, suggests that this approach can produce solutions which lie somewhere on the plane that is distant from the circle. This is not generally a problem when the overall equations are well-conditioned, but when the points $\mathbf{p}_i$ are nearly coplanar, the equations are ill-conditioned and the lack of constraint is more relevant, resulting in potentially distant solutions.

There is also a modified version of (2.7) where d_u is solved implicitly [28, 73]. This approach has been called line of position (LOP) [65]. This is done by solving (2.7) for d_u and then combining pairs of those equations, producing linear equations that are each based on three measurements. This requires the same number of measurements but can introduce divide-by-zero singularities. The numerical advantage is that it only requires inverting a 3×3 matrix, rather than a 4×4 matrix.

Some algorithms use received signal strength (RSS) [29, 50, 74] or gain ratio of arrival (GROA) [75–81] instead of TOA or TDOA. Signal strength measurements produce equations that are geometrically similar to the TOA or TDOA equations presented here.

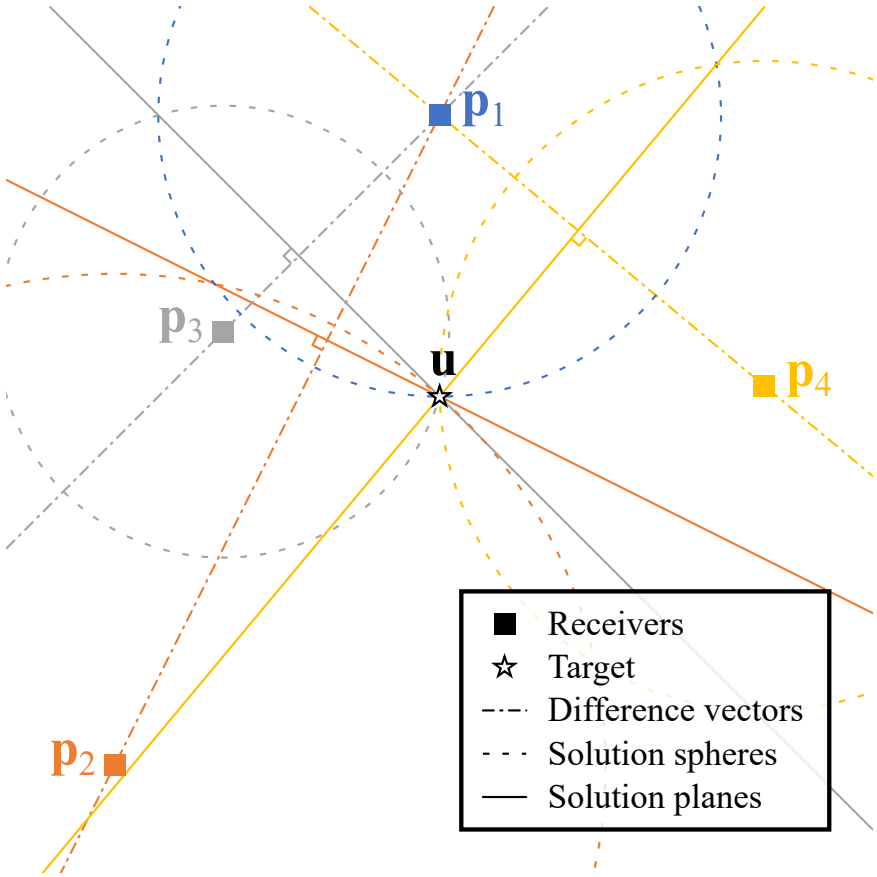

Figure 2.2: Illustration of the linearization of the TDOA localization equations in 2 dimensions, with the differences taken relative to receiver $\mathbf{p}_1$. The solution lies at the intersection of planes (or lines, in 2 dimensions) that are perpendicular to the vectors connecting the pair of receivers in each equation, and that pass through the intersections of the solution spheres.

Azimuth and elevation angle of arrival (AOA)

There are three ways that angle of arrival is typically used in a linear localization equation: azimuth only, azimuth and elevation, and elevation only. Typically, azimuth and/or elevation angles are measured as shown in Fig. 2.3. The general form of the equations can be seen in the equation for an azimuth angle. A given azimuth angle θ_i relative to $\mathbf{p}_i$ gives the equation

$$\frac{y_u - y_i}{x_u - x_i} = \tan\theta_i = \frac{\sin\theta_i}{\cos\theta_i}. \tag{2.8}$$

Putting this in canonical linear equation form suitable for solving by matrix gives the linear azimuth equation

$$x_u \sin\theta_i - y_u \cos\theta_i = x_i \sin\theta_i - y_i \cos\theta_i. \tag{2.9}$$

This equation describes a vertical plane passing through $\mathbf{p}_i$ with a heading of θ. The most important thing to note with this equation is that it uses the sine and cosine, rather than the tangent. This produces an equation that is far more numerically stable than equations using the

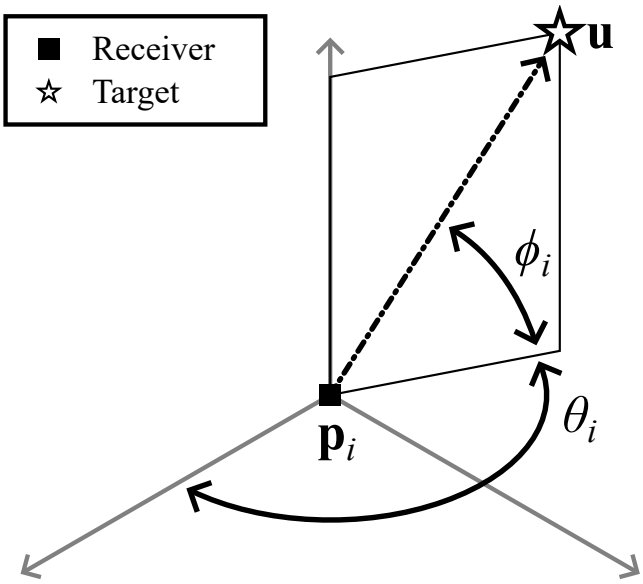

Figure 2.3: Illustration of the typical azimuth and elevation AOA measurements.

tangent. If the tangent of the azimuth is used then the magnitudes of the coefficients blow up when $\theta_i \approx \pm\pi/2$, causing this term to dominate the larger system of linear equations. AOA equations using the tangent appear occasionally in the literature [31, 33, 46, 47, 82–86]. The form shown here, using sine and cosine, is far more common [29, 32, 34–36, 41–43, 49–62, 70–72, 76–78, 87–104].

When elevation angles are used in conjunction with azimuth angles the standard approach is to apply the relationship from Eq. 2.8 to ϕ_i in the vertical plane passing through the θ_i azimuth.

$$\frac{z_u - z_i}{(x_u - x_i)\cos\theta_i + (y_u - y_i)\sin\theta_i} = \tan\phi_i = \frac{\sin\phi_i}{\cos\phi_i}. \tag{2.10}$$

Putting this in canonical linear equation form gives

$$\begin{aligned} x_u \cos\theta_i \sin\phi_i + y_u \cos\theta_i \sin\phi_i - z_u \cos\phi_i = \\ x_i \cos\theta_i \sin\phi_i + y_i \sin\theta_i \sin\phi_i - z_i \cos\phi_i. \end{aligned} \tag{2.11}$$

This equation describes a plane, passing through $\mathbf{p}_i$, perpendicular to the vertical plane described by Eq. 2.9 and rotated ϕ_i from the $x-y$ plane. The key point of this equation is that the intersection of this plane with the plane defined in Eq. 2.9 is the line passing through $\mathbf{u}$ and $\mathbf{p}_i$.

Recently, a single angle triangulation approach has been proposed [105, 106] where each receiver has an independent orientation unit vector $\mathbf{s}_i$ and a single angle ψ_i is measured relative to that vector, as shown in Fig. 2.4. This is one angle of arrival (1AOA). The relationship can be expressed as

$$\cos\psi_i = \frac{(\mathbf{u} - \mathbf{p}_i)^{\mathrm{T}} \mathbf{s}_i}{|\mathbf{u} - \mathbf{p}_i|}. \tag{2.12}$$

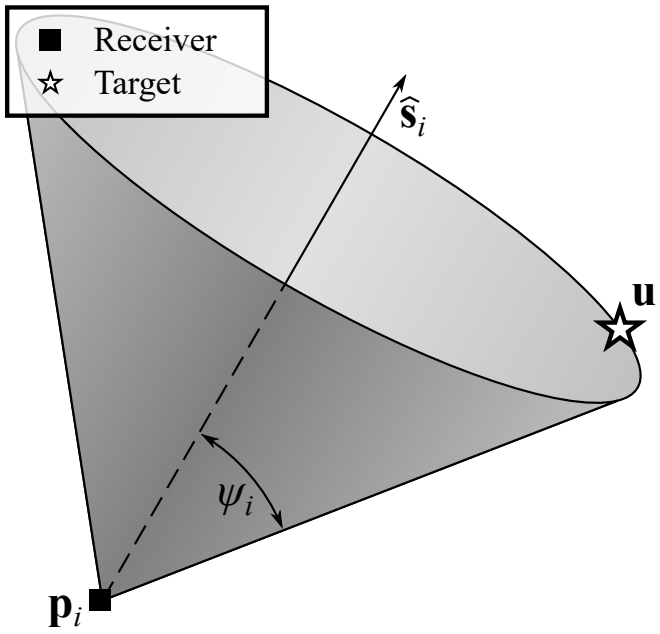

Figure 2.4: Illustration of the arbitrary single AOA measurement. The measurement constrains the solution to lie on the indicated cone.

Breaking the dot product into components and using the fact that $|\mathbf{u} - \mathbf{p}_i| = d_i - d_u$, this becomes

$$\cos\psi_i = \frac{x_{\hat{s}_i}(x_u - x_{p_i}) + y_{\hat{s}_i}(y_u - y_{p_i}) + z_{\hat{s}_i}(z_u - z_{p_i})}{d_i - d_u}, \tag{2.13}$$

which can be rewritten in a linear form as

$$x_{\hat{s}}x_u + y_{\hat{s}_i}y_u + z_{\hat{s}_i}z_u - d_u\cos\psi_i = x_{\hat{s}_i}x_{p_i} + y_{\hat{s}_i}y_{p_i} + z_{\hat{s}_i}z_{p_i} - d_i\cos\psi_i. \tag{2.14}$$

Eq. 2.14 constrains the distance from $\mathbf{u}$ to the line formed by $\mathbf{p}_i + k\mathbf{s}_i$ to be proportional to $d_i - d_u$. The quantity $d_i - d_u$, in turn, constrains $|\mathbf{u} - \mathbf{p}_i|$. The locus of those constraints is the cone shown in Fig. 2.4.

Note that this method, as described here, requires TOA measurements, meaning that it cannot operate in a triangulation-only localization algorithm. In general, localization via triangulation-only is less accurate than localization via multilateration-only [107, 108]. This is largely due to the fact that in multilateration position errors are proportional to measurement error, while in triangulation position errors are proportional to measurement error multiplied by the distance to the target. When the multilateration problem is ill-conditioned, or when the target is close to the vertex of the angle, then the accuracy due to triangulation may be better than from multilateration. This a key motivation for combining TOA and AOA measurements into a single system.

A special case of 1AOA uses $\mathbf{s}_i = \mathbf{z}$, i.e., the angles are all taken relative to vertical, as shown in Fig. 2.5 [2]. In this case, the angle is typically taken relative to the horizontal, similar to the elevation angle in 2AOA[k]. The resulting equation can be derived from Eq. 2.14 by replacing $\mathbf{s}_i$ with $\mathbf{z} = \begin{bmatrix} 0 & 0 & 1 \end{bmatrix}^{\mathrm{T}}$, giving

[k]Note that this angle is the complement of the angle used in Eq. 2.14, which is why Eq. 2.14 uses $\cos\psi_i$ and Eq. 2.15 uses $\sin\phi_i$. The vertical 1AOA equation differs from Eq. 2.11 in that it uses $d_i - d_u$ instead of the azimuth angle to relate the elevation angle to $\mathbf{u}$.

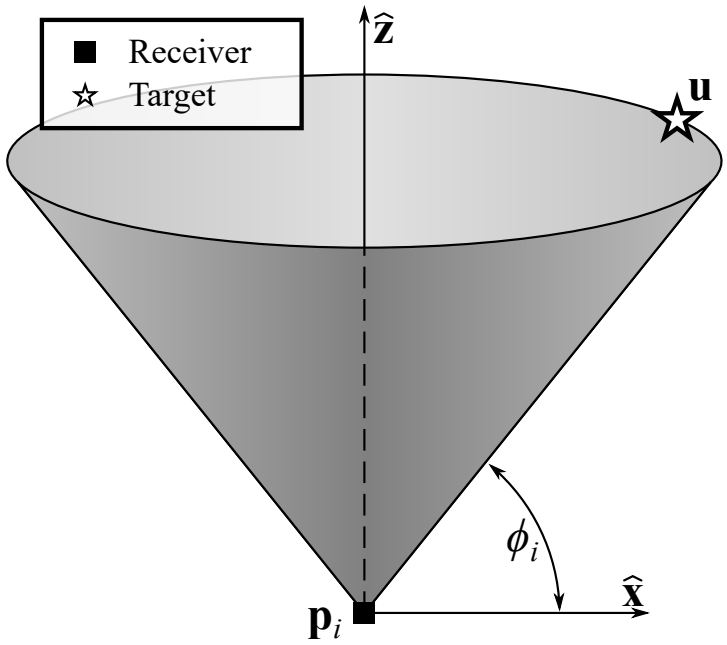

Figure 2.5: Illustration of the vertical AOA measurement. The measurement constrains the solution to lie on the indicated cone.

$$z_u - d_u \sin\phi_i = z_i - d_i \sin\phi_i. \tag{2.15}$$

As with Eq. 2.14, this equation effectively describes a cone, with a vertex at $\mathbf{p}_i$. This type of measurement is helpful in wide area multilateration, where the receivers are spread out over a large area, and are nearly coplanar. In those scenarios, multilateration is not as accurate in the vertical direction, so adding an elevation angle is an efficient way of improving the overall position accuracy.

In recent years, TOA and AOA have been applied to a different localization measure, called direction of arrival (DOA) [98]. When a source is far from all of the receivers, determining a fixed position in space may be impossible. Instead, these methods seek to use measured TOA and AOA to improve the estimate of the true bearing of the target, relative to all of the receivers (i.e., assuming that the target is in the far field and that the angle to each receiver is the same). Additional research on this approach, all performed by the same research group, has focused on determining when to determine DOA or position [95, 99, 109].

Frequency difference of arrival (FDOA)

Frequency difference of arrival (FDOA) involves measuring the received frequency of a signal with an unknown or uncertain transmitted frequency to improve the estimated location parameters of the transmitter. In the general case of passive localization, where the transmitted signal characteristics are not known *a priori* and the signals are not optimized for range-Doppler processing, FDOA can be difficult to implement. Nevertheless, the notion of using FDOA as part of passive localization schemes has been proposed.

In synthetic aperture radar (SAR), FDOA is used to disambiguate returned signals in range and azimuth. By that reasoning, it could be employed to improve the solution in passive localization. It turns out that, when the transmitter velocity is unknown and the receiver velocities are all zero[l], the FDOA measurements do not provide any information on the position of the transmitter. FDOA is therefore primarily useful for measuring the velocity of a target for use in a tracking algorithm.

[l] These conditions are the opposite of the conditions for SAR mapping, where the relative motion of the radar and target is well known.

Given a target moving at point $\mathbf{u}$ with velocity $\mathbf{v}_u$ that transmits a signal with frequency f_u and a wavelength of $\lambda_u = v/f_u$ where v is the propagation speed of the signal, and a receiver moving at $\mathbf{p}_i$ with velocity $\mathbf{v}_i$, the frequency of the received signal is

$$f_i = f_s - \frac{(\mathbf{v}_u - \mathbf{v}_i) \cdot (\mathbf{u} - \mathbf{p}_i)}{\lambda_u \, |\mathbf{u} - \mathbf{p}_i|}. \tag{2.16}$$

By rearranging the equation and using $d_i - d_u = |\mathbf{u} - \mathbf{p}_i|$, this can be rewritten as

$$\lambda_u (f_u - f_i)(d_i - d_u) = (\mathbf{v}_u - \mathbf{v}_i) \cdot (\mathbf{u} - \mathbf{p}_i) \tag{2.17}$$

which, when split into individual terms, is

$$\lambda_u f_u d_i + \lambda_u f_i d_u - \lambda_u f_u d_u - \lambda_u f_i d_i = \mathbf{v}_u \cdot \mathbf{u} - \mathbf{v}_u \cdot \mathbf{p}_i - \mathbf{v}_i \cdot \mathbf{u} + \mathbf{v}_i \cdot \mathbf{p}_i. \tag{2.18}$$

Apart from the $f_u d_u$ and $\mathbf{v}_u \cdot \mathbf{u}$ terms, this equation is already linear in terms of the unknown variables $\mathbf{u}$, d_u, $\mathbf{v}_u$, and f_u. As with Eq. 2.5, one straightforward way to linearize the equation[m] is to take the difference between the equations for two points $\mathbf{p}_i$ and $\mathbf{p}_j$. This produces the equation [64]

[m] This can also be linearized using an approach similar to Norrdine. That approach requires a second nuisance variable, but there is already a second nuisance variable (f_u) in the FDOA equation presented here.

$$\mathbf{u} \cdot (\mathbf{v}_i - \mathbf{v}_j) + \mathbf{v}_u \cdot (\mathbf{p}_i - \mathbf{p}_j) + \lambda_u (f_i - f_j) d_u + \lambda_u (d_i - d_j) f_u = \mathbf{v}_i \cdot \mathbf{p}_i - \mathbf{v}_j \cdot \mathbf{p}_j + \lambda_u d_i f_i - \lambda_u d_j f_j. \tag{2.19}$$

This equation is distinct from the other equations in this section in that it has eight unknowns, rather than just two to four. This makes it harder to visualize the linear geometry represented by these equations. Instead of visualizing the entire 8-dimensional linear system, we consider a simplified version that is sufficient for a wide range of applications. If

the receivers are all located at fixed sites then there is no Doppler shift due to receiver motion, making $\mathbf{v}_i = \mathbf{0}$. This produces a simplified FDOA equation

$$\mathbf{v}_u \cdot (\mathbf{p}_i - \mathbf{p}_j) + \lambda_u(f_i - f_j)d_u + \lambda_u(d_i - d_j)f_u = \lambda_u d_i f_i - \lambda_u d_j f_j. \quad (2.20)$$

The most important detail of this equation is that it does not include the unknown transmitter position $\mathbf{u}$. That means that FDOA cannot be used with stationary receivers to locate a transmitter. Instead, FDOA is mostly useful for calculating the movement of a transmitter, which enables improved tracking.

The solution to this system of equations can be understood in the same way as the TDOA equations in Sec. 2.2.1. The velocity of the transmitter is at or near the intersection of surfaces that are perpendicular to the vectors joining the receiver locations, as shown in Fig. 2.6.

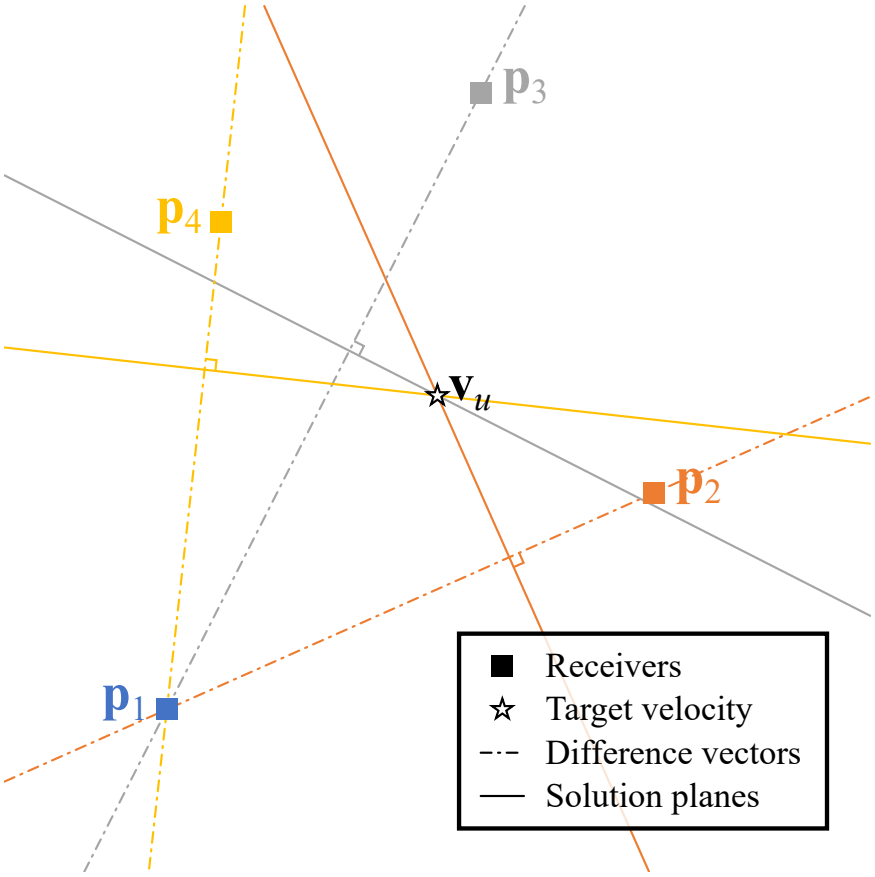

Figure 2.6: Illustration of the linearization of the FDOA equations in 2 dimensions, with the differences taken relative to receiver $\mathbf{p}_1$.The solution lies at the intersection of planes (or lines, in 2 dimensions) that are perpendicular to the vectors connecting the pair of receivers in each equation. The incongruity between using position and speed vectors can be reconciled by noting that velocity vectors and position vectors are proportional to each other, and that the point of the relationship is to show the orientation of the solution planes.

Another reduced form of Eq. 2.19 can be made if the sensor velocities $\mathbf{v}_j$ are non-zero and known (e.g., the orbital velocities of GPS satellites) and $\mathbf{v}_u$ and f_u are assumed to be zero. In that case, Eq. 2.19 reduces to a linear equation of four unknowns. That system of equations can be used to determine $\mathbf{u}$, which lies on a plane perpendicular to the relative receiver velocity vector $\mathbf{v}_i - \mathbf{v}_j$.

FDOA is included in some localization algorithms. Implementations include quadratic [110], iterative [87], and linear [64, 90, 111], and probabilistic [112] methods. It is common for FDOA to be employed in bistatic radar [113–118]. Linear bistatic radar localization is explored in the section below.

Bistatic radar

The localization of a target in a bistatic radar is quite similar to multilateration, using time of arrival to estimate the position of a scattering target. Approaches for solving the bistatic radar problem are presented by Malanowski [119, 120] and Willis [121]. The linear bistatic radar equation from Malanowski for multiple transmitters and a single receiver is

$$x_i x_u + y_i y_u + z_i z_u - r_i r_u = \frac{1}{2}\left(x_i^2 + y_i^2 + z_i^2 - r_i^2\right) \tag{2.21}$$

where r_u is an unknown target-receiver range that is constant for all transmitters[n] and r_i is the measured bistatic range to the target. This equation is equivalent to Eq. 2.7 with the receiver acting as the common node and with a sign change.

[n] In a single transmitter, multiple receiver case, r_u is the transmitter-target range. That includes passive multistatic radar, which is found frequently in the literature.

Malanowski only applies the linear equations to the position variables, considering the r_u as a non-linear variable that needs to be solved independent of $[x_u, y_u, z_u]^{\mathrm{T}}$. He suggests two different approaches for doing so. The first (spherical interpolation, or SI) is nearly linear, but includes a non-linear step, based on similar multilateration algorithms [20, 21]. The second (spherical-intersection, or SX) is similar to the quadratic approach in [18]. As non-linear solutions, neither of those approaches are well-suited for adding additional information such as AOA or FDOA.

Geometry summary

These different localization equations, or others like them, can be used, individually or together, to create localization algorithms suited to most scenarios. The key is to consider the geometric limitations of each technique, and to bring together different techniques that have complementary strength. For example, for tracking aircraft in flight there is a need for 3 dimensional positioning using ground-based sensors that are nearly coplanar. That sensor layout can produce very good localization in 2 dimensions using TOA/TDOA, but the equations are ill-conditioned in the vertical direction. By adding elevation AOA measurements, the problem becomes constrained vertically and the solution becomes more accurate.

This flexibility is the key advantage to linear equations. Most non-linear TDOA [19], TDOA/AOA [91, 93], or TDOA/FDOA [110] methods

do not scale to include more data[o]. Significant effort is required to incorporate different kinds of measurements into quadratic algorithms. This can be seen in the relative complexity of a quadratic TDOA algorithm [18] versus a quadratic TDOA/AOA algorithm [72].

[o]Even Chan's paper [22] starts with a 3 measurement, 2-dimensional quadratic algorithm that does not scale to include more or different measurements.

When combining linear equations, especially when different types of measurements (TOA/TDOA, azimuth AOA, elevation AOA, FDOA, etc.) are used, it is essential to use weighted least squares with an appropriate weighting matrix, or to incorporate the weighting directly into the equations themselves [60]. This is a non-trivial problem that encompasses the bulk of the analytical work in the literature cited here.

2.3 Review of TDOA/AOA Multilateration Approaches

The last 30 years has seen a large volume of papers on passive localization, especially using TDOA and/or AOA techniques. This section reviews examples of these linear approaches from the literature, with particular interest in papers that supplement the TOA or TDOA data with AOA or other data. The wide array of approaches and implementations show the versatility of linear equations when it comes to expanding on the basic TOA/TDOA localization problem.

This review gives some examples of work in general localization, optimized sensor placement, clutter and multipath, cellular telephone localization, wireless device localization, tracking air and space vehicles, acoustic localization, underwater localization, optical multilateration, and object orientation. It also includes a brief review of some work in passive multistatic radar.

2.3.1 General multilateration and triangulation algorithms

Many papers combine 2-dimensional mulilateration and azimuth AOA for more general localization. These employ TDOA [53, 71] and TOA [46, 56]. Rui [122] provides a generalized analysis of the maximum likelihood estimator for 2-dimensional TDOA/AOA localization. Ma [59] adds a non-linear constraint to the linear equations, then creates a linear approximation of that constraint. A method exists for 2-point, two-dimensional TDOA/FDOA/AOA localization [87], using a TDOA/FDOA approach intended for global navigation satellite system (GNSS) localization [110]. A French team implemented a two-point TOA/AOA system [123], with emphasis on the hardware used to measure the signals.

When extending TDOA/AOA methods to three dimensions, there are two standard approaches to the AOA. The simpler approach is to only measure angle in azimuth, which is done for multipath environments [54] and to locate points of failure on a power grid [84]. The more general case also includes elevation angle [94, 96]. A method can add both azimuth and elevation AOA, which gives improved 3-dimensional position [31, 32, 96], or a way to isolate multipath and clutter returns [88, 124, 125]. A rigorous analysis of two angle TDOA/AOA errors is found in [94]. Most papers assume that angle measurements are small, allowing for a small angle approximations in the error terms, but [104] provides an AOA

analysis that does not rely on that assumption. One method employs a reference source at a known location to calibrate the algorithm [61].

A less common TOA/AOA localization approach is to use a single AOA that is not the azimuth angle. This includes two-dimensional[p] [126] and three-dimensional [2, 127] localization using elevation angles only. A more general approach using a single non-azimuth AOA, where the AOA measurements are made relative to arbitrarily oriented vectors, is given in [105, 106].

[p] In a two-dimensional localization problem, a non-azimuth angle lies outside the solution space and cannot be used directly to locate the target. Instead, [126] uses the elevation angles to foreshorten the measured pseudodistances, at which point they use conventional TDOA equations, without a transmitter clock offset, to determine the (x, y) position of the target.

Filtering is not a common feature of TDOA/AOA algorithms but is occasionally included. Filtering approaches include Kalman filtering [128] and a Kalman-like Bayesian filter [129].

Limited sensors

An interesting approach to achieving multiple sensor localization with just two sensors suggests using a stationary sensor and a moving sensor [57]. This enables TDOA/AOA localization from different points using TDOA pairs with the stationary sensor. They also survey approaches based on unmanned aerial vehicle (UAV) platforms, summarizing their accuracy based on environment, geometry, and measurement types [42].

The most extreme version of passive localization with limited sensors is 2-dimensional TOA/AOA multilateration employing a single station. The challenge in such a system is determining the true distance. This is done by using synchronized transmissions [130] or RSS [81, 92]. Both approaches require a target that is either cooperative or at least predictable. A passive single-sensor localization approach in 3 dimensions, with azimuth and elevation angles has been proposed [100]. It assumes that a target is moving at a constant velocity and uses multiple TOA and AOA samples over time to model the target's position and velocity, making it geometrically similar to SAR. Another SAR-like approach employs AOA and FDOA to a 2-dimensional Doppler-triangulation localization method for a target that is moving in a non-linear path [97]. It has also been suggested that using TDOA and AOA from multipath returns could be sufficient to determine the position of a transmitter from a single reference point [68].

Triangulation only

Some papers consider TDOA and AOA and ultimately only implement the latter. One stated reason for excluding multilateration is that "these multilateration techniques systems have several drawbacks mainly related to the requirement of network synchronization, which does not exist in [cellular telephone networks] ." [131] Given the relatively poor accuracy of AOA compared to TDOA, this is a poor choice for wide area applications. Triangulation-only is applied to self-localization [89], 2-dimensional localization [58], and 3-dimensional localization [102]. One paper [132] presents a method of localizing a set of unknown sources and sensors using only azimuth angles. The resulting solution is an approximation of the true relative positions, which must then be rotated, translated, and scaled to approximate the true absolute positions.

Optimized sensor placement

A few papers analyze the problem of optimizing sensor placement for multilateration problems. This is done in 2 dimensions [63, 133, 134] and in 3 dimensions [101]. One [134] determines that the optimal positions for three sensors is in an equilateral triangle. Typically, these methods provide complicated equations that are far removed from the underlying geometry, depriving readers of any general or intuitive understanding of the results.

2.3.2 Multilateration applications

Clutter and multipath

Localization in the presence of multipath propagation and clutter, or non-line of sight (NLOS), has been an important area of research [53, 54, 65, 124, 125]. The multipath signal has a path length and AOA that differ from the true line of sight (LOS) path. This can affect the accuracy of multilateration systems, especially in urban environments. For that reason, it correcting for NLOS has been a focus of Enhanced 911 (E-911) localization [44, 47, 51, 55, 83, 90]. AOA may be employed to correct multilateration path lengths [45] and to determine the optimal beamforming for a multiple-input multiple-output (MIMO) antenna [69]. A proposed self-localization method is proposed for cellular phones employing TOA and AOA in a multipath environment with other cooperative receivers and information from the transmitter [68]. A more algorithmic approach to localization in clutter is presented in [85]. NLOS can also be an issue underwater [88].

Cellular telephone localization

Enhanced 911 (E-911), established by the Wireless Communications and Public Safety Act in 1999 [5], levied a requirement on cellular telephone services to be able to locate phones that have called emergency services. This prompted a flurry of research into passive localization of cellular devices [135]. The addition of AOA has been employed to resolve under-determined localization scenarios, such as when the base stations are all in a line [41]. E-911 research has focused on scenarios with limited reference points [49, 51], which is common for rural environments, and scenarios with significant scattering in 2-dimensions [44, 83] or 3-dimensions [52, 55, 66], which is typical for urban areas. One approach uses the scatterers to help locate the telephone in 3 dimensions [90], using AOA to characterize the locations of the scatterers. E-911 approaches also employ filters [49] and estimators [47]. A few E-911 papers propose localization with triangulation only [136, 137].

Wireless device localization

A common application of multilateration is locating wireless network devices. Methods that incorporate AOA with 2-dimensional multilateration equations do not appear to be popular. One simple system employing two sensors with two TOA and one AOA measurements is [70]. TDOA/AOA measurements are also used to locate interference

sources, either at specific points [138] or in specific directions [139]. The latter uses the TDOA at two close antennas to measure the AOA. TDOA/AOA is also used to distinguish between signal sources [82].

Tracking air and space vehicles

Passive detection is of interest to civil aviation agencies seeking to track aircraft. These applications typically employ aircraft transponder signals such as Airborne Collision Avoidance System (ACAS) Mode S signals [140], L-band digital aeronautical communication system (LDACS) [141], or the Automatic Dependent Surveillance-Broadcast (ADS-B) messages [48, 142]. The approach in [140] is for ground tracking at an airport, rigidly limiting the scenario to two dimensions, and employs RF over fiber (RoF) in order to centralize the detection and processing functions. Some papers respond to the difficulty of 3-dimensional localization in wide area multilateration by only considering the horizontal accuracy, even for aircraft in flight [141, 143].

Multilateration may also be used to track objects in space. A Korean team has employed TOA/AOA localization in tracking space vehicles during launch [144, 145]. A satellite tracking algorithm employs FDOA in addition to TDOA and AOA, using PSO [17]. AOA is not typically applied to GPS, but it has been proposed as part of a GPS augmentation. This includes a case where ground stations, acting as pseudo-satellites, can measure azimuth AOA [146], and where AOA is measured directly to the satellites [147].

Acoustic localization

Acoustic waves may be used for multilateration and AOA measurements. Acoustic signals can experience stronger dispersion than RF signals, making it difficult to employ the relatively wide bandwidth signals that are most effective for TOA measurements. Acoustic localization can be done over distances of meters [148] or over longer distances in 2 dimensions [80] and 3 dimensions [77].

Underwater localization

Underwater multilateration using RF waves and AOA has been proposed as a method to locate invasive weeds [62]. AOA has also been applied to correct ranges in multilateration-only localization underwater [67]. RF attenuation underwater can be severe, which places great importance on placing sensors and selecting which sensors to include in a solution [103, 149].

Optical multilateration

A recent paper [86] uses phase and modulation to measure TOA in optical systems, which it then adds to the angle measurements inherent in an image to produce a hybrid TDOA/AOA optical localization system.

Object orientation

Multilateration with AOA can be used to determine the orientation of a rigid body using a fixed point and sensors positioned on the body [150, 151]. This is a difficult problem with six degrees of freedom (translation in three dimensions and rotation on three axes) that is very different from a traditional localization problem.

2.3.3 Multistatic radar

Bistatic radar uses separate antennas to transmit and receive, which may or may not be located near each other. A multistatic radar employs one or more transmitting antennas and one or more receiving antennas. When a system employs a transmitter (which may be part of the system or may be transmitting signals for some other purpose, such as radio or television broadcasts) and several geographically separated receivers, then the target localization problem becomes quite similar to the problem in multilateration. The problem can be solved with linear equations nearly identical to those presented by Chan [22, 30, 43], with AOA measurements producing equations similar to those given in Sec. 2.2.1 [34, 36, 43]. Including the uncertainty in the sensor locations produces more complicated WLS weights but otherwise does not affect the linear equations [33, 152].

The multistatic radar scenario, when viewed in terms of the signal being reflected from a single target, can be reduced to a multilateration problem where the transmitter is equivalent to a receiver with negative propagation time. As a result of this, multilateration techniques can be applied to multistatic radar, and many multistatic radar algorithms can be applied to multilateration problems. They also share some of the same geometric problems including multipath [116, 153] and vertical ambiguity. Multistatic radar has more difficulties with ghosting [154] than multilateration. Like other surveillance radars, multistatic radars are able to take advantage of Doppler filtering for clutter rejection [117] when the target is moving.

An active area of multistatic radar research is passive multistatic radar using signals from digital radio (DAB) and TV (DVB-T) stations as illuminators [111, 114, 115, 117, 154]. Experimental radars using DVB-T signals can track objects in 2 dimensions with reasonable accuracy [113, 155]. The DAB/DVB-T radar papers cited here do not employ AOA due to their use of small, relatively inexpensive antennas which are inadequate for measuring AOA in azimuth or elevation. Passive multistatic radars require a direct path signal for synchronization, but the direct signal can interfere with the reflected waveforms [116].

A popular approach to solving the multistatic radar localization problem is to maximize a joint probability distribution across multiple receivers [30, 33, 111, 112, 116, 118, 152]. When this approach produces an algorithm for solving the localization problem the resulting equations are often similar to methods for multilateration [30, 33]. Other approaches also produce equations similar to the linear equations for multilateration,

including those employing AOA information [34, 36].

Other algorithmic refinements include adaptive nulling of interference sources [153], tracking algorithms [111, 114, 115], and employing intelligent reflectors [156] in the environment, effectively functioning as passive receivers [157]. Timing is important for all passive localization algorithms. The industry standard is the white rabbit algorithm developed by CERN [158], although other methods have been proposed [142].

2.4 Conclusion

Passive localization has been the topic of extensive research. This has led to a wide range of algorithms that can be employed to locate a transmitter based on TOA and/or AOA. Unfortunately, it can be quite difficult to recognize when two algorithms are using the same equations. Even with deliberate effort, it can be difficult to see the connection between the equations and the underlying geometric problem.

The field of passive localization could greatly benefit from one simple change to how equations are derived. Most papers start their derivations from noisy signal models, which means that the geometric solution is surrounded in a cloak of random vectors and statistical functions. This analysis is important for analyzing and optimizing the algorithm, but it is not necessary to produce the geometric solution.

Our review highlights the utility and adaptability of linear TOA, TDOA, AOA, and FDOA equations. These provide simple building blocks that can be employed to solve a wide range of problems in passive localization. The community was reluctant to use linear equations in this way[q], but the proliferation of papers employing these linear algorithms shows that they have come around to using linear equations to solve localization problems.

[q]Even the seminal works on linear algorithms [22, 119] are reluctant to use fully linear solutions, choosing instead to stop short and finish the solutions using quadratic equations.

Recognizing and understanding the linear equations used in a localization algorithm enables a more intuitive understanding of these algorithms. The equations describe vectors, which can be visualized in terms of the geometry of the scenario. This sort of intuitive understanding can help in avoiding stability issues when implementing localization algorithms.

3 Hybrid Multilateration and Triangulation

This chapter is composed from a paper entitled "Hybrid Multilateration and Triangulation" published in the journal *Positioning* [2]. I hereby confirm that the use of this article is compliant with all publishing agreements.

3.1 Introduction

A key application of multilateration-based localization is locating aircraft in flight. This scenario presents some distinct challenges, most notably that the receivers are typically all on or very close to the ground. In most cases, this will mean that they are very nearly coplanar. In TOA multilateration this creates an ambiguous geometry, where the target can lie above or below the ground, which can usually be resolved by checking the altitude of the aircraft. In TDOA multateration the problem is much more complex. Slight changes in the calculated transmitter offset t_u or transmitter offset pseudodistance $d_u = ct_u$ can produce valid position solutions at a wide range of altitudes above and below the ground, following a near-vertical line or hyperbolic curve. This is independent of algorithm, as the underlying geometry of the problem is unstable, regardless of the method used to solve it [37].

The most common way of resolving this issue in the literature is to simply calculate a 2-dimensional position, ignoring the vertical position entirely [140, 141, 143]. While 2-dimensional localization is acceptable in some applications, it can have serious negative implications for tracking and flight safety. Many recent papers addressing 3-dimensional multilateration, including a few cases of tracking cellular telephones [52, 55, 66], which are typically at or near ground level, include angle of arrival, include angle of arrival information as a way of improving the algorithm's performance [61, 72].

Our approach to mitigating the vertical uncertainty is to add vertical angle of arrival (AOA) measurements. Somewhat surprisingly, this is relatively uncommon in the literature. We were unable to find any papers that used only vertical AOA to improve localization performance, although there is a paper that uses only a single angle of arrival, oriented relative to an arbitrary axis, as part of its localization algorithm [127][a].

This chapter presents an algorithm that combines TDOA multilateration with a vertical AOA to produce a single set of linear equations for

[a] This is an approach that we considered as a generalization of the algorithm presented in this chapter. Ultimately, we decided that this generalization did not expand significantly enough on our earlier approach to warrant fleshing it out more.

determining the location of an unknown transmitter.

3.2 Algorithm

Let $\mathbf{p}_i = [\ x_i \quad y_i \quad z_i\ ]^{\mathrm{T}}, i = 1, 2, \ldots, N$ be the position of N receivers and $\mathbf{u} = [\ x_u \quad y_u \quad z_u\ ]^{\mathrm{T}}$ be the unknown position of a transmitter. The transmitter emits a signal at time t_u that is received at $\mathbf{p}_i$ at time t_i. For each receiver, a pseudo-distance $d_i = ct_i$ is calculated, where c is the speed of light. This pseudodistance is used instead of time in the positioning equations. For each $\mathbf{p}_i$, the angle of arrival of the transmitted signal relative to the $x - y$ plane, ϕ_i is measured. For any $\mathbf{p}_i$ and $\mathbf{p}_j$, the difference between the corresponding parameters is

$$a_i - a_j = \tilde{a}_{i,j}, \tag{3.1}$$

e.g. $\tilde{x}_{i,j} = x_i - x_j$. The vector $\tilde{\mathbf{p}}_{i,j} = \mathbf{p}_i - \mathbf{p}_j$ is the difference vector between the ith and jth receiver locations. The operation $\mathbf{a}' = [\ x_a \quad y_a\ ]^{\mathrm{T}}$ projects of $\mathbf{a}$ onto the xy plane, so that $\mathbf{a} = \left[\ \mathbf{a}'^{\mathrm{T}} \quad z_a\ \right]^{\mathrm{T}}$.

The following sections present the HM algorithm by first deriving a TDOA multilateration algorithm, and then incorporating the measured angle information.

3.2.1 TDOA multilateration-only

Linear equations for solving TDOA multilateration are given in [22]. This section presents a clearer derivation of those equations that is more suited for use in the later steps.

The distance between points $\mathbf{p}_i$ and $\mathbf{u}$ is

$$|\mathbf{u} - \mathbf{p}_i| = |d_u - d_i|. \tag{3.2}$$

Squaring both sides gives

$$|\mathbf{u}|^2 + |\mathbf{p}_i|^2 - 2\mathbf{u} \cdot \mathbf{p}_i = d_u^2 - 2d_u d_i + d_i^2 \tag{3.3}$$

where $\mathbf{a} \cdot \mathbf{b}$ is the dot product. This can be rearranged to yield

$$2\mathbf{u} \cdot \mathbf{p}_i - 2d_u d_i - |\mathbf{u}|^2 + d_u^2 = |\mathbf{p}_i|^2 - d_i^2. \tag{3.4}$$

This is almost linear in terms of the unknown values, but those unknown terms contribute the exact same $-|\mathbf{u}|^2 + d_u^2$ to the equation for each point. This means that they can be eliminated by taking the difference between the equations for two separate points. Taking that difference between the ith and jth equations gives

$$2\mathbf{u} \cdot \tilde{\mathbf{p}}_{i,j} - 2d_u \tilde{d}_{i,j} = |\mathbf{p}_i|^2 - |\mathbf{p}_j|^2 - d_i^2 + d_j^2. \tag{3.5}$$

These are the linear equations from [22], without the measurement error terms. It can be written in matrix form as

$$\mathbf{A}_M \bar{\mathbf{x}} = \mathbf{b}_M \tag{3.6}$$

where $\bar{\mathbf{x}} = \begin{bmatrix} \bar{x}_u & \bar{y}_u & \bar{z}_u & \bar{d}_u \end{bmatrix}^{\mathrm{T}}$ is an estimated value of the unknown values $\mathbf{u}$ and d_u,

$$\begin{aligned} \mathbf{A}_M &= \begin{bmatrix} 2\tilde{\mathbf{p}}'_{2,1} & -2\tilde{d}_{2,1} \\ \vdots & \vdots \\ 2\tilde{\mathbf{p}}'_{N,1} & -2\tilde{d}_{N,1} \end{bmatrix} \\ \mathbf{b}_M &= \begin{bmatrix} |\mathbf{p}_2|^2 - |\mathbf{p}_1|^2 - d_2^2 + d_1^2 \\ \vdots \\ |\mathbf{p}_N|^2 - |\mathbf{p}_1|^2 - d_N^2 + d_1^2 \end{bmatrix}. \end{aligned} \tag{3.7}$$

3.2.2 Vertical AOA-only

For this algorithm, a vertical AOA measurement is taken relative to the horizontal at one or more receivers, as shown in Fig. 3.1. If the measurement is error-free then a given value of ϕ_i places the target on a vertically-oriented cone.

The triangulation algorithm uses the measured values of the angle of the transmitter relative to vertical for each receiver, as shown in Fig. 3.1. Adding this one-dimensional triangulation to the multilateration equations can help to significantly improve the solution in the z direction.

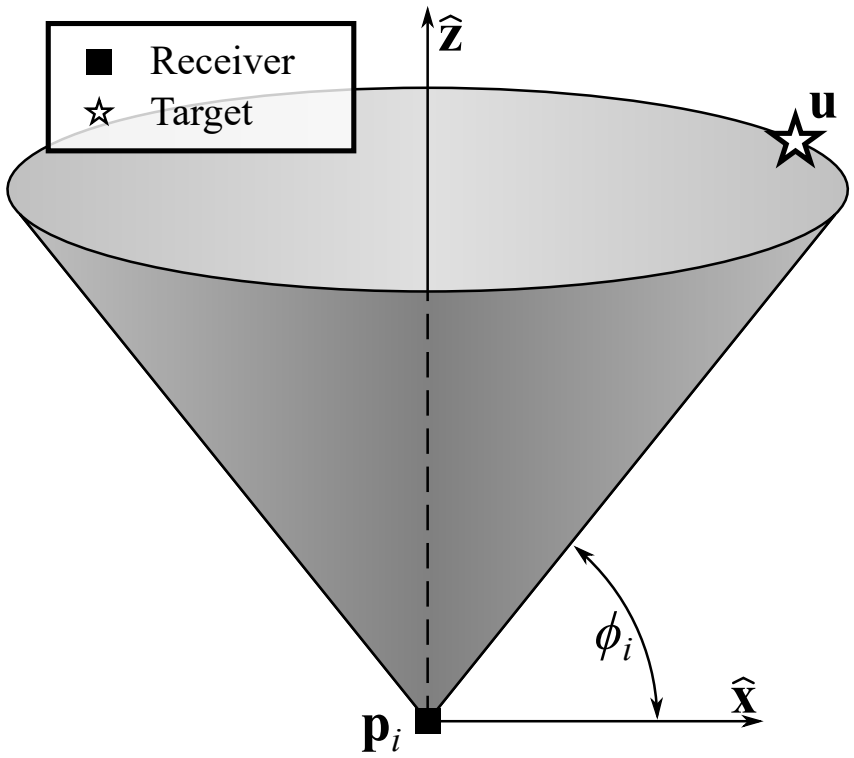

Figure 3.1: Angle measurement for vertical angle of arrival. The measured angle describes a cone containing the transmitter. Note that this figure is identical to Fig. 2.5.

The measured angle ϕ_i relates the distance $|\mathbf{p}_i - \mathbf{u}| = d_i - d_u$ and the difference in elevation $z_u - z_i$ as

$$z_u - z_i = (d_i - d_u) \sin \phi_i. \tag{3.8}$$

This can be rewritten as a linear equation of the unknown variables

$$z_u + d_u \sin \phi_i = z_i + d_i \sin \phi_i, \tag{3.9}$$

which has a matrix form

$$\mathbf{A}_T \bar{\mathbf{x}} = \mathbf{b}_T \tag{3.10}$$

where

$$\begin{aligned} \mathbf{A}_T &= \begin{bmatrix} 0 & 0 & 1 & \sin \phi_1 \\ \vdots & \vdots & \vdots & \vdots \\ 0 & 0 & 1 & \sin \phi_N \end{bmatrix} \\ \mathbf{b}_T &= \begin{bmatrix} z_1 + d_1 \sin \phi_1 \\ \vdots \\ z_N + d_N \sin \phi_N \end{bmatrix}. \end{aligned} \tag{3.11}$$

This is clearly not sufficient for determining $\mathbf{x}'$, but it can be combined with Eq. 3.6 to produce an augmented system of equations that combine TDOA multilateration and triangulation.

$$\begin{bmatrix} \mathbf{A}_M \\ \mathbf{A}_T \end{bmatrix} \bar{\mathbf{x}} = \begin{bmatrix} \mathbf{b}_M \\ \mathbf{b}_T \end{bmatrix}. \tag{3.12}$$

This is how combined TDOA/AOA localization is typically implemented, with linear TDOA equations concatenated with linear AOA equations into a single system of linear equations. In this paper, we go one step further to explicitly tie the z_u value to the triangulation.

3.2.3 Hybrid Multilateration/Triangulation

The hybrid multilateration and triangulation equations are derived by replacing the value z_u in Eq. 3.5 with the value for z_u from Eq. 3.9, producing an equation in terms of x_u, y_u, and d_u, so that

$$2\mathbf{u} \cdot \tilde{\mathbf{p}}'_{i,j} + 2\tilde{z}_{i,j} z_u - 2 d_u \tilde{d}_{i,j} = |\mathbf{p}_i|^2 - |\mathbf{p}_j|^2 - d_i^2 + d_j^2 \tag{3.13}$$

becomes

$$2\mathbf{u} \cdot \tilde{\mathbf{p}}'_{i,j} - 2 d_u \left(\tilde{z}_{i,j} \sin \phi_i + \tilde{d}_{i,j} \right) = |\mathbf{p}_i|^2 - |\mathbf{p}_j|^2 - d_i^2 + d_j^2 - \tilde{z}_{i,j} \left(z_i + d_i \sin \phi_i \right). \tag{3.14}$$

This equation combines multilateration in x and y with triangulation in z, all of which are tied to d_u. These equations are then combined into the hybrid matrix form

$$\mathbf{A}_H \bar{x} = \mathbf{b}_H \tag{3.15}$$

where

$$\mathbf{A}_H = \begin{bmatrix} 2\tilde{\mathbf{p}}'_{2,1} & 0 & -2\left(\tilde{z}_{2,1}\sin\phi_2 + \tilde{d}_{2,1}\right) \\ \vdots & \vdots & \vdots \\ 2\tilde{\mathbf{p}}'_{N,1} & 0 & -2\left(\tilde{z}_{N,1}\sin\phi_N + \tilde{d}_{N,1}\right) \end{bmatrix}$$
$$\mathbf{b}_H = \begin{bmatrix} |\mathbf{p}_2|^2 - |\mathbf{p}_1|^2 - d_2^2 + d_1^2 - 2\tilde{z}_{2,1}\left(z_2 + d_2\sin\phi_2\right) \\ \vdots \\ |\mathbf{p}_N|^2 - |\mathbf{p}_1|^2 - d_N^2 + d_1^2 - 2\tilde{z}_{N,1}\left(z_N + d_N\sin\phi_N\right) \end{bmatrix}. \tag{3.16}$$

The hybrid multilateration equations of Eq. 3.15 are concatenated with the matrices from Eq. 3.12.

$$\begin{bmatrix} \mathbf{A}_H \\ \mathbf{A}_T \end{bmatrix} \bar{\mathbf{x}} = \begin{bmatrix} \mathbf{b}_H \\ \mathbf{b}_T \end{bmatrix}. \tag{3.17}$$

This can be solved using any linear algebra pseudoinverse such as least squares (LS) or weighted least squares (WLS). In most localization algorithms, WLS is employed to minimize the effects of uncertainty of the measurement error on the calculated position[b]. In this case, given that the norms of the rows in $\mathbf{A}_H$ are typically orders of magnitude larger than the norms in the rows of $\mathbf{A}_T$, it is essential to use WLS to bring the rows into roughly the same scale. The next section provides a statistical basis for choosing a good weighting for weighted least squares.

[b] In most cases, the weighting matrix is calculated from the variances of the measurement errors, which are all uniform. This means that the weighting matrix is equivalent to the identity matrix.

3.3 Optimal weighted least squares

To understand the behavior of this algorithm, we must consider the effect of measurement error on its performance. Let the measured pseudodistance be

$$d_i = \hat{d}_i + n_i \tag{3.18}$$

where d_i is the measured pseudodistance at $\mathbf{p}_i$, $\hat{d}_i$ is the noise-free pseudodistance, and n_i is a zero-mean, uncorrelated Gaussian random variable with variance $\sigma^2_{d,i}$. Similarly, let

$$\phi_i = \hat{\phi}_i + m_i \tag{3.19}$$

where ϕ_i is the measured elevation angle at $\mathbf{p}_i$, $\hat{\phi}_i$ is the noise-free elevation angle, and m_i is a zero-mean Gaussian random variable with variance $\sigma^2_{\phi,i}$. These can be written in vector form as

$$\mathbf{d} = \hat{\mathbf{d}} + \mathbf{n} \tag{3.20}$$

and

$$\boldsymbol{\Psi} = \hat{\boldsymbol{\phi}} + \mathbf{m} \tag{3.21}$$

where $\hat{\mathbf{d}} = \begin{bmatrix} \hat{d}_1 & \dots & \hat{d}_N \end{bmatrix}^{\mathrm{T}}$, $\mathbf{n} = \begin{bmatrix} n_1 & \dots & n_N \end{bmatrix}^{\mathrm{T}}$, $\hat{\boldsymbol{\phi}} = \begin{bmatrix} \hat{\phi}_1 & \dots & \hat{\phi}_N \end{bmatrix}^{\mathrm{T}}$, and $\mathbf{m} = \begin{bmatrix} m_1 & \dots & m_N \end{bmatrix}^{\mathrm{T}}$. These noise vectors have covariance matrices

$$\mathrm{E}(\mathbf{n}\mathbf{n}^{\mathrm{T}}) = \mathbf{Q}_n = \begin{bmatrix} \sigma_{d,1} & \mathbf{0}_{(1\times N-1)} \\ \mathbf{0}_{N-1\times 1} & \mathbf{Q}'_n \end{bmatrix} \tag{3.22}$$

and

$$\mathrm{E}(\mathbf{m}\mathbf{m}^{\mathrm{T}}) = \mathbf{Q}_\phi \tag{3.23}$$

where $\mathbf{Q}'_n = \mathrm{E}(\mathbf{n}'\mathbf{n}'^{\mathrm{T}})$, and $\mathbf{n}' = [n_2, \dots, n_N]^{\mathrm{T}}$.

The effects of noise on the system can be found by considering the weighted residue vector

$$\boldsymbol{\psi} = \begin{bmatrix} \mathbf{W}_H & \mathbf{0} \\ \mathbf{0} & \mathbf{W}_T \end{bmatrix} \left(\begin{bmatrix} \mathbf{b}_H \\ \mathbf{b}_T \end{bmatrix} - \begin{bmatrix} \mathbf{A}_H \\ \mathbf{A}_T \end{bmatrix} \bar{\mathbf{x}} \right) \tag{3.24}$$

where $\mathbf{W}_H = \mathrm{diag}(w_{H,2}, \dots, w_{H,N})$ and $\mathbf{W}_T = \mathrm{diag}(w_{T,1}, \dots, w_{T,N})$ are diagonal weighting matrices. If the measurements are noise-free then $\boldsymbol{\psi} = \mathbf{0}$. The effects of noise can be found by breaking down $\mathbf{A}_H$, $\mathbf{A}_T$, $\mathbf{b}_H$, and $\mathbf{b}_T$ into noisy and noise-free components by substituting Eqs. 3.20 and 3.21 into Eqs. 3.16 and 3.11. To simplify the resulting equations, we consider the value of $\sin\phi_i$ for when m_i is small.

$$\begin{aligned} \sin\phi_i &= \sin\left(\hat{\phi}_i + m_i\right) \\ &= \sin\hat{\phi}_i \cos m_i + \cos\hat{\phi}_i \sin m_i \\ &\approx \sin\hat{\phi}_i + m_i \cos\hat{\phi}_i. \end{aligned} \tag{3.25}$$

This gives

$$\begin{aligned} \mathbf{A}_H &\approx \hat{\mathbf{A}}_H + \begin{bmatrix} 0 & 0 & 0 & -2m_2\tilde{z}_{2,1}\cos\hat{\phi}_2 - 2(n_2 - n_1) \\ \vdots & \vdots & \vdots & \vdots \\ 0 & 0 & 0 & -2m_N\tilde{z}_{N,1}\cos\hat{\phi}_N - 2(n_N - n_1) \end{bmatrix} \\ \mathbf{A}_T &\approx \hat{\mathbf{A}}_T + \begin{bmatrix} 0 & 0 & 0 & m_1\cos\hat{\phi}_1 \\ \vdots & \vdots & \vdots & \vdots \\ 0 & 0 & 0 & m_N\cos\hat{\phi}_n \end{bmatrix} \\ \mathbf{b}_H &\approx \hat{\mathbf{b}}_H + \begin{bmatrix} -2\hat{d}_2 n_2 - n_2^2 + 2\hat{d}_1 n_1 + n_1^2 \\ \vdots \\ -2\hat{d}_N n_N - n_N^2 + 2\hat{d}_1 n_1 + n_1^2 \end{bmatrix} + \\ &\quad \begin{bmatrix} -2\tilde{z}_{2,1}(n_2\sin\hat{\phi}_2 + (\hat{d}_2 + n_2)m_2\cos\hat{\phi}_2)) \\ \vdots \\ -2\tilde{z}_{N,1}(n_N\sin\hat{\phi}_N + (\hat{d}_N + n_N)m_N\cos\hat{\phi}_N)) \end{bmatrix} \end{aligned} \tag{3.26}$$

[c] The fact that the noise-free measurements produce a residue of zero can be seen in two ways. First, if the noise terms are all zero then the equations describe $\bar{\mathbf{x}}$ exactly. Second, the expected value of the noisy terms in Eq. 3.26 are all zero as long as the time or distance measurement error is has an average value of zero with the same variance at all points.

Applying these to Eq. 3.24 and using the fact that the noise-free measurements produce a residue of $\boldsymbol{\psi} = \mathbf{0}$[c], the residue can be written as

$$\begin{aligned}\boldsymbol{\psi} = \sum_{i=2}^{N} w_{H,i} \Big[2\tilde{z}_{i,1} \left(d_u m_i \cos\hat{\phi}_i - n_i \sin\hat{\phi}_i - (\hat{d}_i + n_i) m_i \cos\hat{\phi}_i \right) + \\ 2d_u(n_i - n_1) - 2\hat{d}_i n_i - n_i^2 + 2\hat{d}_1 n_1 + n_1^2 \Big] + \\ \sum_{i=1}^{N} w_{T,i} \left[n_i \sin\hat{\phi}_i + (\hat{d}_i + n_i) m_i \cos\hat{\phi}_i - d_u m_i \cos\hat{\phi}_i \right]\end{aligned} \tag{3.27}$$

The optimal weights weighted least squares are the weights such that the expected value $\boldsymbol{\Psi} = E\left[\boldsymbol{\psi}\boldsymbol{\psi}^{\mathrm{T}}\right] \approx \mathbf{I}$. While this can be done with some mathematical rigor, the same result can be achieved intuitively by examining Eq. 3.27 and considering the square of each sum term[d]. For this analysis, we assume that

$$\begin{aligned} |\tilde{z}_{i,1}| < |d_u| < |\hat{d}_i| \\ \sigma_{\phi,i}^2 \cos^2\hat{\phi}_i \ll \sigma_{d,i}^2. \end{aligned} \tag{3.28}$$

[d]There are several issues with this approach, most notably that the hybrid terms all include n_1, which means that there will be some non-zero cross-correlation between those equations. For this derivation we ignore this cross correlation. For weighting matrices, findinging the correct magnitude is more important than obtaining an exact value.

For the $w_{H,i}$ terms, the dominant contributors to $\boldsymbol{\Psi}$ are the $-2\hat{d}_i n_i + 2\hat{d}_1 n_1$ terms. The expected value of those terms within $\boldsymbol{\Psi}$ is $4w_{H,i}^2\sigma_{d,i}^2(\hat{d}_i^2 + \hat{d}_1^2) \approx 8w_{H,i}^2\sigma_{d,i}^2\hat{d}_i^2$. Since this should be approximately equal to 1, we find that

$$w_{H,i} \approx \frac{1}{\sqrt{8}\sigma_{d,i}\hat{d}_i}. \tag{3.29}$$

For the $w_{T,i}$ terms, the dominant contributor to $\boldsymbol{\Psi}$ is the $w_{T,i}\hat{d}_i m_i \cos\hat{\phi}_i$ term. The expected value of this term within $\boldsymbol{\Psi}$ is $w_{T,i}^2\hat{d}_i^2\sigma_{\phi,i}^2\cos^2\hat{\phi}_i$. Since this should be approximately equal to 1, we find that

$$w_{T,i} \approx \frac{1}{\hat{d}_i\sigma_{\phi,i}\cos\hat{\phi}_i}. \tag{3.30}$$

When the values of d_i and z_i are all roughly the same and $z_i \approx z_u$, the weights can be further simplified. In that case, the $\hat{d}_i$ terms are all equal and can be omitted, and the $\cos\hat{\phi}_i \approx 1$, giving a weighting matrix of

$$\mathbf{W} = \mathrm{diag}\left(\frac{1}{\sqrt{8}\sigma_{d,2}}, \ldots, \frac{1}{\sqrt{8}\sigma_{d,N}}, \frac{1}{\sigma_{\phi,1}}, \ldots, \frac{1}{\sigma_{\phi,1}} \right). \tag{3.31}$$

These approximations only apply when the inequalities of Eq. 3.28 hold. When they do not, and in particular when $\sigma_{\phi,i}^2$ is not several orders of magnitude smaller than $\sigma_{d,i}$, then better weighting coefficients are given

by

$$w_{H,i} = \left| \tilde{z}_{i,1} \left[(d_u - \hat{d}_i - \sigma_{d,i})\sigma_{\phi,i} \cos\hat{\phi}_i - \sigma_{d,i} \sin\hat{\phi}_i \right] + (d_u - \hat{d}_i)\sigma_{d,i} - (d_u - \hat{d}_1)\sigma_{d,1} - (\sigma_{d,i}^2 - \sigma_{d,1}^2)/2 \right|^{-1} \tag{3.32}$$

$$w_{T,i} = \left| \sigma_{d,i} \sin\hat{\phi}_i + (\hat{d}_i + \sigma_{d,i} - d_u)\sigma_{\phi,i} \cos\hat{\phi}_i \right|^{-1}.$$

In calculating the weights using Eq. 3.32, the measured values can generally be used instead of the noise-free values. The unknown value d_u can be set to 0, approximated as being roughly equal to the d_i or $|\mathbf{p}_i|$ values, or estimated by solving the equations with less optimal weights.

Note that these derivations are quite rough. This is intentional. The key to a successful application of weighted least squares is to weight the equations based on how much information they contribute to the overall problem. Without any additional information about the quality of each equation, the best weighted least squares is one that has every equation contribute the same amount to the overall solution. This means that each equation should be scaled to the point that their magnitudes are roughly equal. This matches the results of every weighted least squares analysis that I have observed in the literature. Relevantly, the result in Eq. 3.29 is consistent with the weights given in [22] and the result in Eq. 3.30 is consistent with the weights given in [105]. The results are not very sensitive to small changes in the weighting matrix. As long as the weighting matrix scales $\mathbf{A}_T$ and $\mathbf{b}_T$ more than it scales $\mathbf{A}_H$ and $\mathbf{b}_H$ by a factor that is roughly the same magnitude as the average value of $|\mathbf{p}_i - \mathbf{p}_1|$, the solution is statistically indistinguishable from a solution prepared using a more precisely calculated weighting matrix.

3.4 Stability

Multilateration algorithms are sensitive to the positions where the measurements are taken. If the reference point locations are not sufficiently distributed, then the algorithm can fail. This is a problem with terrestrial multilateration systems that are tracking aircraft over a large area. In a system, the reference points are likely to be approximately coplanar, which makes it difficult for a multilateration algorithm to distinguish between points that are at orthogonally opposite positions relative to that plane.

In analyzing the algorithm, we are primarily concerned with scenarios where the reference points are coplanar or nearly coplanar. For most scenarios the transmitter is not in the same plane. The stability of the approach depends on the stability of the matrix $\left(\mathbf{A}^{\mathrm{T}}\mathbf{A}\right)^{-1}$, where $\mathbf{A} = \begin{bmatrix} A_H^{\mathrm{T}} & A_T^{\mathrm{T}} \end{bmatrix}^{\mathrm{T}}$, given by

$$\begin{bmatrix} 4\tilde{x}_{i,0}^2 & 4\tilde{x}_{i,0}\tilde{y}_{i,0} & 0 & -\tilde{x}_{i,0}(\tilde{d}_{i,0}+\tilde{z}_{i,0}\cos\phi_i) \\ 4\tilde{x}_{i,0}\tilde{y}_{i,0} & 4\tilde{y}_{i,0}^2 & 0 & -\tilde{y}_{i,0}(\tilde{d}_{i,0}+\tilde{z}_{i,0}\cos\phi_i) \\ 0 & 0 & 0 & 0 \\ -\tilde{x}_{i,0}(\tilde{d}_{i,0}+\tilde{z}_{i,0}\cos\phi_i) & -\tilde{y}_{i,0}(\tilde{d}_{i,0}+\tilde{z}_{i,0}\cos\phi_i) & 0 & (\tilde{d}_{i,0}+\tilde{z}_{i,0}\cos\phi_i)^2 \end{bmatrix} + \begin{bmatrix} 0 & 0 & 0 & 0 \\ 0 & 0 & 0 & 0 \\ 0 & 0 & 1 & \cos\phi_i \\ 0 & 0 & \cos\phi_i & \cos^2\phi_i \end{bmatrix}. \tag{3.33}$$

The following sections analytically demonstrate the instability of the algorithm for a few specific special cases of receiver layouts. It also considers several other receiver configurations to gain insight into the stability of the algorithm.

3.4.1 Linear Deployment

If the receivers are in a line where $x_i = x_j \forall i, j$ then the first row and column of $\mathbf{A}^{\mathrm{T}}\mathbf{A}$ are uniformly zero, and $\mathbf{A}^{\mathrm{T}}\mathbf{A}$ has no inverse. The same holds for when $y_i = y_j \forall i, j$, which leads to all zeros in the second row and column.

For other linear arrangements, consider a line of receivers located at $(x_i, y_i, z_i) = (ak_i + x_0, bk_i + x_0, z_i)$ for some $a, b, k_1, \ldots, k_n$ where k_i is a scalar representing the location of the receiver on the line. Then $\tilde{x}_{i,0} = ak_i$ and $\tilde{y}_{i,0} = bk_i$. Let $K = \sum k_i^2$. Then

$$\mathbf{A}^{\mathrm{T}}\mathbf{A} = \begin{bmatrix} 4a^2K & 4abK & 0 & -\sum_i ak_i\tilde{d}'_{i,0} \\ 4abK & 4b^2K & 0 & -\sum_i bk_i\tilde{d}'_{i,0} \\ 0 & 0 & N & \sum_i \cos\phi_i \\ -\sum_i ak_i\tilde{d}'_{i,0} & -\sum_i bk_i\tilde{d}'_{i,0} & \sum_i \cos\phi_i & \sum_i \left(\cos^2\phi_i + \tilde{d}'_{i,0}\right) \end{bmatrix} \tag{3.34}$$

where $\tilde{d}'_{i,0} = \tilde{d}_{i,0} + \tilde{z}_{i,0}\cos\phi_i$. The first two columns of that matrix are $a\mathbf{x}$ and $b\mathbf{x}$ where

$$\mathbf{x} = \begin{bmatrix} 4aK & 4bK & 0 & -\sum_i k_i\tilde{d}'_{i,0} \end{bmatrix}^{\mathrm{T}}. \tag{3.35}$$

This means that those two columns are not linearly independent and that $\mathbf{A}^{\mathrm{T}}\mathbf{A}$ is deficient. Therefore any linear arrangement of sensors produces a deficient $\mathbf{A}^{\mathrm{T}}\mathbf{A}$ matrix.

3.4.2 Circular Deployment

Let the receivers be located on a circle, such that the location of each sensor is $(\hat{x} + r\cos\phi_i, \hat{y} + r\sin\phi_i, \hat{z})$, and the transmitter located at $(\hat{x}, \hat{y}, z_s)$. The values of $\tilde{d}_{i,s} = \sqrt{r^2 + (z - \hat{z})^2} + d_s$ are the same for all of the sensors, so that $\tilde{d}_{i,0} = 0$. Similarly, $\tilde{z}_{i,0} = 0$ for all sensors. Since the horizontal and vertical distance from the transmitter to each sensor is the same,

$$\phi_i = \tan^{-1}\frac{z_s - \hat{z}}{r}$$

is the same for all sensors. This results in

$$\begin{aligned}
\mathbf{A}^{\mathrm{T}}\mathbf{A} &= \sum_{i=1}^{N} \begin{bmatrix} 4\tilde{x}_{i,0}^2 & 4\tilde{x}_{i,0}\tilde{y}_{i,0} & 0 & -\tilde{x}_{i,0} \\ 4\tilde{x}_{i,0}\tilde{y}_{i,0} & 4\tilde{y}_{i,0}^2 & 0 & -\tilde{y}_{i,0} \\ 0 & 0 & 1 & \cos\phi_i \\ -\tilde{x}_{i,0}(0+0\cos\phi_i) & -\tilde{y}_{i,0}(0+0\cos\phi_i) & \cos\phi_i & \cos^2\phi_i \end{bmatrix} \\
&= \sum_{i=1}^{N} \begin{bmatrix} 4\tilde{x}_{i,0}^2 & 4\tilde{x}_{i,0}\tilde{y}_{i,0} & 0 & 0 \\ 4\tilde{x}_{i,0}\tilde{y}_{i,0} & 4\tilde{y}_{i,0}^2 & 0 & 0 \\ 0 & 0 & 1 & \cos\phi_i \\ 0 & 0 & \cos\phi_i & \cos^2\phi_i \end{bmatrix} \\
&= \begin{bmatrix} \sum_{i=1}^{N} 4\tilde{x}_{i,0}^2 & \sum_{i=1}^{N} 4\tilde{x}_{i,0}y_{i,0} & 0 & 0 \\ \sum_{i=1}^{N} 4\tilde{x}_{i,0}y_{i,0} & \sum_{i=1}^{N} 4\tilde{y}_{i,0}^2 & 0 & 0 \\ 0 & 0 & N & N\cos\phi_0 \\ 0 & 0 & N\cos\phi_0 & N\cos^2\phi_0 \end{bmatrix}
\end{aligned} \tag{3.36}$$

The third and fourth columns are equal to $N[\ 0 \quad 0 \quad 1 \quad \cos\phi_0\ ]^{\mathrm{T}}$ and $N\cos\phi_0[\ 0 \quad 0 \quad 1 \quad \cos\phi_0\ ]^{\mathrm{T}}$, so the columns of $\mathbf{A}^{\mathrm{T}}\mathbf{A}$ are linearly dependent and $\mathbf{A}^{\mathrm{T}}\mathbf{A}$ is deficient.

Therefore, an arrangement of receivers on a circle cannot produce a solution when the transmitter is located exactly equidistant from the receivers at the center of the circle. This holds whether the receivers are evenly or unevenly spaced, and whether the receivers are around the whole circle or located exclusively along an arc of the circle. This pole of instability is only present when the transmitter is at the center of the circle. As the transmitter moves away from the center of the circle the instability disappears.

The behavior of the HM algorithm with a circular configuration of receivers can be seen in Fig. 3.2. The HM algorithm is compared to a similar algorithm that only uses multilateration (ML) [27]. Both plots show the deviation as a function of transmitter position relative to the receivers at the positions shown. Gaussian error with a standard deviation of 1 m was added to the true pseudodistances and a Gaussian error with a standard deviation of 1° was added to the true elevation values.[e] Note that the scales are different for the two images.

This shows a problem with using a multilateration algorithm in that scenario that needs to be corrected to give realistic comparable results between the two algorithms. A comparison of the scales in Fig. 3.2 shows that HM algorithm out-performs the ML algorithm by at least 60 dB meters, which is a factor of 1,000,000:1. This is due to the fact that the receivers were coplanar. In any algorithm that relies solely on multilateration, having all of the reference points in a single plane creates an ambiguity. The algorithm cannot distinguish between points above the plane and points below the plane. To resolve this the simulations were performed using receiver locations with $\sigma_z = 20$ m of Gaussian random variation added to their height. This is the near-coplanar configuration used in all of the remaining simulations in this paper. The results are

[e] Additionally, a Gaussian error with a standard deviation of 100 m was added to the pseudodistances used by the HM algorithm. This term did not affect the results because it was constant across all of the pseudodistances and therefore cancelled when the $\tilde{d}_{i,j}$ terms were calculated.

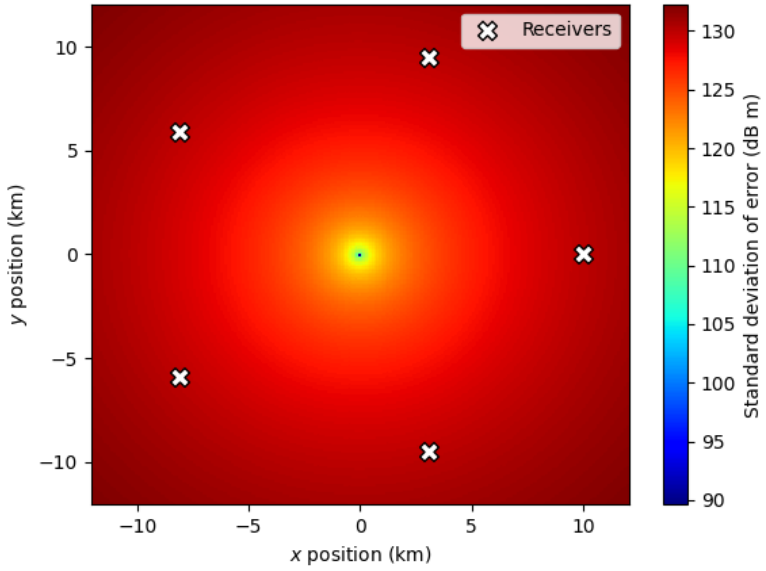

(a) ML

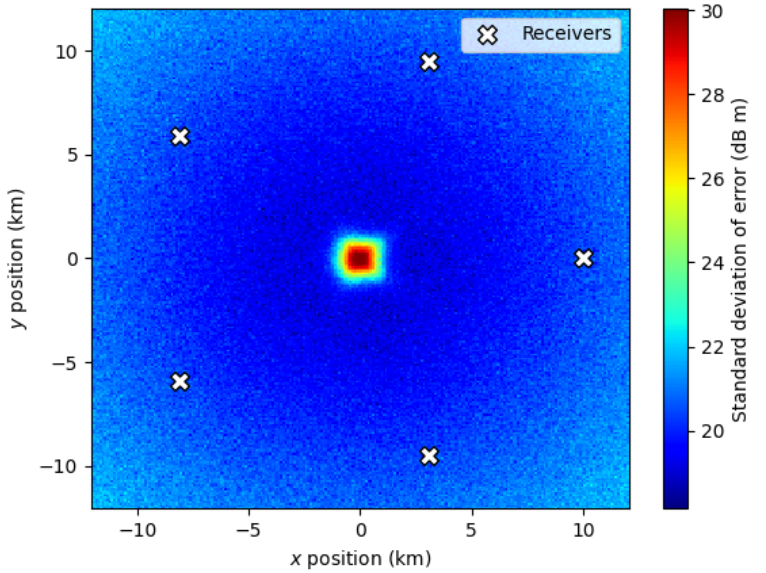

(b) HM

Figure 3.2: Standard deviation of a multilateration (ML) algorithm and the hybrid multilateration (HM) algorithm error as a function of transmitter location with coplanar receivers. The ML algorithm has sizeable error with all receivers on the same plane. It cannot distinguish between transmitters with a positive z coordinate and those with a negative z coordinate. Note that the two figures use different scales for the standard deviation of the error.

shown in Fig. 3.3. The HM algorithm still produces significantly lower error except at its point of instability.

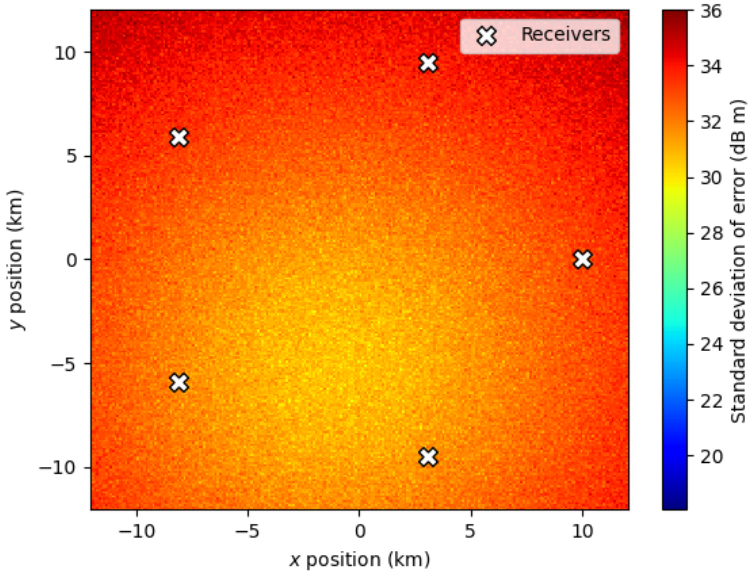

(a) ML

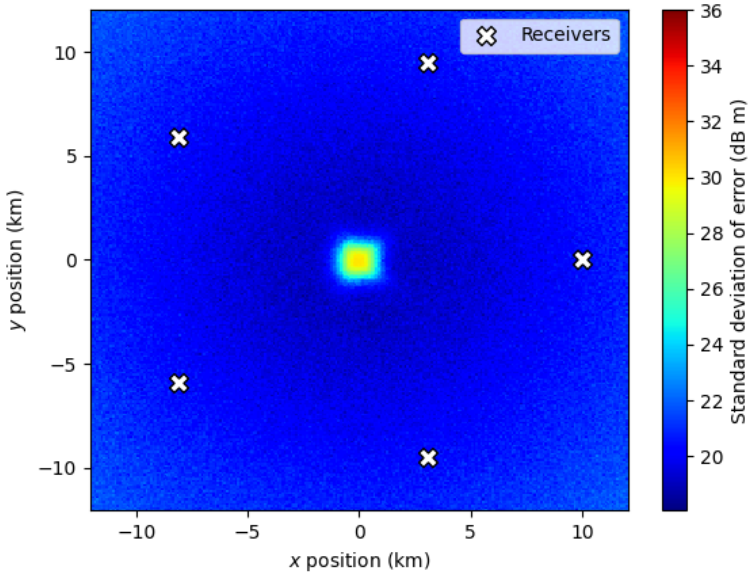

(b) HM

Figure 3.3: Standard deviation of ML and HM algorithm error as a function of transmitter location with near-coplanar receivers. The ML error is about 6 to 10 times larger at all points apart from the center where the HM algorithm is unstable.

The choice of $\sigma_z = 20\,\text{m}$ is based on the underlying scenario that the ground level varies by less than 20 m. The performance of both

algorithms is affected by this vertical perturbation of receiver positions, but for small variation of height only the ML algorithm is significantly affected. A plot of the position error as a function of σ_z is shown in Fig. 3.4. Accuracy of the ML algorithm increases as the vertical separation between receivers increases. The HM algorithm performs equally well across a range of local topological variation. This means that the HM algorithm performs better than the ML algorithm when the receivers are more planar and the ML performs better when the receivers have significant vertical variation. In the scenario analyzed in Fig. 3.4 the vertical relief must have a standard deviation of about $\sigma_z = 500$ meters (27 dB meters) before the two algorithms perform equally well. The near-coplanar simulations in this paper use vertical standard deviation of $\sigma_z = 20$ meters (13 dB meters).

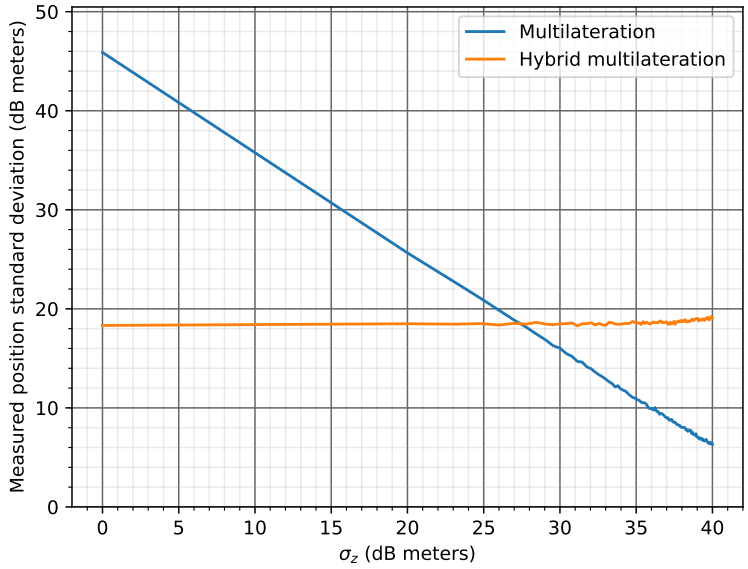

Figure 3.4: Algorithm comparison as a function of vertical variance using a central receiver in the same configuration shown in Fig. 3.6 with the transmitter directly above the central receiver.

Moving one of the sensors outward from the circle by a small distance creates two poles of instability along the axis that contains the point that was moved. Moving one sensor inward by a small distance creates two poles of instability that are located on a line perpendicular to the axis that contains the point that was moved. Plots of the convergence are shown in Fig. 3.5. This shows that small changes from a strictly circular configuration aren't enough to remove the instability.

The circular non-convergence problem can be resolved by moving one of the sensors to the center of the circle and rearranging the other sensors evenly around a circle. This eliminates the pole of instability at the center of the circle, as shown in Fig. 3.6. The HM algorithm performs better than the ML algorithm in this configuration, producing errors less

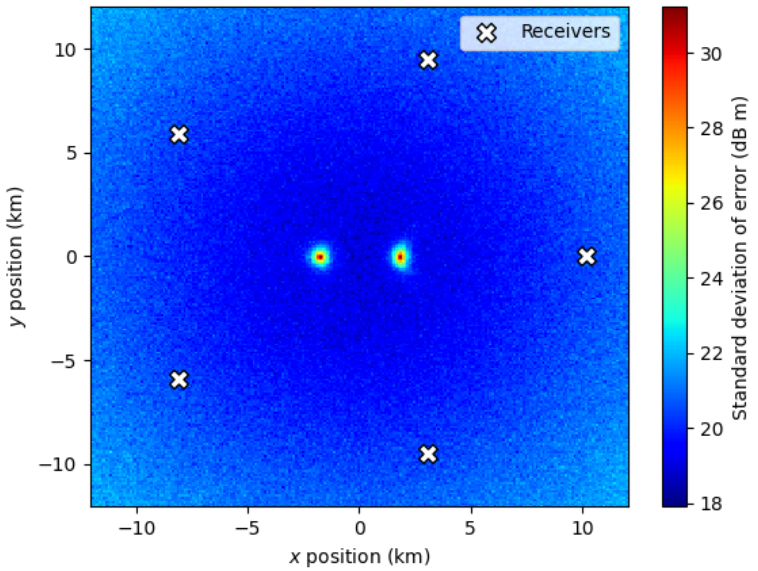

(a) Receiver moved outward

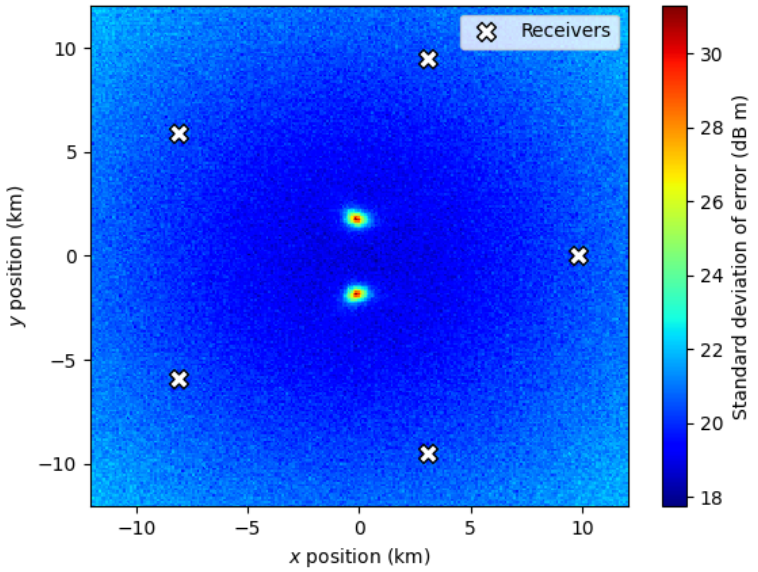

(b) Receiver moved inward

Figure 3.5: Standard deviation of the HM algorithm error. The right-most point is displaced 400 m in the x-direction from the circle containing the other points. This shows that the HM algorithm still has points of instability when small changes are made to the circular receiver configuration.

than 5% of the ML algorithm errors at most points.

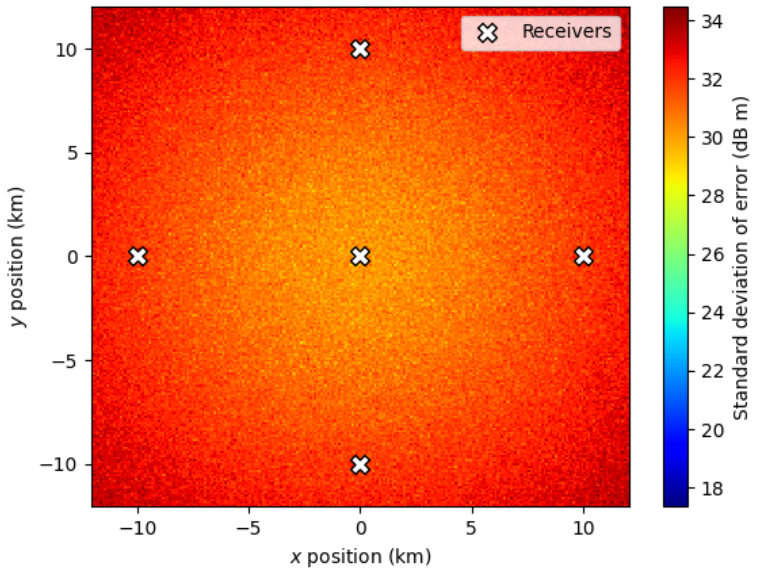

(a) ML

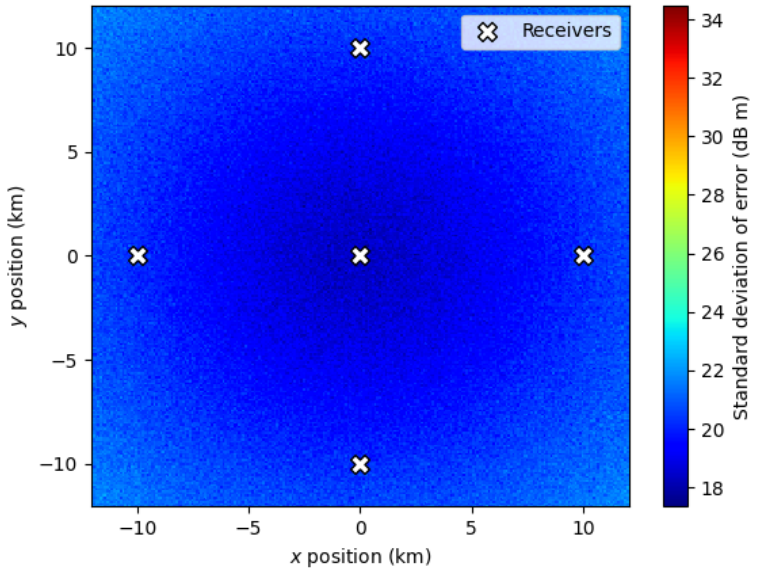

(b) HM

Figure 3.6: Comparison of the standard deviation of the ML and HM algorithm error for near-coplanar receivers with a central receiver. The HM algorithm no longer has a point of instability. The ML error is 10 times larger than the HM error at every point.

3.4.3 Other Receiver Configurations

Circular or near-circular receiver arrangements are undesirable because they create a pole of instability. This instability isn't present in other receiver configurations. This section considers the stability of the HM algorithm with other receiver configurations.

A delta, or V, configuration places the receivers along two lines that meet at a point. This works relatively well with the ML algorithm, which performs roughly the same as it did in the circular configurations. With the HM algorithm this configuration induces a line of relative instability in the direction that the V is pointing, as shown in Fig. 3.7. The HM algorithm still out-performs the ML algorithm, producing about 10% as much error even in the places where it was not performing as well.

Another configuration is a wye or Y configuration. This consists of a central point and the receivers placed on three lines radiating outward from the center. The Y configuration is very similar to the circular configuration with a receiver in the center, as seen in Fig. 3.8. The HM algorithm produces significantly less error at every point.

The performance of the scenarios in this section and Fig. 3.9 is summarized in Table 3.1. Note that these ranges include the values from outside the sensor perimeter.

Scenario	Fig	ML min	ML max	HM min	HM max
Circular	3.3	29.1	36.1	18.0	30.1
Circular (outward)	3.5a	—	—	17.9	31.8
Circular (inward)	3.5b	—	—	18.0	32.0
Eye	3.6	28.9	34.5	17.3	22.4
Delta	3.7	26.8	34.8	15.4	24.3
Wye	3.8	29.1	39.3	15.3	22.6
Lattice	3.9	25.8	41.0	17.0	24.5

Table 3.1: Range of error in the scenarios presented in this section. All values are standard deviation of error and are given in dB meters.

3.5 Implementation Factors

A number of factors should be taken into consideration when implementing the HM algorithm. They include the desired coverage area, the number and location of receivers, and the utilization of those receivers in the calculations. Each of these are addressed in the following section.

The HM algorithm works best when the transmitter is located somewhere between the receivers. As such, the optimal arrangement is to have receivers surrounding the area of interest.

3.5.1 Coverage Area

The coverage area places some requirements or constraints on the employment of this algorithm. The algorithm is built around the assumption that all of the angles are measured relative to a common vertical direction. This can be a problem if the coverage area gets wide enough

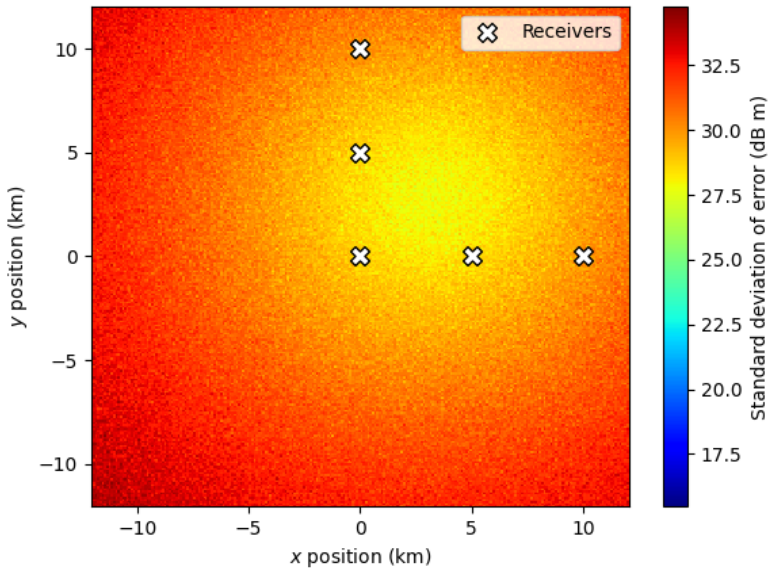

(a) ML

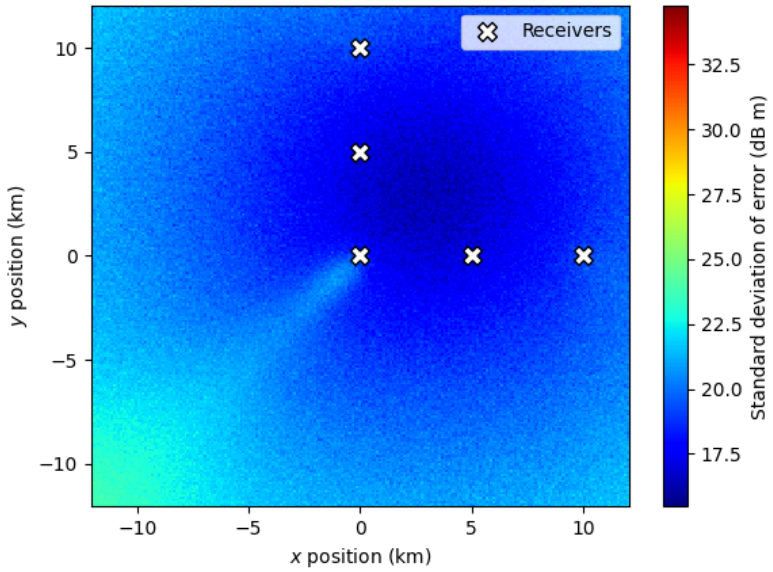

(b) HM

Figure 3.7: Comparison of the standard deviation of the ML and HM algorithm error for near-coplanar receivers in a delta configuration. The HM algorithm performs well over most of the area, but is relatively unstable as the transmitter moves away from the receivers in one direction. It still outperforms the ML algorithm at every point.

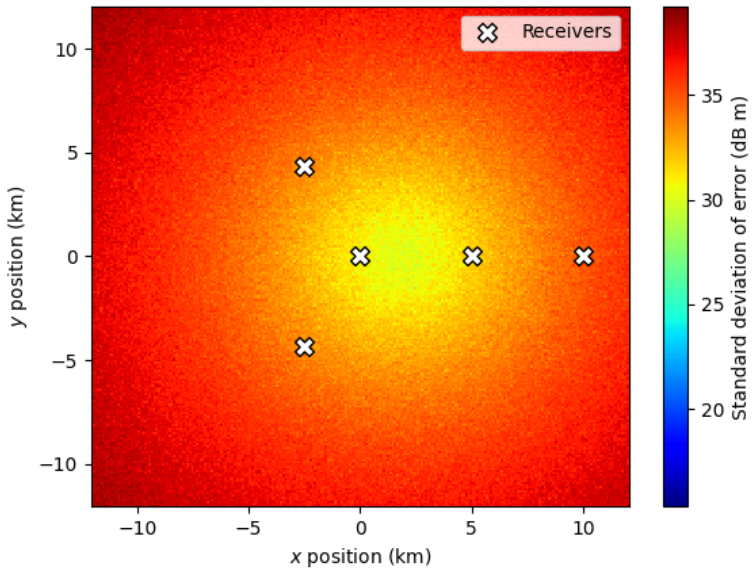

(a) ML

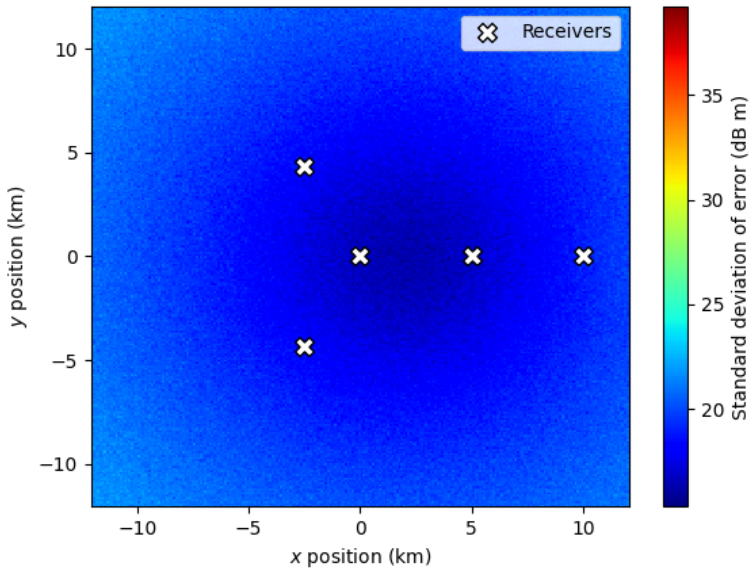

(b) HM

Figure 3.8: Comparison of the standard deviation of the ML and HM algorithm error for near-coplanar receivers in a Y configuration. The HM algorithm performs better at every point.

for the curvature of the Earth to start introducing error into the angle measurements. The two solutions to this are to limit the coverage area or to orient the receivers to a shared vertical that may be different from the local vertical.

The alternative is to orient all the sensors so that they measure angle with respect to parallel vertical axes. This presents a significant challenge installing and maintaining the receiver antennas as it is relatively easy to measure whether an object is aligned to vertical and difficult to align it to a specific deviation from vertical. In a wide area deployment the receivers need to be aligned to an angle that is slightly off from vertical or bias is introduced to the resulting measured angles which produces more position error from the algorithm.

The size of a limited coverage area affects the accuracy of the calculated position. An inherent problem with triangulation is that triangulation errors are proportional to the error in measuring the angle and to the distance from the vertex of the measured angles. This triangulation error must be considered when determining the size of the coverage area and the spacing of sensors within it. A denser deployment of sensors allows for more angular error because the distance from transmitter to receiver does not contribute as much to the overall triangulation error. Receivers deployed less than 44 km apart have less than 1° difference in their local vertical direction which may be sufficient for a given application, depending on the tolerance for angular error.

Coverage area can also be expanded by using a wider array of receivers and then only including the closest measurement to the transmitter, determined by the time of arrival of the signal, in the calculations. This keeps the triangulation error in any given calculation small while allowing for a larger coverage area at the expense of requiring more receivers.

3.5.2 Receiver positions

The stability analysis in Section 4.3 demonstrated that the algorithm works best when the transmitter is within a polygon surrounding the receivers. Some coverage outside that boundary may be possible, any positions calculated outside the perimeter contain additional error due to the geometric problems with multilateration and the fact that a fixed angular measurement produces more error the farther it is from the point of measurement.

Spacing of sensors affects the accuracy of the algorithm. The inclusion of triangulation in the algorithm means that more distance between the transmitter and receiver induces a larger position error for the same angle error. The optimal spacing depends on the accuracy of angular measurements and the required positional accuracy.

3.5.3 Number of Receivers

The best performance is achieved when the transmitter is inside the perimeter created by the receivers. The performance is also affected by

the spacing between the receivers. These two constraints will dictate the number of receivers required.

The most efficient spacing may be an equilateral triangular lattice pattern, which puts receivers close to any transmitter within its coverage area. A plot of this type of scenario and the resulting stability is shown in Fig. 3.9. The simulations show that this lattice arrangement gives consistent coverage over the area bounded by the sensors, with less stable responses outside of that area.

3.5.4 Selection of Sensors

The HM algorithm requires at least 5 receivers to accurately calculate the position of a transmitter. If a system has more than 5 receivers then there are three options for dealing with the extra sensors.

- The extra sensors can be omitted from the calculations. In this case, the sensors with the highest signal-to-noise ratio are typically the best ones to use in the calculation.
- The extra sensors can be included in the calculations. The algorithm can easily accommodate additional measurements. If there is error in the extra measurements it could degrade the quality of the calculations.
- The calculations can be done using weighted measurements. Weighting the measurements according to a factor such as the signal to noise ratio can be a way to include the extra information from additional sensors without harming the calculated result. This is done by weighting each row of $\mathbf{A}_H$ and $\mathbf{b}_H$ according to the quality of the data in that row.

3.6 Conclusion

Incorporating triangulation measurements into a multilateration system produces significant improvement in the accuracy of the ML algorithm. Its ability to accurately calculate height while using sensors on or near the ground makes it useful in real-world scenarios where objects are being tracked in 3 dimensions. It can make multilateration useful for tracking aircraft in flight over a wide area. This could include tracking aircraft in flight near airports or drone swarms.

Except for a few particular cases the algorithm performs well in a variety of sensor configurations. When the receivers are nearly coplanar it consistently out-performs a multilateration-only algorithm. Adapting the algorithm for receivers that do not share a common vertical direction is an area for further research.

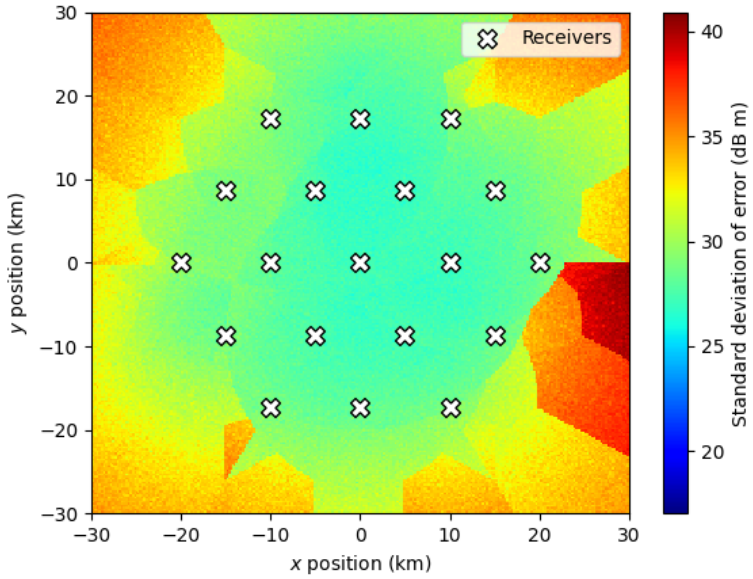

(a) ML

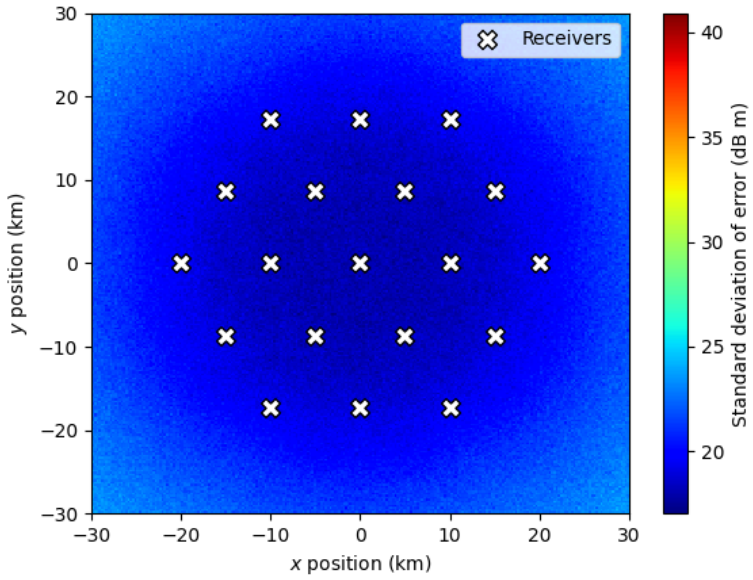

(b) HM

Figure 3.9: Comparison of the standard deviation of the ML and HM algorithm error for near-coplanar receivers in a triangular lattice configuration. The patterns in the ML figure are a result of the vertical deviation that was added to the receiver locations. Both algorithms show an increase in error as the transmitter moves outside the region containing the receivers.

4 Multilateration Using a priori Position Estimates

This chapter is composed from a paper entitled "Multilateration Using A Priori Position Estimates" published in the journal *IEEE Transactions on Radar Systems* [3]. © 2023 IEEE. Reprinted, with permission from Widdison, E. and Long, D. G. "Multilateration Using A Priori Position Estimates," *IEEE Transactions on Radar Systems,* Aug 2023. I hereby confirm that the use of this article is compliant with all publishing agreements.

4.1 Introduction

Multilateration is a process whereby an unknown position of an object can be determined using the distance between its location and several known points. The unknown location lies at the intersection of the spheres centered at the known points with the corresponding radii.

One application of this is to determine the location of a transmitter by recording the time that a single transmitted waveform is received at several different locations. If the positions of these locations are known and their clocks are adequately synchronized, then by using the time of arrival (TOA), the position of the transmitter and the time of its transmission can be determined. [135] This can work without the cooperation of the transmitter.

Multilateration algorithms can be broadly grouped into three categories: iterative, closed-form non-linear, and linear. Iterative methods [12, 15, 159] often perform well but take longer to compute than closed-form methods and can converge to the wrong solution [16]. Closed-form non-linear methods, such as quadratic methods [18, 19], explicitly give the multiple solutions produced by iterative methods but are not always scalable and are not generally compatible with other forms of information such as AOA [2, 31, 32, 41, 96] and FDOA [64, 90, 110]. Linear methods are easily expanded to include additional data [64, 75], but require at least one extra measurement [22, 27] and can be less stable when the linear equations are ill-conditioned[a]. When there are enough measurements[b] the three families of methods have similar accuracy.

One shortcoming of most closed-form solutions to the multilateration problem is that they do not have a way of incorporating or exploiting any a priori information about the target's location to calculate its position [160]. From the perspective of a single sensor, the target can lie anywhere on a

[a] The numerical stability problem can also affect iterative and quadratic methods. Many iterative and quadratic methods also involve matrix inversion and become unstable when those matrices are ill-conditioned.

[b] Three dimensional TDOA multilateration requires at least 5 measurements, corresponding to the 3 spatial dimensions, the unknown clock offset, and one extra degree of freedom to help linearize the equations.

sphere.The motivation for this paper is to incorporate an a priori position estimate as a constraint on the multilateration problem. This is done by using linear approximations of the spherical surfaces, at the a priori estimate position. This geometry has been employed to determine the maximum accuracy of a localization algorithm [37], but not as a way of updating a location estimate.

For the purposes of this paper, the creation and maintenance of the a priori estimate is not considered a part of the algorithm. The initial a priori estimate can come from a wide range of sources. This can include location via surveillance radar, location via unconstrained multilateration, or using self-reported position information from transponder systems such as ADS-B. This method also be used to create improved positions of objects in a swarm, using an average or group position as the a priori estimate.

This paper presents the derivation of the algorithm. Section III analyzes the sources can of error, including measurement error and error created because the true position differs from the estimate. This later error sets a minimum accuracy for the algorithm which can be iteratively improved. Section IV compares the new algorithm with linear TDOA multilateration across a range of wide area multilateration scenarios.

4.2 Differential multilateration algorithm

In this paper, vectors representing a point in space are written in bold, e.g., $\mathbf{a}$ and vectors representing a difference between two points are written with an overbar, e.g., $\bar{c}$.

Conventional multilateration uses a set of distances from a set of known points to a target to determine the position of the target. The target is located at the intersection of a set of spheres. If the target is far from the known points then the spheres can be approximated by planes tangent to the sphere at or near the location of the target. Choosing the point of tangency requires some *a priori* knowledge of the position of the target.

The proposed new algorithm takes an estimated target position $\mathbf{b}$ and uses it to produce planar approximations of the spheres used in conventional multilateration. The planar approximations of the spheres are perpendicular to the vectors from the known points $\mathbf{p}_i$ to the estimated position $\mathbf{b}$, which is adjusted based on the measured pseudodistance and estimated transmitter pseudodistance, as shown in Fig. 4.1.

Let $\mathbf{a} = \mathbf{b} + \bar{c}$ be the unknown position of a transmitter relative to the known estimate $\mathbf{b}$ and let $\mathbf{p}_i, i = 1, \ldots, N$ be the positions of N receivers. The transmitter emits a signal at unknown time t_a which is received at $\mathbf{p}_i$ at time t_i. Pseudodistances

$$\begin{aligned} d_a &= t_a v \\ d_i &= t_i v \end{aligned} \tag{4.1}$$

are calculated, where v is the propagation speed of the signal, which

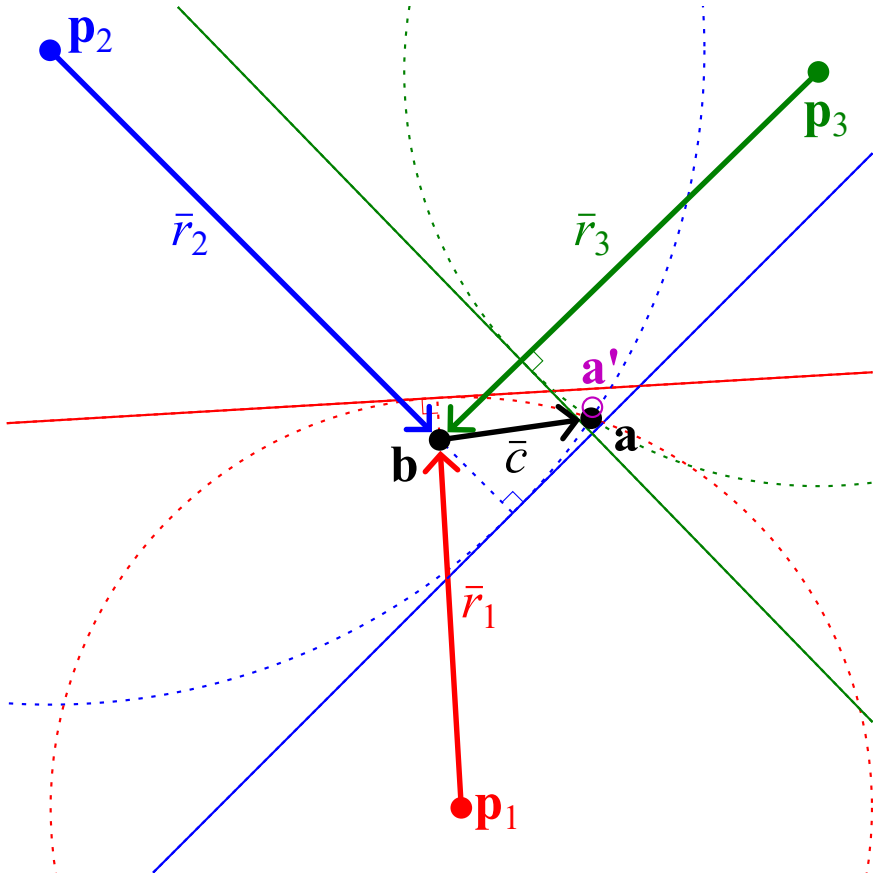

Figure 4.1: The multilateration scenario. Points in space are shown as dots while vectors representing the difference between two points are shown as arrows. The solid lines are the planar approximations of the spheres passing through **a**, shown as dotted lines. This method places the target at the incircle of the triangle they form, marked as **a'**.

is typically the speed of light, c. The distance between transmitter and receiver is then $|\mathbf{a} - \mathbf{p}_i| = d_i - d_a$.

For each point $\mathbf{p}_i$, let $\bar{r}_i = \mathbf{b} - \mathbf{p}_i$ be the radial vector for that point. The planar approximation of a sphere of radius $(d_i - d_a) = d\,|\bar{r}_i|$ centered at $\mathbf{p}_i$, perpendicular to $\bar{r}_i$, is the set of points orthogonal to $\bar{r}_i$ at $\mathbf{p}_i + d\bar{r}_i$ such that

$$\langle (\mathbf{a} - \mathbf{p}_i) - d\bar{r}_i, \bar{r}_i \rangle = 0. \tag{4.2}$$

This is equivalent to

$$\langle \mathbf{a}, \bar{r}_i \rangle + d_a\,|\bar{r}_i| = d_i\,|\bar{r}_i| + \langle \mathbf{p}_i, \bar{r}_i \rangle\,, \tag{4.3}$$

which can be normalized by dividing by $|\bar{r}_i|$ to produce

$$\langle \mathbf{a}, \hat{r}_i \rangle + d_a = d_i + \langle \mathbf{p}_i, \hat{r}_i \rangle \tag{4.4}$$

where $\hat{r}_i = \bar{r}_i / |\bar{r}_i|$ is the unit vector in the direction of $\bar{r}_i$. In 3-dimensional space this is a linear equation of four unknowns. These equations, taken across four or more points, can be expressed as a matrix equation of the

form

$$\begin{aligned}
\mathbf{A} &= \left[\begin{array}{c|c} \hat{r}_1^{\mathrm{T}} & 1 \\ \vdots & \vdots \\ \hat{r}_N^{\mathrm{T}} & 1 \end{array}\right] \\
\mathbf{x} &= \begin{bmatrix} \mathbf{a}' \\ d_a' \end{bmatrix} \\
\mathbf{y} &= \begin{bmatrix} d_1 + \langle \mathbf{p}_1, \hat{r}_1 \rangle \\ \vdots \\ d_N + \langle \mathbf{p}_N, \hat{r}_N \rangle \end{bmatrix} \\
\mathbf{A}\mathbf{x} &= \mathbf{y}
\end{aligned} \tag{4.5}$$

where $\mathbf{a}'$ is the calculated position and d_a' is the calculated pseudodistance associated with the signal transmission time. The unknowns can be calculated directly as $\mathbf{x} = \mathbf{A}^{-1}\mathbf{y}$ if $\mathbf{A}$ is square or via least squares as $\mathbf{x} = \left(\mathbf{A}^{\mathrm{T}}\mathbf{A}\right)^{-1}\mathbf{A}^{\mathrm{T}}\mathbf{y}$.

This method produces estimates of the target position that are at least as accurate as those from traditional multilateration as long as the measurement error is small enough relative to the error due to using a planar approximation of the multilateration spheres. The general stability of this method is analyzed in Sec. 4.3 and the errors due to approximating the spheres as planes is analyzed in Sec. 4.3.2.

4.2.1 Two dimensional algorithm

This algorithm, as written, can be used in an D-dimensional space, but here is only used for $D = 2, 3$. For a target and reference points in 3 dimensions, at least four reference points are required to determine the location of the target. The $D = 2$ case requires only 3 reference points, along with some care to implement correctly.

In a 2-dimensional implementation the assumption is that the target lies on a 2-dimensional plane. Since 2-dimensional scenarios typically constrain the solution space and not the locations of receivers, the positions of the reference points may be somewhere other than directly on that plane. The algorithm uses the propagation speed in the plane, which in this case needs to account for the difference between the slant range between the transmitter and receiver, and the projection of that range onto the plane. If $\bar{r}_i = \begin{bmatrix} x_i & y_i & z_i \end{bmatrix}^{\mathrm{T}}$ and the target is assumed to lie in the xy plane then the projected pseudodistance

$$d_i = t_i v_i = t_i v \cos\phi_i \tag{4.6}$$

where

$$\tan\phi_i = \frac{z_i}{\sqrt{x_i^2 + y_i^2}}. \tag{4.7}$$

Alternately, this is

$$d_i = t_i v \left(\frac{\sqrt{x_i^2 + y_i^2}}{|\bar{r}_i|} \right). \tag{4.8}$$

With this adjustment of the pseudodistance, compared to Eq. 4.1, the 2 dimensional algorithm can be implemented using Eq. 4.5 with **A** of size $N \times 3$.

4.3 Numerical stability

4.3.1 Unstable cases

There are two cases where the **A** matrix is singular. When the receivers are all coplanar[c] and equidistant from the estimate point (the coplanar equidistant case, i.e. the receivers lie on a circle and the estimate point is on the line that is equidistant from all points on the circle, Fig. 4.2a), or when the receivers are coplanar with the estimate point (the coplanar case, Fig. 4.2b). In both of these cases, the **A** matrix is not full rank and cannot be inverted. It is possible for a scenario to experience both instability conditions at the same time.

[c]In this section, the term "coplanar" is based on a 3 dimensional algorithm. More generally, these instability cases require that $D + 1$ receivers lie in a $D - 1$ dimensional subspace of a D dimensional space. In the 2 dimensional case this condition only applies when at least three points are colinear and equidistant from the reference point. However, three points cannot be colinear and all equidistant from a fourth point. Therefore the coplanar equidistant condition cannot apply in 2 dimensions.

Multilateration algorithms cannot generally work when the receivers are all coplanar. The proposed algorithm is numerically stable when the receivers are coplanar as long as the *a priori* estimate point is not also coplanar with them and the receivers are not all equidistant from the estimate point.

The coplanar equidistant case is equivalent to all the receivers lying on a circle with the estimate point on the line perpendicular to the circle and passing through the center. To see why this case does not produce a full rank matrix, consider the case where the radial unit vectors are all of the form $\hat{r}_i = \begin{bmatrix} r\cos\theta_i & r\sin\theta_i & z \end{bmatrix}^{\mathrm{T}}$, where θ_i is the bearing from the estimate point to the ith receiver. This produces the matrix

$$\mathbf{A} = \begin{bmatrix} r\cos\theta_1 & r\sin\theta_1 & z & 1 \\ \vdots & \vdots & \vdots & \vdots \\ r\cos\theta_N & r\sin\theta_N & z & 1 \end{bmatrix}. \tag{4.9}$$

The right two columns of **A** have the same value in each row, so the columns are multiples of each other. This means the matrix **A** has, at most, rank 3, when it needs to be rank 4 to be inverted and produce a valid estimate of **a'**.

If the receivers lie on any plane other than one parallel to the xy plane then the **A** matrix can be converted into this form by a coordinate transformation, which means that the matrix is rank deficient for any set of coplanar receivers that are equidistant from the transmitter.

In the second unstable case, the receivers and estimate points are all coplanar. This can be examined by considering the case where the radial vectors all lie on the xy plane and are of the form $\hat{r}_i = \begin{bmatrix} x_i & y_i & 0 \end{bmatrix}^{\mathrm{T}}$.

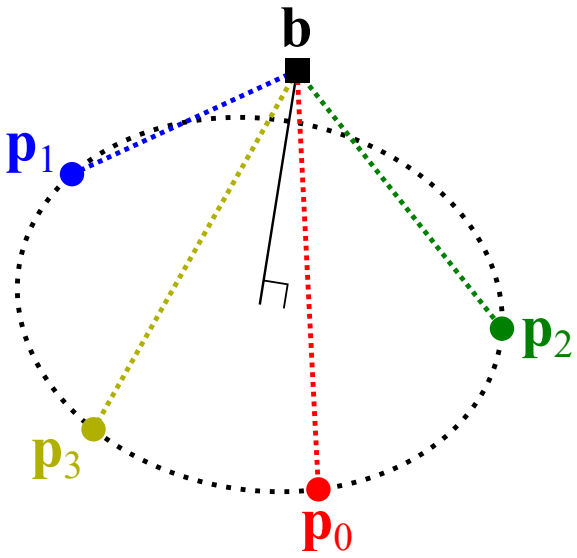

(a) Coplanar equidistant case

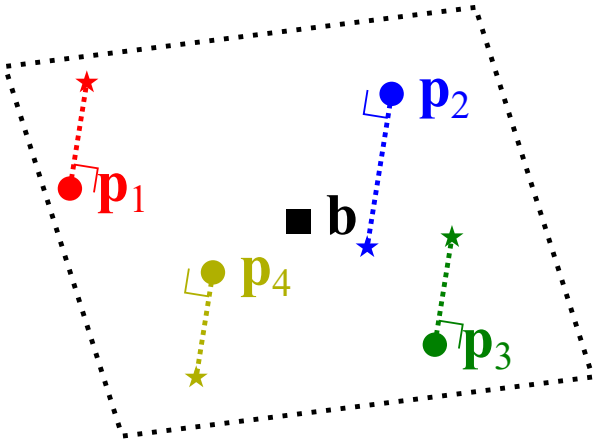

(b) Coplanar case

Figure 4.2: A depiction of numerically unstable scenarios, with the estimate position marked as a square and the receiver positions marked as circles. In (a), the coplanar equidistant case, the receivers all lie on a circle and the estimate lies on the axis of symmetry of that circle. In (b) the receivers all lie on the same plane as the estimate. The points marked by stars are included to show that the receiver positions are equivalent to non-coplanar points that have been projected onto a single plane.

This produces the **A** matrix

$$\mathbf{A} = \begin{bmatrix} x_1 & y_1 & 0 & 1 \\ \vdots & \vdots & \vdots & \vdots \\ x_N & y_N & 0 & 1 \end{bmatrix}. \tag{4.10}$$

With one column equal to zero, this matrix is also deficient. As with the coplanar equidistant receiver case, any set of receivers that are coplanar with the estimate can, with a coordinate transformation, be put in this form and is rank deficient.

These instability cases depend only on the receiver locations and the estimate point. One way to ensure that these conditions are never met is to ensure that the receivers are not coplanar. If the target's position can be assumed to be out of the plane containing the receivers, for example, if the target is an airplane with some minimum altitude, then it is sufficient to ensure that the receivers do not lie in a circle. With a large number of receivers this is unlikely to occur accidentally, but when only 4 receivers are used some care should be taken in choosing suitable locations for the receivers.

4.3.2 Planar approximation error

In this algorithm, the use of planes to approximate spheres introduces some error into the results. When radii of the spheres are large then this estimate is relatively accurate locally around **b**. The approximation is less accurate when the target is farther from the radial line passing through the *a priori* estimate. This section quantifies that error.

Using this algorithm, the correct position is calculated when the measured pseudodistance[d] d_i is adjusted to match the projection of the target's true position onto the radial vector. The measured pseudodistance represents the slant range to the target, which is the hypotenuse of a right triangle with the projected distance as one of its legs. The difference between these two distances is the planar approximation error, or planar error e_i, as shown in Fig. 4.3.

[d] To improve the readability of the derivations in this section, we ignore the transmitter pseudodistance, and assume that the pseudodistance d_i is a true distance, with $d_a = 0$. This does not affect the results of the derivation. If $d_a \neq 0$ then the first line in Eq. 4.12 starts $e_i = d_i - d_a - (\tilde{d}_i - d_a) = d_i - \tilde{d}_i \ldots$, with the rest of the derivation following identically.

The distance to the target is $d_i = |\mathbf{a} - \mathbf{p}_i| = |\bar{r}_i + \bar{c}|$ and the length of the projection of $\mathbf{a} - \mathbf{p}_i = \bar{r}_i + \bar{c}$ onto $\bar{r}_i$ is

$$\tilde{d}_i = \frac{\langle \bar{r}_i + \bar{c}, \bar{r}_i \rangle}{|\bar{r}_i|}. \tag{4.11}$$

The planar error is

$$\begin{aligned} e_i &= d_i - \tilde{d}_i = |\bar{r}_i + \bar{c}| - \frac{\langle \bar{r}_i + \bar{c}, \bar{r}_i \rangle}{|\bar{r}_i|} \\ e_i &= \sqrt{\langle \bar{r}_i + \bar{c}, \bar{r}_i + \bar{c} \rangle} - \frac{\langle \bar{r}_i + \bar{c}, \bar{r}_i \rangle}{|\bar{r}_i|} \\ e_i &= \sqrt{|\bar{r}_i|^2 + 2\langle \bar{r}_i, \bar{c} \rangle + |\bar{c}|^2} - |\bar{r}_i| - \frac{\langle \bar{r}_i, \bar{c} \rangle}{|\bar{r}_i|}. \end{aligned} \tag{4.12}$$

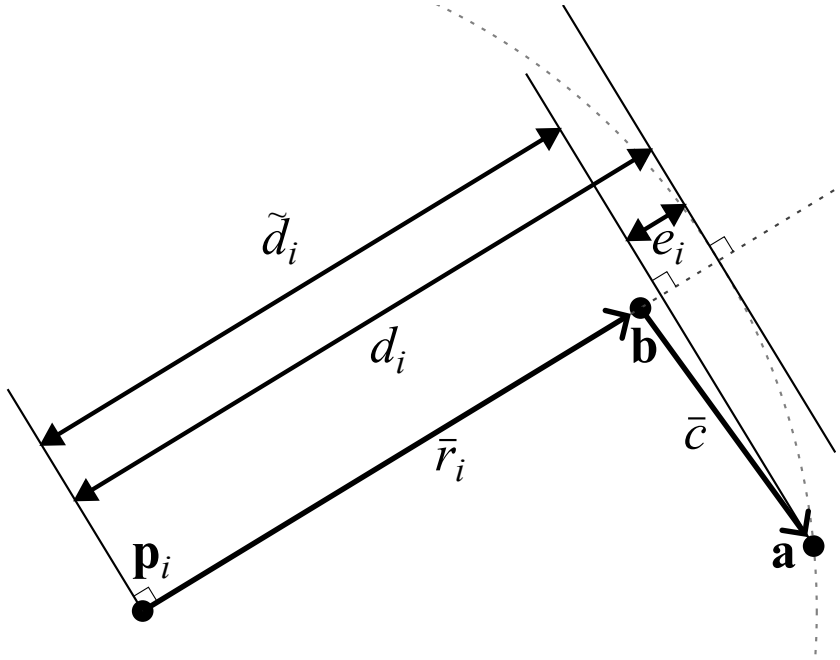

Figure 4.3: The planar error and pseudodistance for a single receiver. The planar error e_i in this figure is exaggerated by the small value of $|\bar{r}_i|$ and relatively large displacement between the target **a** and the radial vector $\bar{r}_i$.

The radical term can be approximated by factoring out $|\bar{r}_i|^2$ and using the binomial expansion

$$(1+a)^n = 1 + na + \frac{1}{2!}n(n-1)a^2 + \frac{1}{3!}n(n-1)(n-2)a^3 + \cdots . \quad (4.13)$$

[e]The algorithm is not suitable when $|\bar{r}_i| \gg |\bar{c}|$ is not true. The worst case considered in this paper is shown in Fig. 4.6 where the average value of $|\bar{r}_i|/|\bar{c}|$ is $10/\sqrt{3}$. In that scenario, the algorithm in Eq. 4.5 is unable to reduce the standard deviation of the error in the calculated position below 100 m.

Because $|\bar{r}_i| \gg |\bar{c}|$, the first order terms and the first half of the second order terms are sufficient to estimate the error[e].

$$\begin{aligned} e_i &\approx |\bar{r}_i|\left(1 + \frac{\langle \bar{r}_i, \bar{c}\rangle}{|\bar{r}_i|^2} + \frac{|\bar{c}|^2}{2\,|\bar{r}_i|^2} - \frac{\langle \bar{r}_i, \bar{c}\rangle^2}{2\,|\bar{r}_i|^4}\right) - |\bar{r}_i| - \frac{\langle \bar{r}_i, \bar{c}\rangle}{|\bar{r}_i|} \\ e_i &\approx \frac{|\bar{c}|^2 - \langle \hat{r}_i, \bar{c}\rangle^2}{2\,|\bar{r}_i|}. \end{aligned} \quad (4.14)$$

This is equal to the square of the length of the component of $\bar{c}$ that is orthogonal to $\bar{r}_i$. Since $|\bar{c}| \geq |\langle \hat{r}_i, \bar{c}\rangle|$, the planar error is within the range

$$0 \leq e_i \leq \frac{|\bar{c}|^2}{2\,|\bar{r}_i|} \quad (4.15)$$

If $\bar{c}$ follows a D-dimensional multivariate normal distribution with variance σ_c^2, i.e., each element of $\bar{c}$ follows a normal distribution with

zero mean and variance σ_c^2, then the expected value of e_i is

$$\begin{aligned} E(e_i) &= E\left(\frac{|\bar{c}|^2 - \langle \hat{r}_i, \bar{c}\rangle^2}{2|\bar{r}_i|}\right) \\ &= \frac{1}{2|\bar{r}_i|}\left[E\left(|\bar{c}|^2\right) - E\left(\langle \hat{r}_i, \bar{c}\rangle^2\right)\right] \\ &= \frac{1}{2|\bar{r}_i|}\left[D\sigma_c^2 - \sigma_c^2\right] \\ &= \frac{(D-1)\sigma_c^2}{2|\bar{r}_i|}. \end{aligned} \tag{4.16}$$

This agrees with the mean of a chi-squared distribution with $D-1$ degrees of freedom [161, pp.62-63], scaled by σ_{e_i}, and agrees with the way that Eq. 4.14 subtracts one degree of freedom from the D-dimensional normal distribution of $\bar{c}$. The variance of the planar error is given by scaling the chi-squared variance of $2(D-1)$ by $\sigma_{e_i}^2$ to get

$$\sigma_{e_i}^2 = \frac{(D-1)\sigma_c^4}{2|\bar{r}_i|^2}. \tag{4.17}$$

When $D = 3$, this gives $\sigma_{e_i} = \sigma_c^2/|\bar{r}_i|$.

When solving the equations, the d'_a term should account for any bias due to the mean value of e_i. The degradation of the calculated position is due to the variance of the error terms, $\sigma_{e_i}^2$. This combines with the variance of the measurement error, $\sigma_{d_i}^2$, to produce the total error in the calculated position. This means that the position error is dominated by the planar error when $\sigma_{d_i}^2 < \sigma_{e_i}^2$, which creates a performance floor which can be seen in Figs. 4.4-4.9. The floor occurs at the level where the planar error limits the accuracy of the measured position, which corresponding to $\sigma_d \geq \sigma_{e_i}$, as seen in Fig. 4.4.

4.3.3 Statistical optimization

To improve the performance of this algorithm, we consider the statistical effects of measurement noise and planar error on the computations.

Let the noisy measurements be $\tilde{d}_i = d_i + n_i + e_i$ where n_i is a Gaussian random variable representing the noise, and let $\mathbf{n} = [n_1, \ldots, n_N]^{\mathrm{T}}$ be a vector of the measurement noise. The noisy measurement also includes the planar error term, which can be concatenated to form the planar error vector $\mathbf{e} = [e_1, \ldots, e_N]^{\mathrm{T}}$. We can assume that the measurement noise is zero mean and uncorrelated with the planar error, with covariance

$$\mathrm{E}(\mathbf{n}\mathbf{n}^{\mathrm{T}}) = \mathbf{Q}_n. \tag{4.18}$$

The mean of $\mathbf{e}$ is

$$\boldsymbol{\mu}_{\mathbf{e}} = \mathrm{E}(\mathbf{e}) = \begin{bmatrix} \frac{(D-1)\sigma_c^2}{2|\bar{r}_1|} \\ \vdots \\ \frac{(D-1)\sigma_c^2}{2|\bar{r}_N|} \end{bmatrix} = \frac{D-1}{2}\sigma_c^2\mathbf{r}', \tag{4.19}$$

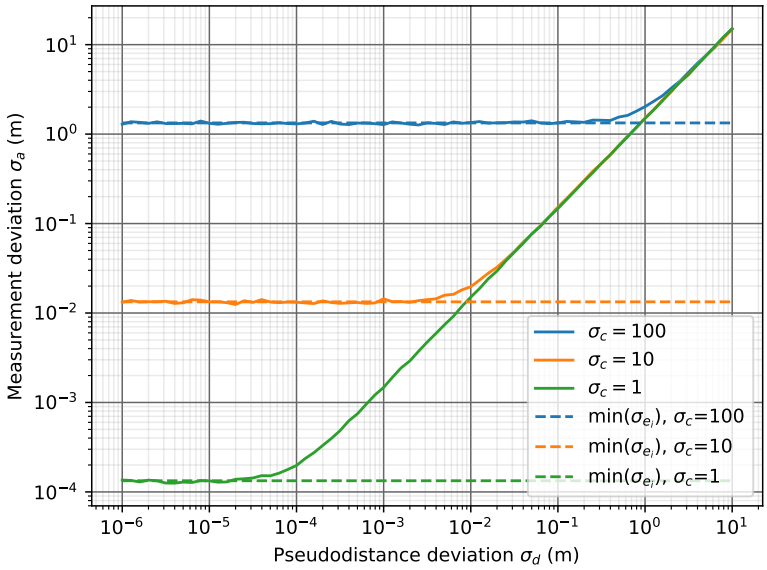

Figure 4.4: Simulations of planar noise with 4 receivers and different levels of σ_c. The theoretical minimum measurement error is marked by the horizontal dotted lines. The receivers are located in a tetrahedron, centered on the transmitter, with each receiver 7.5 km from the transmitter.

where $\mathbf{r}' = [|\bar{r}_1|^{-1}, \ldots, |\bar{r}_N|^{-1}]^{\mathrm{T}}$. Because the planar error has a non-zero mean we need the correlation matrix $\mathbf{R}_e = E[\mathbf{e}\mathbf{e}^{\mathrm{T}}]$ rather than the covariance matrix $\mathbf{Q}_e = E[(\mathbf{e} - \boldsymbol{\mu}_e)(\mathbf{e} - \boldsymbol{\mu}_e)^{\mathrm{T}}]$. The elements of $\mathbf{R}_e$ are[f]

[f] $\mathrm{E}(|\bar{c}|^4) = (2D + D^2)\sigma_c^4 = D(D+2)\sigma_c^4$, $\mathrm{E}(|\bar{c}|^2 \langle \hat{r}_i, \bar{c}\rangle^2) = (D+2)\sigma_c^4$, and $\mathrm{E}(\langle \hat{r}_i, \bar{c}\rangle^2 \langle \hat{r}_j, \bar{c}\rangle^2) = (2\langle \hat{r}_i, \hat{r}_j\rangle^2 + 1)\sigma_c^4$. The first value is derived from the variance and mean of the chi square distribution. The others are determined experimentally.

$$
\begin{aligned}
R_{e,ij} &= E[e_i e_j] = \mathrm{E}\left[\frac{|\bar{c}|^2 - \langle \hat{r}_i, \bar{c}\rangle^2}{2|\bar{r}_i|}\frac{|\bar{c}|^2 - \langle \hat{r}_j, \bar{c}\rangle^2}{2|\bar{r}_j|}\right] \\
&= \frac{1}{4|\bar{r}_i||\bar{r}_j|}\mathrm{E}\left[|\bar{c}|^4 - |\bar{c}|^2\left(\langle \hat{r}_i, \bar{c}\rangle^2 + \langle \hat{r}_j, \bar{c}\rangle^2\right) + \right. \\
&\qquad \left. \langle \hat{r}_i, \bar{c}\rangle^2 \langle \hat{r}_j, \bar{c}\rangle^2\right] \\
&= \frac{\sigma_c^4}{4|\bar{r}_i||\bar{r}_j|}\left(2D + D^2 - 2(D+2) + 2\langle \hat{r}_i, \hat{r}_j\rangle^2 + 1\right) \\
&= \frac{D^2 - 3 + 2\langle \hat{r}_i, \hat{r}_j\rangle^2}{4|\bar{r}_i||\bar{r}_j|}\sigma_c^4. \qquad (4.20)
\end{aligned}
$$

This noise model changes Eq. 4.5 to

$$\begin{aligned}
\mathbf{A} &= \left[\begin{array}{c|c} \hat{r}_1^{\mathrm{T}} & 1 \\ \vdots & \vdots \\ \hat{r}_N^{\mathrm{T}} & 1 \end{array}\right] \\
\mathbf{x} &= \left[\begin{array}{c} \mathbf{a}' \\ \tilde{d}_a' \end{array}\right] \\
\mathbf{y} &= \left[\begin{array}{c} d_1 + \langle \mathbf{p}_1, \hat{r}_1 \rangle \\ \vdots \\ d_N + \langle \mathbf{p}_N, \hat{r}_N \rangle \end{array}\right] + \mathbf{n} + \mathbf{e} \\
\mathbf{A}\mathbf{x} &= \mathbf{y}
\end{aligned} \tag{4.21}$$

where $\mathbf{x}, \mathbf{a}, \tilde{d}_a, \mathbf{y}$ are the noisy versions of $\mathbf{x}, \mathbf{a}, d_a, \mathbf{y}$ respectively.

The position error is therefore equal to

$$\boldsymbol{\psi} = \mathbf{x} - \mathbf{x} = \mathbf{x} + \mathbf{A}^{\dagger}(\mathbf{n} + \mathbf{e}) - \mathbf{x} = \mathbf{A}^{\dagger}(\mathbf{n} + \mathbf{e}) \tag{4.22}$$

where $\mathbf{A}^{\dagger}$ is the inverse or pseudoinverse of $\mathbf{A}$. The expected value of this error is

$$\begin{aligned}
\mathrm{E}(\boldsymbol{\psi}) &= \mathbf{A}^{\dagger}[\mathrm{E}(\mathbf{n}) + \mathrm{E}(\mathbf{e})] \\
&= \mathbf{A}^{\dagger}\boldsymbol{\mu}_{\mathbf{e}}.
\end{aligned} \tag{4.23}$$

The variance of the position error can be expressed as

$$\begin{aligned}
\mathrm{E}(\boldsymbol{\psi}\boldsymbol{\psi}^{\mathrm{T}}) &= \mathrm{E}\left[\mathbf{A}^{\dagger}(\mathbf{n} + \mathbf{e})(\mathbf{n} + \mathbf{e})^{\mathrm{T}}\mathbf{A}^{\dagger^{\mathrm{T}}}\right] \\
&= \mathbf{A}^{\dagger}\mathbf{Q}_n\mathbf{A}^{\dagger^{\mathrm{T}}} + \mathbf{A}^{\dagger}\mathbf{Q}_e\mathbf{A}^{\dagger^{\mathrm{T}}}.
\end{aligned} \tag{4.24}$$

Using weighted least squares (WLS), this is

$$\mathrm{E}(\boldsymbol{\psi}\boldsymbol{\psi}^{\mathrm{T}}) = (\mathbf{A}^{\mathrm{T}}\mathbf{W}\mathbf{A})^{-1}\mathbf{A}^{\mathrm{T}}\mathbf{W}(\mathbf{Q}_n + \mathbf{Q}_e)\mathbf{W}\mathbf{A}(\mathbf{A}^{\mathrm{T}}\mathbf{W}\mathbf{A})^{-1}. \tag{4.25}$$

This suggests that the total error can be minimized by applying WLS with

$$\mathbf{W} = (\mathbf{Q}_n + \mathbf{R}_e)^{-1} \tag{4.26}$$

and

$$\mathbf{x} = \left(\mathbf{A}^{\mathrm{T}}\mathbf{W}\mathbf{A}\right)^{-1}\mathbf{A}^{\mathrm{T}}\mathbf{W}\mathbf{y}. \tag{4.27}$$

In practice, incorporating the $\mathbf{R}_e$ planar error correlation does not significantly improve the calculated position estimate, as shown in Fig. 4.5. In some cases, where σ_d^2 is small and $\sigma_c^2/|\bar{r}_i|$ is large, the $\mathbf{Q}_n + \mathbf{R}_e$ matrix is ill-conditioned. Therefore, we suggest using $\mathbf{W} = \mathbf{Q}_n^{-1}$ rather than the value from Eq. 4.26, and address the effects of planar error by the iterative approach presented in Sec. 4.3.4.

The equations in this algorithm are nearly identical to those used by Lee [37] to determine the geometric dilution of precision (GDOP) of a

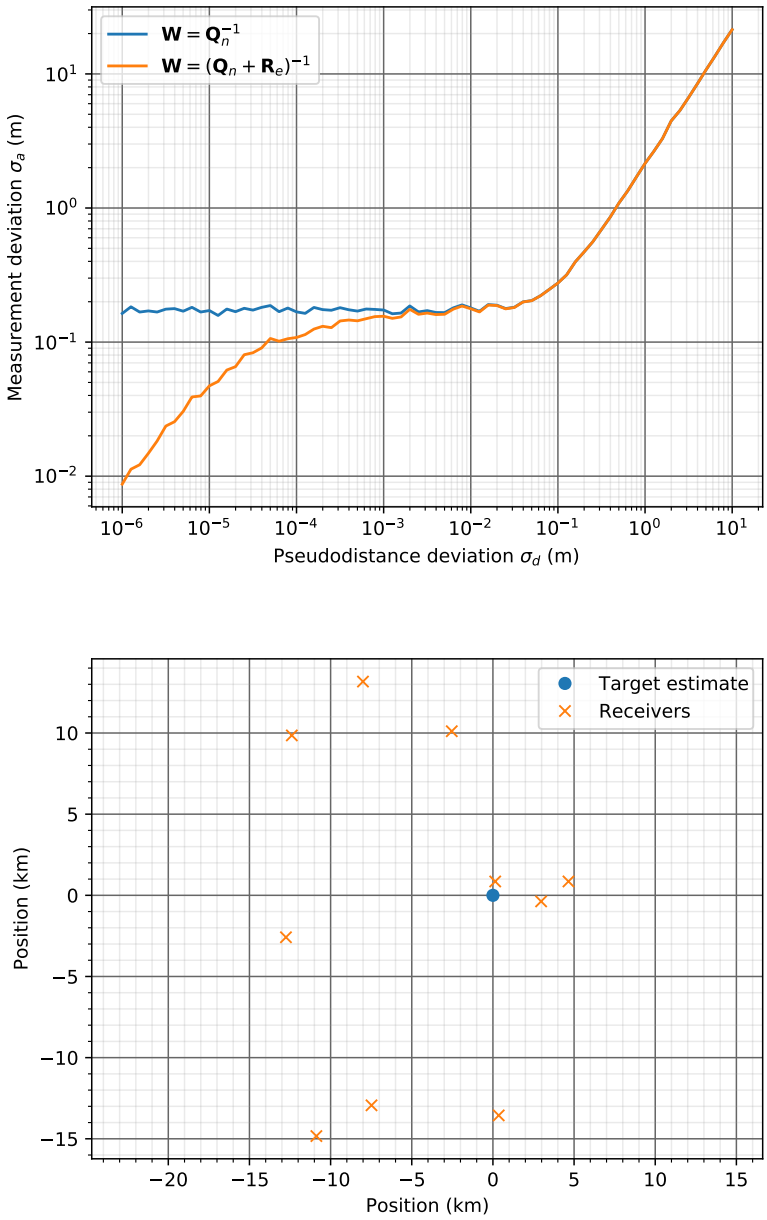

Figure 4.5: Demonstration of weighted least squares solution accuracy, with 10 receivers randomly distributed as shown and $\sigma_c = 10\,\text{m}$. Note that the weighted solutions are identical when the measurement error dominates ($\sigma_d > 0.01\,\text{m}$), and that including $\mathbf{R}_e$ in the weighting only makes relatively small gains except in cases with extremely low measurement errors ($\sigma_d < 1\,\text{mm}$).

multilateration scenario. The only difference is that Lee used the true position of the target while this uses an approximation. This means that when the estimate error σ_c^2 is small the measurement error asymptotically approaches the GDOP. For multilateration where the pseudodistance errors are zero mean Gaussian variables, the Cramér-Rao lower bound (CRLB) is equal to the GDOP [162].

4.3.4 Multi-pass algorithm

The planar bias error can be reduced by using the calculated position to adjust the pseudodistances and then recalculate. This can be done using the direct calculation in Eq. 4.12 or the approximation in Eq. 4.14, using $\mathbf{a}'$ to determine an estimate of $\bar{c}$, which in turn is used to estimate the errors. The updated pseudodistances are $d_i' = d_i - e_i$ and the updated position $\mathbf{a}''$ is given by

$$\begin{aligned} \mathbf{x}' &= \begin{bmatrix} \mathbf{a}'' \\ d_a'' \end{bmatrix} \\ \mathbf{y}' &= \begin{bmatrix} d_1' + \langle \mathbf{p}_1, \hat{r}_1 \rangle \\ \vdots \\ d_N' + \langle \mathbf{p}_N, \hat{r}_N \rangle \end{bmatrix} \\ \mathbf{A}\mathbf{x}' &= \mathbf{y}' \end{aligned} \tag{4.28}$$

Because $\mathbf{A}$ is unchanged from the original algorithm, the second pass can reuse the same $\mathbf{A}^\dagger$ from the first pass, which reduces the computational cost of performing multiple passes. The second pass reduces the minimum measurement error by a factor of roughly $\sigma_c / |\bar{r}_i|$.

This step can be iterated more than once. Each time the original distances are updated using the new calculated position.

$$d_i^{(n+1)} = d_i - \left(\left| \mathbf{a}^{(n)} - \mathbf{p}_i \right| - \left\langle \mathbf{a}^{(n)} - \mathbf{p}_i, \hat{r}_i \right\rangle \right). \tag{4.29}$$

As the algorithm is iterated, the average error is reduced. Fig. 4.6 shows the algorithm's performance against a target with $\sigma_c = 1\,\text{km}$ and four receivers in a tetrahedral formation at a distance of 10 km from the reference point. The results are shown for 1 through 10 passes of the algorithm. After eight iterations (the first pass and seven update passes) the average planar error is less than the level for $\sigma_c = 10\,\text{m}$ with one pass under the same conditions. If the multi-pass algorithm is used then it should be stopped when $|\mathbf{a}^{(n+1)} - \mathbf{a}^{(n)}| < \epsilon$ for some value of ϵ, or after some number of iterations, whichever comes first. The multi-pass algorithm should only be used when the variance of the measurement error is very small.

4.4 Performance verification

To evaluate the performance of this algorithm we compare it to the linear multilateration approach from [22], using the optimal weighting as given

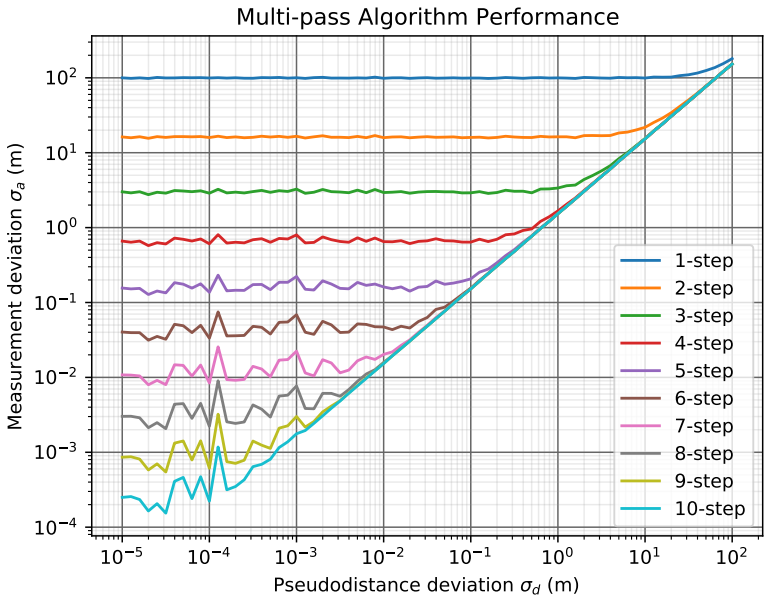

Figure 4.6: Improvements in position from iterating the algorithm. The receivers are located in a regular tetrahedron centered on and 10 km away from the estimate point. The position accuracy is $\sigma_c = 1$ km.

in equations (11) through (14a). This is compared to the single-pass method as given in Eq. 4.27.

We apply these methods to three different scenarios, each using five receivers, showing horizontal and vertical errors on separate graphs. The scenarios are:

- spherically uniform, with receivers spread equally around a sphere [163] centered on the transmitter, shown in Fig. 4.7,
- circular, with receivers spread evenly in a circle around the transmitter, which is above the center of the circle, with some random vertical perturbation to prevent both algorithms from having singular matrices, shown in Fig. 4.8, and
- random, with receivers randomly distributed in a box of size 30 km × 30 km × 500 m, shown in Fig. 4.9.

The specific receiver locations are given in Table 4.1. The transmitter is located at $\mathbf{a} = [0, 0, 0]^{\mathrm{T}}$ in the spherically uniform scenario and at $\mathbf{a} = [0, 0, 1000]^{\mathrm{T}}$ meters in the other two scenarios.

In every scenario, when the measurement noise variance was greater than the variance of the planar error the proposed algorithm performed better than traditional linear multilateration. The performance difference was especially pronounced in the circular scenario where the receivers are nearly coplanar and traditional linear multilateration has very poor accuracy vertically [164, 165].

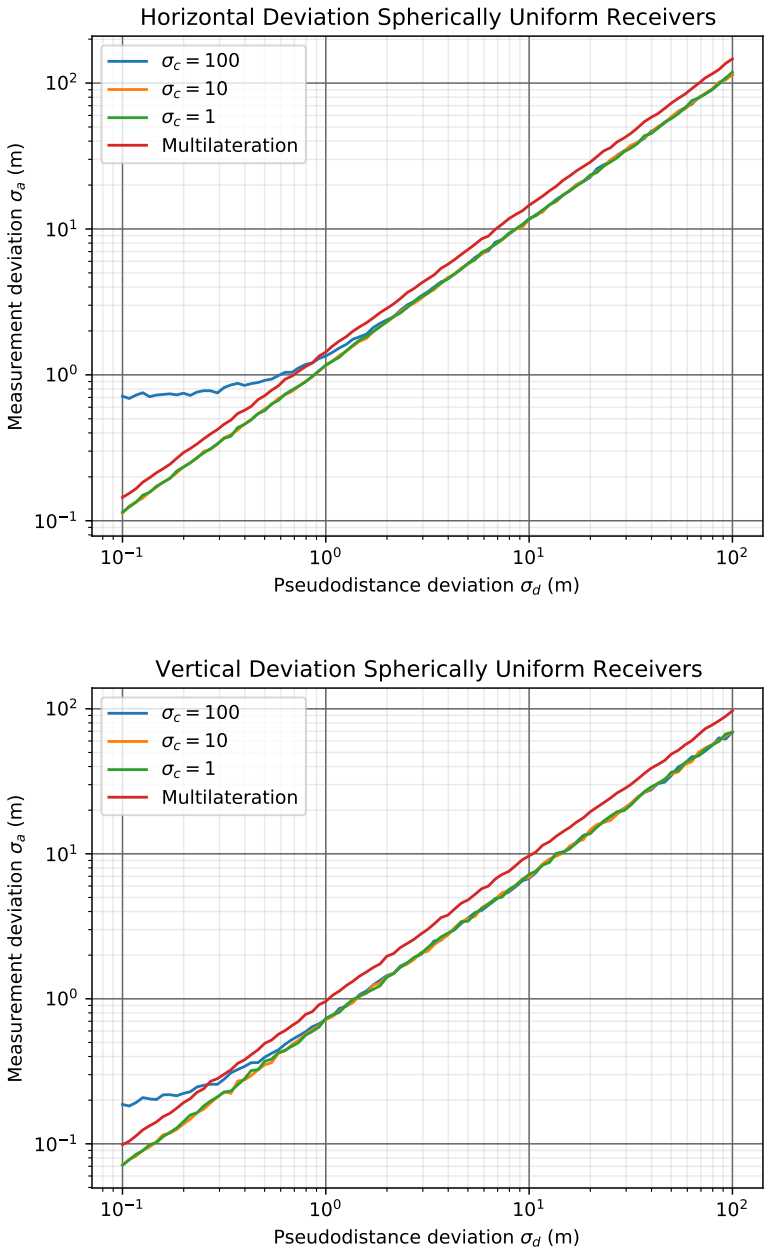

Figure 4.7: Comparison of the differential multilateration algorithm with traditional multilateration with spherically uniform receivers. The new algorithm matches or exceeds performance except when planar error exceeds the measurement error.

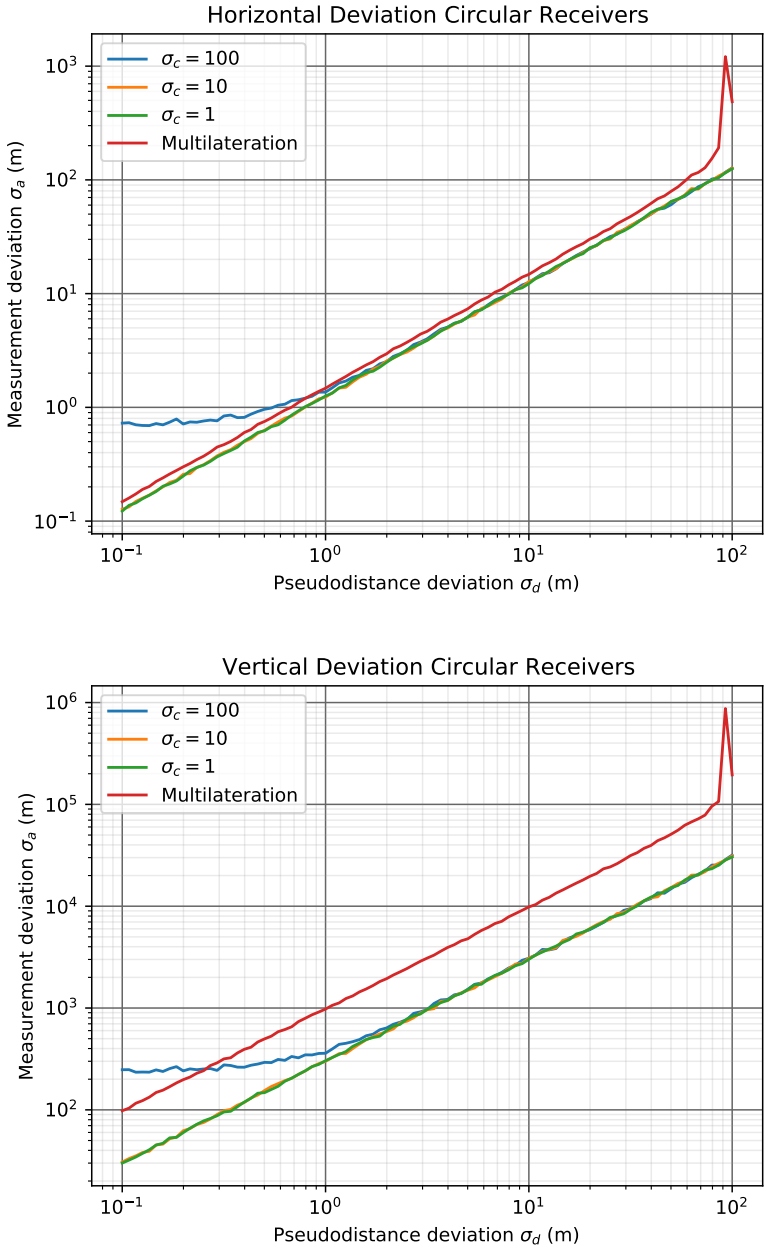

Figure 4.8: Comparison of the differential multilateration algorithm with traditional multilateration with receivers in a nearly planar circular arrangement. This scenario is ill-conditioned for both methods, with only the small vertical deviations in receiver locations preventing both algorithms from producing singular matrices. The conventional multilateration algorithm became unstable with $\sigma_d > 100\,\text{m}$.

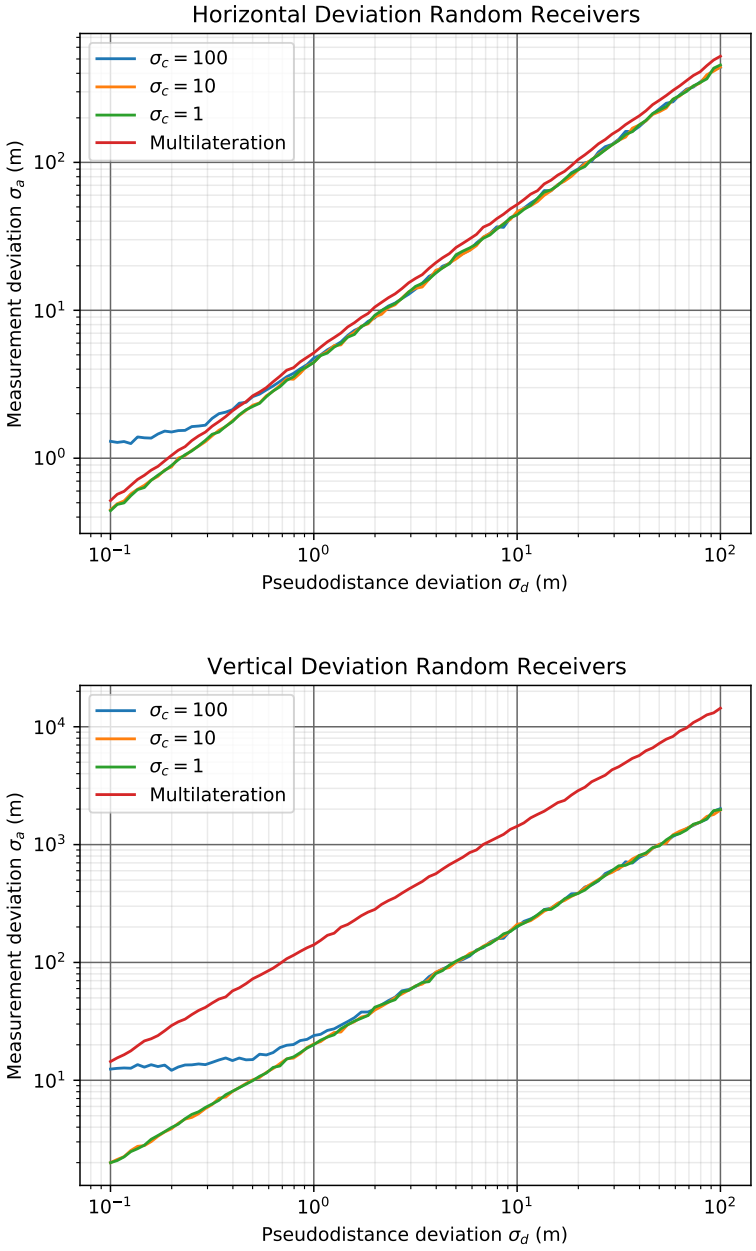

Figure 4.9: Comparison of the differential multilateration algorithm with traditional multilateration with receivers randomly located in a 30 km × 30 km × 500 m box, centered 1 km below the estimated target position **a**. The new algorithm performed significantly better whenever the planar error was not the dominant source of measurement variance.

Table 4.1: Receiver locations for performance verification scenarios. All figures are given in meters.

Spherical			
point	x	y	z
$\mathbf{p}_1$	0	0	8000
$\mathbf{p}_2$	12000	0	0
$\mathbf{p}_3$	-5500	9526	0
$\mathbf{p}_4$	-4500	-7794	0
$\mathbf{p}_5$	0	0	-10000
Circular			
point	x	y	z
$\mathbf{p}_1$	9500	0	-3
$\mathbf{p}_2$	3090	9511	-9
$\mathbf{p}_3$	-8090	5878	12
$\mathbf{p}_4$	-8090	-5878	6
$\mathbf{p}_5$	3090	-9511	9
Random			
point	x	y	z
$\mathbf{p}_1$	12653	-1716	108
$\mathbf{p}_2$	7384	14813	67
$\mathbf{p}_3$	7896	6170	-99
$\mathbf{p}_4$	9637	-7515	182
$\mathbf{p}_5$	6563	2165	-36

4.5 Conclusion

The algorithm presented here improves on traditional mutlilateration algorithms at obtaining an accurate 3-dimensional position in typical wide area multilateration scenarios. This comes at the cost of requiring an initial measurement and a target tracking algorithm to maintain the quality of the estimate. It more numerically stable in typical wide area multilateration scenarios than traditional multilateration. This method reduces the number of measurements required by one, allowing for 3-dimensional localization with only four measurements instead of at least five for linear TDOA multilateration.

The key benefit of this algorithm is that it is well-suited for incorporation into a tracking algorithm. At any point in time the calculation of the estimate is linear, allowing for tracking with a simple Kalman filter rather than one of the non-linear extensions. It can also be employed for tracking swarms of objects where a central point within the swarm can act as an estimate for the position of an individual transmitter, and each calculated transmitter location contributes to the estimate of the swarm position.

To implement this algorithm, an *a priori* estimate for the location of a target must be available. As such it requires that an initial position be available. This can be acquired with a different multilateration algorithm or by using some other sensor such as a radar. The accuracy of the

algorithm is limited when the estimate is not accurate enough. The statistics, in Eq. 4.17, and simulations, in Fig. 4.6, show that in a wide area multilateration scenario the variance of the estimate error can be quite large without irreparably degrading the performance of the algorithm.

With its initial estimate and linear equations, this is naturally suited for use in a tracking algorithm. It uses an estimate of the current position of an object to calculate an updated position, and all the calculations are linear functions. A Kalman filter should be able to both track the target and provide quality estimates of updated positions for use with future samples.

This algorithm could be used to measure and possibly track individual objects in a swarm. A traditional radar may not be able to distinguish individual objects in a swarm, but by using the radar's position as the estimate for the swarm as a whole, and then applying this algorithm to signals sent between members of the swarm, it may be possible to determine the positions of individual objects.

5 Conclusion

5.1 Contributions and Publications

This dissertation clarifies and expands on the algorithms for linear localization. This is done by performing a broad review of the localization approaches since linear multilateration was introduced in 1994, covering both the equations employed in localization algorithms and the applications for those algorithms. I develop two new localization algorithms to aid with wide area multilateration. One combines TDOA and vertical AOA measurements to improve the accuracy of the vertical position estimate. The other uses an *a priori* estimate to create a linear approximation of the localization problem.

The literature review provides the a unique, clear catalog of linear TOA, TDOA, AOA, and FDOA equations. It shows how the equations relate geometrically to the general, non-linear localization problem. This relationship is key to building a strong, intuitive understanding of linear localization algorithms. That, in turn, aids in identifying scenarios where linear localization algorithms are numerically or geometrically unstable. The linear equations identified can be combined to form hybrid localization algorithms. This includes the option of using fewer or simpler measurements than might seem obvious at first, such as using 1AOA to measure vertical position rather than measuring both azimuth and elevation AOA. The literature review has been submitted for peer review [4].

I present a review of passive localization applications in the literature. This covers a wide range of scenarios and of approaches used to address those scenarios. This includes a brief survey of passive multistatic radar applications.

This dissertation presents a unique approach to combining TDOA and AOA measurements to reduce vertical angle error. The combination of TDOA and vertical AOA, rather than 2-angle AOA, was unique in the literature, Vertical-only AOA algorithms are uncommon in the literature[a]. This algorithm is unique in that it explicitly constrains the vertical position to the AOA measurement. The algorithm performs significantly better than linear TDOA in wide area multilateration scenarios. This paper has been published in a peer-reviewed journal [2].

[a] The first and only instance I found of a combined TDOA/1AOA algorithm was in a conference paper [127] published less than two months after my paper.

The second algorithm is a novel variation of the multilateration problem. The TDOA measurements normally constrain the solution to lie at the intersection of several spheres. In this approach, an *a priori*

estimate is used to approximate those spheres as planes, producing linear equations. When the approximation is sufficiently close to the true position of the target, the resulting equations are at least as accurate as conventional TDOA multilateration, and performs significantly better when the scenario employs receiver locations that are nearly coplanar. An iterative variation is presented that can improve the calculated position estimate when the original estimate is far enough from the true position that it contributes to the calculated position error. This algorithm is well-suited for use in tracking algorithms. This has been published in a peer-reviewed journal [3].

5.2 Future Work

The work presented in this dissertation suggests several areas for future research:

- The analysis in Ch. 2 focuses on a geometric understanding of the noise-free localization problem, including identifying similarities in the equations employed in solving the passive localization problem. The analysis of the problem with measurement noise is a significant undertaking in the papers cited in that chapter. There is significant commonality between the statistical analyses presented in those papers. This commonality can be explored and the statistical problem may potentially be generalized, which would make it easier to exploit the benefits of linear localization equations in general localization problems. Ideally this generalization would encompass the common TOA, TDOA, and AOA equations separately and together. This type of generalization has been done before for a more general localization problem [38, 39], which was later simplified into a more intuitive linear form [37].

- The literature review in this dissertation barely touched the massive body of work being produced on multistatic radars. It would be very beneficial for me to expand that review and identify the approaches, applications, implementations, and limitations of multistatic radar, and especially passive multistatic radar.

- The hybrid multilateration algorithm of Ch. 3 only works when the sensors are all oriented in the same direction. This is a reasonable assumption across relatively small areas where the local vertical only diverges slightly. Over larger areas, this divergence becomes much more pronounced. An alternative to the hybrid multilateration algorithm here would use a more arbitrary sensor orientation, such as the one described in [105]. This would be a more conventional TDOA/AOA algorithm, but I am unaware of any algorithm that employs that particular combination of measurements. This would be very similar to the approach in [127]. That paper is quite short and would benefit from a clearer presentation and more detailed

analysis, including analyzing how the spacing and orientation of the sensors affect the accuracy of the algorithm.

- The algorithm in Ch. 4 is merely the foundation of a more general tracking algorithm. The linear localization algorithm is well-suited for incorporation into a Kalman filter, which would need some work to develop explicitly. Some work would be required to determine an approach for swarm tracking using this algorithm, including the rules for updating both the individual object tracks and the swarm center estimate. This approach can also be combined with AOA or FDOA to create an even better estimate for tracking a target.

- It may be possible to apply the approach from the hybrid multilateration algorithm to the *a priori* algorithm presented here.

- The *a priori* algorithm can be combined with AOA or FDOA measurements in a more conventional concatenated linear system. Adding FDOA measurements, producing a direct estimate of the target velocity, would be a natural choice if the equations are incorporated into a tracking algorithm.

References

1 Grant, R., *The Radar Game: Understanding Stealth and Aircraft Survivability*, ser. Next American century series. IRIS Independent Research, 1998. cited on p. 1

2 Widdison, E. and Long, D. G., "Hybrid Multilateration and Triangulation," *Positioning*, vol. 12, 2021, pp. 1–15. DOI: 10.4236/pos.2021.121001 cited on pp. 2, 3, 11, 16, 21, 27, 49, 69

3 Widdison, E. and Long, D. G., "Multilateration Using A Priori Position Estimates," *IEEE Transactions on Radar Systems*, vol. 1, 2023, pp. 455–462. DOI: 10.1109/trs.2023.3305471 cited on pp. 2, 4, 49, 70

4 Widdison, E. and Long, D. G., "A Review of Linear Multilateration Techniques and Applications," *IEEE Access*, 2023, In Review. cited on pp. 2, 3, 5, 69, 89

5 106th Congress, *Public Law 106-81*, January 1999. URL: https://www.congress.gov/106/plaws/publ81/PLAW-106publ81.htm. cited on pp. 5, 22

6 Iliev, N. and Paprotny, I., "Review and Comparison of Spatial Localization Methods for Low-Power Wireless Sensor Networks," *IEEE Sensors Journal*, vol. 15, no. 10, 2015, pp. 5971–5987. DOI: 10.1109/jsen.2015.2450742 cited on p. 6

7 Gao, W., Kim, S., Bosse, H., Haitjema, H., Chen, Y., Lu, X., Knapp, W., Weckenmann, A., Estler, W., and Kunzmann, H., "Measurement technologies for precision positioning," *CIRP Annals*, vol. 64, no. 2, 2015, pp. 773–796. DOI: 10.1016/j.cirp.2015.05.009 cited on p. 6

8 Yang, T., Cabani, A., and Chafouk, H., "A Survey of Recent Indoor Localization Scenarios and Methodologies," *Sensors*, vol. 21, no. 23, 2021. DOI: 10.3390/s21238086 cited on p. 6

9 Tahat, A., Kaddoum, G., Yousefi, S., Valaee, S., and Gagnon, F., "A Look at the Recent Wireless Positioning Techniques With a Focus on Algorithms for Moving Receivers," *IEEE Access*, vol. 4, 2016, pp. 6652–6680. DOI: 10.1109/access.2016.2606486 cited on p. 6

10 Zhang, Q., Zhang, Q., Wu, Z., Zhao, Y., Li, H., and Pan, W., "Application overview and development trend of passive radar in civil aviation," *The Journal of Engineering*, vol. 2019, no. 20, 2019, pp. 6737–6740. DOI: 10.1049/joe.2019.0577 cited on p. 6

11 Marquardt, D. W., "An Algorithm for Least-Squares Estimation of Nonlinear Parameters," *Journal of the Society for Industrial and Applied Mathematics*, vol. 11, no. 2, 1963, pp. 431–441. DOI: 10.1137/0111030 cited on pp. 6, 11

12 FOY, W. H., "Position-Location Solutions by Taylor-Series Estimation," *IEEE Transactions on Aerospace and Electronic Systems*, vol. AES-12, no. 2, 1976, pp. 187–194. DOI: 10.1109/taes.1976.308294 cited on pp. 6, 49

cited on p. 6 13 McClarren, R. G., *Chapter 13 - open root finding methods*, *Computational Nuclear Engineering and Radiological Science Using Python*, McClarren, R. G., Ed., Academic Press, 2018, pp. 229–249. DOI: 10.1016/b978-0-12-812253-2.00015-7

cited on p. 7 14 Milnor, J., "On the concept of attractor," *Communications in Mathematical Physics*, vol. 99, no. 2, 1985, pp. 177–195. DOI: 10.1007/bf01212280

cited on pp. 7, 49 15 Kennedy, J. and Eberhart, R., "Particle swarm optimization," *Proceedings of ICNN'95 - International Conference on Neural Networks*, vol. 4, 1995, 1942–1948 vol.4. DOI: 10.1109/icnn.1995.488968

cited on pp. 7, 11, 49 16 Fresno, J. M., Robles, G., Martínez-Tarifa, J. M., and Stewart, B. G., "Survey on the Performance of Source Localization Algorithms," *Sensors*, vol. 17, no. 11, 2017. DOI: 10.3390/s17112666

cited on pp. 7, 23 17 Bin, Y. Z., Lei, W., Qun, C. P., and Nan, L. A., "Passive satellite localization using TDOA/FDOA/AOA measurements," *IEEE Conference Anthology*, 2013, pp. 1–5. DOI: 10.1109/anthology.2013.6784815

cited on pp. 7, 19, 20, 49 18 Bancroft, S., "An Algebraic Solution of the GPS Equations," *IEEE Transactions on Aerospace and Electronic Systems*, vol. AES-21, no. 1, 1985, pp. 56–59. DOI: 10.1109/taes.1985.310538

cited on pp. 7, 19, 49 19 Bucher, R. and Misra, D., "A Synthesizable VHDL Model of the Exact Solution for Three-dimensional Hyperbolic Positioning System," *VLSI Design*, vol. 15, no. 2, 2002, pp. 507–520. DOI: 10.1080/1065514021000012129

cited on pp. 7, 19 20 Smith, J. and Abel, J., "Closed-form least-squares source location estimation from range-difference measurements," *IEEE Transactions on Acoustics, Speech, and Signal Processing*, vol. 35, no. 12, 1987, pp. 1661–1669. DOI: 10.1109/tassp.1987.1165089

cited on pp. 7, 19 21 Friedlander, B., "A passive localization algorithm and its accuracy analysis," *IEEE Journal of Oceanic Engineering*, vol. 12, no. 1, 1987, pp. 234–245. DOI: 10.1109/joe.1987.1145216

cited on pp. 7, 11, 20, 24, 25, 28, 34, 49, 61, 89 22 Chan, Y. and Ho, K., "A simple and efficient estimator for hyperbolic location," *IEEE Transactions on Signal Processing*, vol. 42, no. 8, 1994, pp. 1905–1915. DOI: 10.1109/78.301830

cited on p. 8 23 Bishop, A. N., Fidan, B., Doğançay, K., Anderson, B. D., and Pathirana, P. N., "Exploiting geometry for improved hybrid AOA/TDOA-based localization," *Signal Processing*, vol. 88, no. 7, 2008, pp. 1775–1791. DOI: 10.1016/j.sigpro.2008.01.015

cited on pp. 8, 11 24 Chen, J., Hudson, R., and Yao, K., "Maximum-likelihood source localization and unknown sensor location estimation for wideband signals in the near-field," *IEEE Transactions on Signal Processing*, vol. 50, no. 8, 2002, pp. 1843–1854. DOI: 10.1109/tsp.2002.800420

cited on p. 8 25 Gaarder, N., "On estimating the location of a signal source," *IEEE Transactions on Information Theory*, vol. 15, no. 5, 1969, pp. 570–576. DOI: 10.1109/tit.1969.1054362

cited on pp. 8, 11

26 Norrdine, A., "Direkte Lösung des räumlichen Bogenschnitts mit Methoden der Linearen Algebra," *Allgemeine Vermessungs-Nachrichten (AVN)*, vol. 1, 2008, pp. 7–9.

27 Norrdine, A., "An Algebraic Solution to the Multilateration Problem," *2012 International Conference on Indoor Positioning and Indoor Navigation*, November 2012. cited on pp. 8, 11, 36, 49, 89

28 Bakhoum, E. G., "Closed-form solution of hyperbolic geolocation equations," *IEEE Transactions on Aerospace and Electronic Systems*, vol. 42, no. 4, 2006, pp. 1396–1404. DOI: 10.1109/taes.2006.314580 cited on pp. 8, 12

29 Heydari, A. and Aghabozorgi, M., "Joint RSSD/AOA Source Localization: Bias Analysis and Asymptotically Efficient Estimator," *Wireless Personal Communications*, vol. 114, 3 2020, pp. 2643–2661. DOI: 10.1007/s11277-020-07495-9 cited on pp. 8, 12, 14

30 Wang, J., Qin, Z., Gao, F., and Wei, S., "An Approximate Maximum Likelihood Algorithm for Target Localization in Multistatic Passive Radar," *Chinese Journal of Electronics*, vol. 28, no. 1, 2019, pp. 195–201. DOI: 10.1049/cje.2018.02.018 cited on pp. 8, 11, 24

31 Zhou, Y., Wang, Y., Nie, R., Cheng, Q., and Zhu, G., "Optimal Location Method of Spontaneous Data Fusion based on TDOA / AOA," *2021 OES China Ocean Acoustics (COA)*, 2021, pp. 885–889. DOI: 10.1109/coa50123.2021.9519960 cited on pp. 8, 14, 20, 49

32 Liu, Z., Zhao, Y., Jin, K., Hu, D., Wang, R., and Zhao, Y., "Algebraic distributed source localisation algorithm using TDOA and AOA measurements," *The Journal of Engineering*, vol. 2019, no. 19, 2019, pp. 5962–5966. DOI: 10.1049/joe.2019.0372 cited on pp. 8, 14, 20, 49

33 Huang, D., Zhao, Y., Hu, D., and Zhao, Y., "3D TDOA/AOA Localization in MIMO Passive Radar with Transmitter and Receiver Position Errors." *Mathematical Problems in Engineering*, 2022, pp. 1–15. DOI: 10.1155/2022/9964332 cited on pp. 8, 11, 14, 24

34 Kazemi, S. A. R., Amiri, R., and Behnia, F., "Efficient Convex Solution for 3-D Localization in MIMO Radars Using Delay and Angle Measurements," *IEEE Communications Letters*, vol. 23, no. 12, 2019, pp. 2219–2223. DOI: 10.1109/lcomm.2019.2948175 cited on pp. 8, 11, 14, 24, 25

35 Amiri, R., Behnia, F., and Zamani, H., "Efficient 3-D Positioning Using Time-Delay and AOA Measurements in MIMO Radar Systems," *IEEE Communications Letters*, vol. 21, no. 12, 2017, pp. 2614–2617. DOI: 10.1109/lcomm.2017.2742945 cited on pp. 8, 11, 14

36 Huang, G. and Zhu, Y., "Robust Localization in Distributed MIMO Radar Using Delay and Angle Measurements with Impulsive Noise Robust TD/AOA Localization in Impulsive Noise," *International Journal of Antennas and Propagation*, vol. 2021, Alejos, A., Ed., 2021, p. 1 531 234. DOI: 10.1155/2021/1531234 cited on pp. 8, 14, 24, 25

37 Lee, H. B., "Accuracy of Range-Range and Range-Sum Multilateration Systems," *IEEE Transactions on Aerospace and Electronic Systems*, vol. AES-11, no. 6, 1975, pp. 1346–1361. DOI: 10.1109/taes.1975.308191 cited on pp. 9, 27, 50, 59, 70

cited on pp. 9, 70
38 Lee, H. B., "A Novel Procedure for Assessing the Accuracy of Hyperbolic Multilateration Systems," *IEEE Transactions on Aerospace and Electronic Systems*, vol. AES-11, no. 1, 1975, pp. 2–15. DOI: 10.1109/taes.1975.308023

cited on pp. 9, 70
39 Lee, H. B., "Accuracy Limitations of Hyperbolic Multilateration Systems," *IEEE Transactions on Aerospace and Electronic Systems*, vol. AES-11, no. 1, 1975, pp. 16–29. DOI: 10.1109/taes.1975.308024

cited on p. 11
40 Wang, X., Wang, Z., and O'Dea, B., "A TOA-based location algorithm reducing the errors due to non-line-of-sight (NLOS) propagation," *IEEE Transactions on Vehicular Technology*, vol. 52, no. 1, 2003, pp. 112–116. DOI: 10.1109/tvt.2002.807158

cited on pp. 11, 14, 22, 49
41 Cong, L. and Zhuang, W., "Hybrid TDOA/AOA mobile user location for wideband CDMA cellular systems," *IEEE Transactions on Wireless Communications*, vol. 1, no. 3, 2002, pp. 439–447. DOI: 10.1109/twc.2002.800542

cited on pp. 11, 14, 21
42 Bachevsky, S. V., Fokin, G. A., Simonov, A. N., and Sevidov, V. V., "Positioning of radio emission sources with unmanned aerial vehicles using TDOA-AOA measurement processing," *Journal of Physics: Conference Series*, vol. 1368, no. 4, November 2019, p. 042 040. DOI: 10.1088/1742-6596/1368/4/042040

cited on pp. 11, 14, 24
43 Wang, J., Qin, Z., Bi, Y., Wei, S., and Luo, F., "Target localisation in multistatic radar using BR, TDOA, and AOA measurements," *The Journal of Engineering*, vol. 2019, no. 19, 2019, pp. 6052–6056. DOI: 10.1049/joe.2019.0128

cited on pp. 11, 22
44 Chan, Y.-T., Tsui, W.-Y., So, H.-C., and Ching, P.-c., "Time-of-arrival based localization under NLOS conditions," *IEEE Transactions on Vehicular Technology*, vol. 55, no. 1, 2006, pp. 17–24. DOI: 10.1109/tvt.2005.861207

cited on pp. 11, 22
45 Soleimani, M. A. and Sharafat, A. R., "A novel geometric approach for mitigating NLOS effects in wireless location estimation," *2011 19th Iranian Conference on Electrical Engineering*, 2011, pp. 1–6.

cited on pp. 11, 14, 20
46 Chang, A.-C. and Chang, J.-C., "Robust Mobile Location Estimation Using Hybrid TOA/AOA Measurements in Cellular Systems," *Wireless Personal Communications*, vol. 65, no. 1, 2012, pp. 1–13. DOI: 10.1007/s11277-011-0224-8

cited on pp. 11, 14, 22
47 Telung-Pan, Chang, J.-C., and Shen, C.-C., "Hybrid TOA/AOA measurements based on the Wiener estimator for cellular network," *2015 IEEE 12th International Conference on Networking, Sensing and Control*, 2015, pp. 405–409. DOI: 10.1109/icnsc.2015.7116071

cited on pp. 11, 23
48 Jheng, S.-L., Jan, S.-S., Chen, Y.-H., and Lo, S., "1090 MHz ADS-B-Based Wide Area Multilateration System for Alternative Positioning Navigation and Timing," *IEEE Sensors Journal*, vol. 20, no. 16, 2020, pp. 9490–9501. DOI: 10.1109/jsen.2020.2988514

cited on pp. 11, 14, 22
49 Zhang, V. Y., Wong, A. K.-s., Woo, K. T., and Ouyang, R. W., "Hybrid TOA/AOA-Based Mobile Localization with and without Tracking in CDMA Cellular Networks," *2010 IEEE Wireless Communication and Networking Conference*, 2010, pp. 1–6. DOI: 10.1109/wcnc.2010.5506585

50 Chan, Y., Chan, F., Read, W., Jackson, B., and Lee, B., "Hybrid localization of an emitter by combining angle-of-arrival and received signal strength measurements," *2014 IEEE 27th Canadian Conference on Electrical and Computer Engineering (CCECE)*, 2014, pp. 1–5. DOI: 10.1109/ccece.2014.6900968 cited on pp. 11, 12, 14

51 Chen, C.-L. and Feng, K.-T., "An efficient geometry-constrained location estimation algorithm for NLOS environments," *2005 International Conference on Wireless Networks, Communications and Mobile Computing*, vol. 1, 2005, 244–249 vol.1. DOI: 10.1109/wirles.2005.1549417 cited on pp. 11, 14, 22

52 Chen, C.-L. and Feng, K.-T., "Hybrid location estimation and tracking system for mobile devices," *2005 IEEE 61st Vehicular Technology Conference*, vol. 4, 2005, 2648–2652 Vol. 4. DOI: 10.1109/vetecs.2005.1543815 cited on pp. 11, 14, 22, 27

53 Abdul-Latif, O., Shepherd, P., and Pennock, S., "TDOA/AOA Data Fusion for Enhancing Positioning in an Ultra Wideband System," *2007 IEEE International Conference on Signal Processing and Communications*, 2007, pp. 1531–1534. DOI: 10.1109/icspc.2007.4728623 cited on pp. 11, 14, 20, 22

54 Feng, K.-T., Chen, C.-L., and Chen, C.-H., "GALE: An Enhanced Geometry-Assisted Location Estimation Algorithm for NLOS Environments," *IEEE Transactions on Mobile Computing*, vol. 7, no. 2, 2008, pp. 199–213. DOI: 10.1109/tmc.2007.70721 cited on pp. 11, 14, 20, 22

55 Tseng, P.-H. and Feng, K.-T., "Hybrid Network/Satellite-Based Location Estimation and Tracking Systems for Wireless Networks," *IEEE Transactions on Vehicular Technology*, vol. 58, no. 9, 2009, pp. 5174–5189. DOI: 10.1109/tvt.2009.2023222 cited on pp. 11, 14, 22, 27, 90

56 Noroozi, A. and Sebt, M. A., "Algebraic solution of source location estimation using TDOA and AOA measurements," *2017 Iranian Conference on Electrical Engineering (ICEE)*, 2017, pp. 1609–1614. DOI: 10.1109/iraniancee.2017.7985303 cited on pp. 11, 14, 20

57 Fokin, G., "Passive Geolocation with Unmanned Aerial Vehicles using TDOA-AOA Measurement Processing," *2019 21st International Conference on Advanced Communication Technology (ICACT)*, 2019, pp. 360–365. DOI: 10.23919/icact.2019.8702023 cited on pp. 11, 14, 21

58 Nguyen, N. H. and Doğançay, K., "Closed-Form Algebraic Solutions for Angle-of-Arrival Source Localization With Bayesian Priors," *IEEE Transactions on Wireless Communications*, vol. 18, no. 8, 2019, pp. 3827–3842. DOI: 10.1109/twc.2019.2918516 cited on pp. 11, 14, 21

59 Ma, C., Klukas, R., and Lachapelle, G., "An enhanced two-step least squared approach for TDOA/AOA wireless location," *IEEE International Conference on Communications, 2003. ICC '03.* Vol. 2, 2003, 987–991 vol.2. DOI: 10.1109/icc.2003.1204495 cited on pp. 11, 14, 20

60 Li, W., Tang, Q., Huang, C., Ren, C., and Li, Y., "A New Close Form Location Algorithm with AOA and TDOA for Mobile User," *Wireless Personal Communications*, vol. 97, 2 2017, pp. 3061–3080. DOI: 10.1007/s11277-017-4661-x cited on pp. 11, 14, 20

cited on pp. 11, 14, 21, 27

[61] Zhang, F., Sun, Y., and Wan, Q., "Calibrating the error from sensor position uncertainty in TDOA-AOA localization," *Signal Processing*, vol. 166, 2020, p. 107 213. DOI: 10.1016/j.sigpro.2019.07.006 cited on pp. 11, 14, 23

[62] Zhang, Z., Lin, Y., and Jin, B., "Underwater TDOA/AOA joint localization algorithm based on hybrid invasive weed optimization algorithm," *IET Communications*, vol. 15, no. 19, 2021, pp. 2376–2389. DOI: 10.1049/cmu2.12277 cited on pp. 11, 22

[63] Abdulla, Y., El-Hennawy, H., and Mahrous, S., "The effect of base stations configurations on the accuracy of hyperbolic position location in macro-cellular and microcellular GSM systems," *Proceedings of the Eighteenth National Radio Science Conference. NRSC'2001 (IEEE Cat. No.01EX462)*, vol. 1, 2001, 303–313 vol.1. DOI: 10.1109/nrsc.2001.929240 cited on pp. 11, 17, 19, 49

[64] Ho, K. and Xu, W., "An accurate algebraic solution for moving source location using TDOA and FDOA measurements," *IEEE Transactions on Signal Processing*, vol. 52, no. 9, 2004, pp. 2453–2463. DOI: 10.1109/tsp.2004.831921 cited on pp. 11, 12, 22

[65] Mahajan, S. and Singh, Y. N., "Enhanced mobile station localization using a hybrid TOA/AOA map-matching algorithm," *TENCON 2009 - 2009 IEEE Region 10 Conference*, 2009, pp. 1–6. DOI: 10.1109/tencon.2009.5396198 cited on pp. 11, 22, 27

[66] Chen, C.-Y. and Wu, W.-R., "Three-Dimensional Positioning for LTE Systems," *IEEE Transactions on Vehicular Technology*, vol. 66, no. 4, 2017, pp. 3220–3234. DOI: 10.1109/tvt.2016.2593697 cited on pp. 11, 23

[67] Zhang, L., Zhang, T., Shin, H.-S., and Xu, X., "Efficient Underwater Acoustical Localization Method Based On Time Difference and Bearing Measurements," *IEEE Transactions on Instrumentation and Measurement*, vol. 70, 2021, pp. 1–16. DOI: 10.1109/tim.2020.3045193 cited on pp. 11, 21, 22

[68] Wu, S., Feng, Q., Huang, W., and Xu, K., "Linear Cooperative Localization Algorithm with TOA/ AOA/ AOD and Multipath," *2021 World Conference on Computing and Communication Technologies (WCCCT)*, 2021, pp. 47–51. DOI: 10.1109/wccct52091.2021.00016 cited on pp. 11, 22

[69] Son, J., Keum, I., Ahn, Y., and Shim, B., "D-TLoc: Deep Learning-aided Hybrid TDOA/AOA-based Localization," *2022 IEEE VTS Asia Pacific Wireless Communications Symposium (APWCS)*, 2022, pp. 47–50. DOI: 10.1109/apwcs55727.2022.9906489 cited on pp. 11, 14, 22

[70] Chen, H.-Y. and Chou, T.-Y., "Hybrid TDOA/AOA Mobile User Location with Artificial Neural Networks," *2008 IEEE International Conference on Networking, Sensing and Control*, 2008, pp. 847–852. DOI: 10.1109/icnsc.2008.4525334 cited on pp. 11, 14, 20

[71] Nur-A-Alam, M. and Haque, M. M., "A least square approach for TDOA/AOA wireless location in WCDMA system," *2008 11th International Conference on Computer and Information Technology*, 2008, pp. 686–690. DOI: 10.1109/iccitechn.2008.4803072 cited on pp. 11, 14, 20, 27

72 Xinghu, Z., Tan Sihong, S., and Yew Hong, T., "An integrated closed-form fusion algorithm for TDOA/AOA," *2016 19th International Conference on Information Fusion (FUSION)*, 2016, pp. 1622–1629.

73 Chaitanya, D. E. and Rao, G. S., "Unknown Radio Source Localization Based on a Modified Closed form Solution Using TDOA Measurement Technique," *Procedia Computer Science*, vol. 87, 2016, pp. 184–189. DOI: 10.1016/j.procs.2016.05.146 cited on p. 12

74 Ketabalian, H., Biguesh, M., and Sheikhi, A., "A Closed-Form Solution for Localization Based on RSS," *IEEE Transactions on Aerospace and Electronic Systems*, vol. 56, no. 2, 2020, pp. 912–923. DOI: 10.1109/taes.2019.2929998 cited on p. 12

75 Ho, K. C. and Sun, M., "Passive Source Localization Using Time Differences of Arrival and Gain Ratios of Arrival," *IEEE Transactions on Signal Processing*, vol. 56, no. 2, 2008, pp. 464–477. DOI: 10.1109/tsp.2007.906728 cited on pp. 12, 49

76 Luo, J.-A., Zhang, X.-P., and Wang, Z., "A new passive source localization method using AOA-GROA-TDOA in wireless sensor array networks and its Cramér-Rao bound analysis," *2013 IEEE International Conference on Acoustics, Speech and Signal Processing*, 2013, pp. 4031–4035. DOI: 10.1109/icassp.2013.6638416 cited on pp. 12, 14

77 Ji-An, L., Si-Wei, P., Dong-Liang, P., Zhi, W., and Yan-Jun, L., "Source Localization in Acoustic Sensor Networks via Constrained Least-Squares Optimization Using AOA and GROA Measurements." *Sensors (14248220)*, vol. 18, no. 4, 2018, p. 937. DOI: 10.3390/s18040937 cited on pp. 12, 14, 23

78 Li, W., Wang, L., Xiao, M., Li, Y., and Zhang, H., "Closed Form Solution for 3D Localization Based on Joint RSS and AOA Measurements for Mobile Communications," *IEEE Access*, vol. 8, 2020, pp. 12 632–12 643. DOI: 10.1109/access.2019.2962811 cited on pp. 12, 14

79 Sun, T. and Dong, C., "Efficient source positioning method based on two stations using GROA and AOA measurements," *IET Signal Processing*, vol. 14, no. 2, 2020, pp. 56–63. DOI: 10.1049/iet-spr.2019.0003 cited on p. 12

80 Luo, J.-A., Zhang, X.-P., Wang, Z., and Lai, X.-P., "On the Accuracy of Passive Source Localization Using Acoustic Sensor Array Networks," *IEEE Sensors Journal*, vol. 17, no. 6, 2017, pp. 1795–1809. DOI: 10.1109/jsen.2017.2657646 cited on pp. 12, 23

81 Le, A. T., Tran, L. C., Huang, X., Ritz, C., Dutkiewicz, E., Phung, S. L., Bouzerdoum, A., and Franklin, D., "Unbalanced Hybrid AOA/RSSI Localization for Simplified Wireless Sensor Networks." *Sensors (14248220)*, vol. 20, no. 14, 2020, p. 3838. DOI: 10.3390/s20143838 cited on pp. 12, 21

82 Zeng, Y. and Li, O., "A new algorithm for signal emitter recognition," *2010 International Conference on Image Analysis and Signal Processing*, 2010, pp. 446–449. DOI: 10.1109/iasp.2010.5476079 cited on pp. 14, 23

83 Deligiannis, N. and Louvros, S., "Hybrid TOA–AOA Location Positioning Techniques in GSM Networks," *Wireless Personal Communications*, vol. 54, 2 2010, pp. 321–348. DOI: 10.1007/s11277-009-9728-x cited on pp. 14, 22

cited on pp. 14, 20

84 Dhara, S., Koley, C., and Chakravorti, S., "Methods for Localization of Partial Discharge Sources within Air Insulated Electrical Substation," *2018 20th National Power Systems Conference (NPSC)*, 2018, pp. 1–6. DOI: 10.1109/npsc.2018.8771788

cited on pp. 14, 22

85 Luo, R., Yan, L., Deng, P., and Kuang, Y., "Hybrid TOA/AOA Virtual Station Localization Based on Scattering Signal Identification for GNSS-Denied Urban or Indoor NLOS Environments," *Applied Sciences*, vol. 12, no. 23, 2022. DOI: 10.3390/app122312157

cited on pp. 14, 23

86 Liu, Z., Stevens, N., and Conde, M. H., "Visible Light Positioning Using Arrays of Time-of- Flight Pixels," *2022 IEEE Sensors*, 2022, pp. 1–4. DOI: 10.1109/sensors52175.2022.9967030

cited on pp. 14, 19, 20

87 McDonald, K. and Kuklinski, W., "Track maintenance and positional estimation via ground moving target indicator and geolocation data fusion," *Proceedings of the 2001 IEEE Radar Conference (Cat. No.01CH37200)*, 2001, pp. 239–245. DOI: 10.1109/nrc.2001.922984

cited on pp. 14, 20, 22

88 Zhang, V. Y. and Wong, A. K.-S., "Combined AOA and TOA NLOS Localization With Nonlinear Programming in Severe Multipath Environments," *2009 IEEE Wireless Communications and Networking Conference*, 2009, pp. 1–6. DOI: 10.1109/wcnc.2009.4917631

cited on pp. 14, 21

89 Shao, H.-J., Zhang, X.-P., and Wang, Z., "Novel closed-form auxiliary variables based algorithms for sensor node localization using AOA," *2014 IEEE International Conference on Acoustics, Speech and Signal Processing (ICASSP)*, 2014, pp. 1414–1418. DOI: 10.1109/icassp.2014.6853830

cited on pp. 14, 19, 22, 49

90 Ramlall, R., Chen, J., and Swindlehurst, A. L., "Non-line-of-sight mobile station positioning algorithm using TOA, AOA, and Doppler-shift," *2014 Ubiquitous Positioning Indoor Navigation and Location Based Service (UPINLBS)*, 2014, pp. 180–184. DOI: 10.1109/upinlbs.2014.7033726

cited on pp. 14, 19

91 Yin, J., Wan, Q., Yang, S., and Ho, K. C., "A Simple and Accurate TDOA-AOA Localization Method Using Two Stations," *IEEE Signal Processing Letters*, vol. 23, no. 1, 2016, pp. 144–148. DOI: 10.1109/lsp.2015.2505138

cited on pp. 14, 21

92 Kalpana, R. and Baskaran, M., "TAR: TOA-AOA Based Random Transmission Directed Localization," *Wireless Personal Communications*, vol. 90, 2 2016, pp. 889–902. DOI: 10.1007/s11277-016-3237-5

cited on pp. 14, 19

93 Sun, Y., Zhou, Z.-p., Tang, S.-l., Ding, X. K., Yin, J., and Wan, Q., "3D hybrid TOA-AOA source localization using an active and a passive station," *2016 IEEE 13th International Conference on Signal Processing (ICSP)*, 2016, pp. 257–260. DOI: 10.1109/icsp.2016.7877836

cited on pp. 14, 20

94 Hao, B., Zhao, Y., Li, Z., and Wan, P., "A sensor selection method for TDOA and AOA localization in the presence of sensor errors," *2017 IEEE/CIC International Conference on Communications in China (ICCC)*, 2017, pp. 1–6. DOI: 10.1109/iccchina.2017.8330350

cited on pp. 14, 16

95 Wang, Y. and Ho, K. C., "TDOA Positioning Irrespective of Source Range," *IEEE Transactions on Signal Processing*, vol. 65, no. 6, 2017, pp. 1447–1460. DOI: 10.1109/tsp.2016.2630030

96 Zhao, Y., Li, Z., Hao, B., Si, J., and Wan, P., "Bias reduced method for TDOA and AOA localization in the presence of sensor errors," *2017 IEEE International Conference on Communications (ICC)*, 2017, pp. 1–6. DOI: 10.1109/icc.2017.7997043 cited on pp. 14, 20, 49

97 Hung Nguyen, N. and Doğançay, K., "Improved Weighted Instrumental Variable Estimator for Doppler-Bearing Source Localization in Heavy Noise," *2018 IEEE International Conference on Acoustics, Speech and Signal Processing (ICASSP)*, 2018, pp. 3529–3533. DOI: 10.1109/icassp.2018.8461284 cited on pp. 14, 21

98 Wang, Y. and Ho, K. C., "Unified Near-Field and Far-Field Localization for AOA and Hybrid AOA-TDOA Positionings," *IEEE Transactions on Wireless Communications*, vol. 17, no. 2, 2018, pp. 1242–1254. DOI: 10.1109/twc.2017.2777457 cited on pp. 14, 16

99 Wang, Y., Ho, K., and Wang, G., "A Unified Estimator for Source Positioning and DOA Estimation Using AOA," *2018 IEEE International Conference on Acoustics, Speech and Signal Processing (ICASSP)*, 2018, pp. 3201–3205. DOI: 10.1109/icassp.2018.8461492 cited on pp. 14, 16

100 Zhao, Y., Qi, W., Liu, P., Chen, L., and Lin, J., "Accurate 3D localisation of mobile target using single station with AOA–TDOA measurements," *IET Radar, Sonar & Navigation*, vol. 14, no. 6, 2020, pp. 954–965. DOI: 10.1049/iet-rsn.2019.0600 cited on pp. 14, 21

101 Zhou, R., Chen, J., Tan, W., Yan, Q., and Cai, C., "Optimal 3D Angle of Arrival Sensor Placement with Gaussian Priors," *Entropy*, vol. 23, no. 11, 2021. DOI: 10.3390/e23111379 cited on pp. 14, 22

102 Xiang, P., Wang, G., and Ho, D. K. C., "Bias Reduced Semidefinite Relaxation Method for AOA Object Localization in 3-D," *2022 IEEE 12th Sensor Array and Multichannel Signal Processing Workshop (SAM)*, 2022, pp. 91–95. DOI: 10.1109/sam53842.2022.9827814 cited on pp. 14, 21

103 Zhou, R., Chen, J., Tan, W., and Cai, C., "Sensor Selection for Optimal Target localization with 3-D Angle of Arrival Estimation in Underwater Wireless Sensor Networks," *Journal of Marine Science and Engineering*, vol. 10, no. 2, 2022. DOI: 10.3390/jmse10020245 cited on pp. 14, 23

104 Imani, S., Peimany, M., Hasankhan, M. J., and Feraidooni, M. M., "Bistatic target localization based on inaccurate TDOA-AOA measurements," *Signal, Image and Video Processing*, vol. 16, 1 2022, pp. 239–245. DOI: 10.1007/s11760-021-01985-4 cited on pp. 14, 20

105 Sun, Y., Ho, K. C., Gao, L., Zou, J., Yang, Y., and Chen, L., "Three Dimensional Source Localization Using Arrival Angles from Linear Arrays: Analytical Investigation and Optimal Solution," *IEEE Transactions on Signal Processing*, vol. 70, 2022, pp. 1864–1879. DOI: 10.1109/tsp.2022.3163889 cited on pp. 14, 21, 34, 70

106 Zou, J., Sun, Y., and Wan, Q., "A Novel 3-D Localization Scheme Using 1-D Angle Measurements," *IEEE Sensors Letters*, vol. 4, no. 6, 2020, pp. 1–4. DOI: 10.1109/lsens.2020.2992704 cited on pp. 14, 21

cited on p. 15

[107] Lee, Y. W., Kim, J. S., and Chung, W. G., "Position location error analysis by AOA and TDOA using a common channel model for CDMA cellular environments," *VTC2000-Spring. 2000 IEEE 51st Vehicular Technology Conference Proceedings (Cat. No.00CH37026)*, vol. 3, 2000, 2394–2397 vol.3. DOI: 10.1109/vetecs.2000.851701

cited on p. 15

[108] Kim, J. and Chung, W., "A spatio-temporal channel model for position location techniques via AOA and TDOA," *IEEE VTS 53rd Vehicular Technology Conference, Spring 2001. Proceedings (Cat. No.01CH37202)*, vol. 1, 2001, 233–237 vol.1. DOI: 10.1109/vetecs.2001.944838

cited on p. 16

[109] Sun, Y., Ho, K. C., and Wan, Q., "Eigenspace Solution for AOA Localization in Modified Polar Representation," *IEEE Transactions on Signal Processing*, vol. 68, 2020, pp. 2256–2271. DOI: 10.1109/tsp.2020.2981773

cited on pp. 19, 20, 49

[110] Ho, K. and Chan, Y., "Geolocation of a known altitude object from TDOA and FDOA measurements," *IEEE Transactions on Aerospace and Electronic Systems*, vol. 33, no. 3, 1997, pp. 770–783. DOI: 10.1109/7.599239

cited on pp. 19, 24, 25

[111] Shi, Y. F., Park, S. H., and Song, T. L., "Multitarget tracking in cluttered environment for a multistatic passive radar system under the DAB/DVB network," *EURASIP Journal on Advances in Signal Processing*, vol. 2017, no. 1, 2017, p. 11. DOI: 10.1186/s13634-017-0445-4

cited on pp. 19, 24

[112] Hack, D. E., Patton, L. K., Kerrick, A. D., and Saville, M. A., "Direct Cartesian detection, localization, and de-ghosting for passive multistatic radar," *2012 IEEE 7th Sensor Array and Multichannel Signal Processing Workshop (SAM)*, 2012, pp. 45–48. DOI: 10.1109/sam.2012.6250538

cited on pp. 19, 24

[113] Jie, S., Fu-qing, C., Cai-sheng, Z., and You, H., "Experimental results of maritime moving target detection based on passive bistatic radar using non-cooperative radar illuminators," *The Journal of Engineering*, vol. 2019, no. 20, 2019, pp. 6763–6766. DOI: 10.1049/joe.2019.0586

cited on pp. 19, 24, 25

[114] Li, X., Zhao, C., Lu, X., and Wei, W., "DA-PMHT for Multistatic Passive Radar Multitarget Tracking in Dense Clutter Environment," *IEEE Access*, vol. 7, 2019, pp. 49 316–49 326. DOI: 10.1109/access.2019.2907789

cited on pp. 19, 24, 25

[115] Lyu, X. and Wang, J., "Sequential Multi-Sensor JPDA for Target Tracking in Passive Multi-Static Radar With Range and Doppler Measurements," *IEEE Access*, vol. 7, 2019, pp. 34 488–34 498. DOI: 10.1109/access.2019.2905265

cited on pp. 19, 24

[116] Tong, J., Gaoming, H., Wei, T., and Huafu, P., "Cramér–Rao Lower Bound Analysis for Stochastic Model Based Target Parameter Estimation in Multistatic Passive Radar With Direct-Path Interference," *IEEE Access*, vol. 7, 2019, pp. 106 761–106 772. DOI: 10.1109/access.2019.2926353

cited on pp. 19, 24

[117] Zhao, Z., Zhou, X., Weng, T., Zhou, X., and Zhang, K., "Target detection approach for DRM-based passive bistatic radar," *The Journal of Engineering*, vol. 2019, no. 21, 2019, pp. 7868–7871. DOI: 10.1049/joe.2019.0657

cited on pp. 19, 24

[118] Zaimbashi, A. and Greco, M. S., "Multistatic Passive Radar Target Detection Under Uncalibrated Receivers With Direct-Path Interference," *IEEE Transactions on Aerospace and Electronic Systems*, vol. 58, no. 6, 2022, pp. 5443–5455. DOI: 10.1109/taes.2022.3171532

119 Malanowski, M. and Kulpa, K., "Two Methods for Target Localization in Multistatic Passive Radar," *IEEE Transactions on Aerospace and Electronic Systems*, vol. 48, no. 1, 2012, pp. 572–580. DOI: 10.1109/taes.2012.6129656 cited on pp. 19, 25

120 Malanowski, M., *Signal Processing for Passive Bistatic Radar*. Artech House, 2019. cited on p. 19

121 Nicholas J., W., *Bistatic Radar.* SciTech Publishing, 2005. cited on p. 19

122 Rui, L. and Ho, K. C., "Bias analysis of source localization using the maximum likelihood estimator," *2012 IEEE International Conference on Acoustics, Speech and Signal Processing (ICASSP)*, 2012, pp. 2605–2608. DOI: 10.1109/icassp.2012.6288450 cited on p. 20

123 Loyez, C., Bocquet, M., and Haddadi, K., "Six-Port Technology for 5G Millimeter-Wave Localization Systems," *2018 International Conference on Electromagnetics in Advanced Applications (ICEAA)*, 2018, pp. 272–275. DOI: 10.1109/iceaa.2018.8520353 cited on p. 20

124 Hu, B., Tian, H., and Fan, S., "Millimeter Wave LOS/NLOS Identification and Localization via Mean-Shift Clustering," *2019 IEEE 30th Annual International Symposium on Personal, Indoor and Mobile Radio Communications (PIMRC)*, 2019, pp. 1–7. DOI: 10.1109/pimrc.2019.8904260 cited on pp. 20, 22

125 Xu, C., Wang, Z., Wang, Y., Wang, Z., and Yu, L., "Three Passive TDOA-AOA Receivers-Based Flying-UAV Positioning in Extreme Environments," *IEEE Sensors Journal*, vol. 20, no. 16, 2020, pp. 9589–9595. DOI: 10.1109/jsen.2020.2988920 cited on pp. 20, 22

126 Le, A. T., Tran, L. C., Huang, X., Ritz, C., Dutkiewicz, E., Bouzerdoum, A., and Franklin, D., "Hybrid TOA/AOA Localization with 1D Angle Estimation in UAV-assisted WSN," *2020 14th International Conference on Signal Processing and Communication Systems (ICSPCS)*, 2020, pp. 1–6. DOI: 10.1109/icspcs50536.2020.9310043 cited on p. 21

127 Hu, Q., Peng, Y., Wan, Q., Hu, Z., Wang, Z., and Zhu, Y., "A Novel 3-D Localization Scheme Using 1-D AOA and TDOA Measurements," *2021 IEEE 94th Vehicular Technology Conference (VTC2021-Fall)*, 2021, pp. 1–5. DOI: 10.1109/vtc2021-fall52928.2021.9625269 cited on pp. 21, 27, 69, 70

128 Tu, X., Zhang, H., Cui, X., and Gulliver, T. A., "3-D TDOA/AOA location based on Extended Kalman Filter," *Proceedings of the 9th International Symposium on Antennas, Propagation and EM Theory*, 2010, pp. 473–476. DOI: 10.1109/isape.2010.5696504 cited on p. 21

129 Chen, M., Mao, X., and Zhao, C., "Direct Localization of Emitters Based on Sparse Bayesian Learning," *IEEE Transactions on Vehicular Technology*, vol. 68, no. 6, 2019, pp. 5769–5781. DOI: 10.1109/tvt.2019.2910831 cited on p. 21

130 Zhang, H., Cui, X., An, B., and Gulliver, T. A., "A distance and angle estimated method based on single UWB station," *2013 IEEE International Conference on Signal Processing, Communication and Computing (ICSPCC 2013)*, 2013, pp. 1–6. DOI: 10.1109/icspcc.2013.6663885 cited on p. 21

131 Osa, V., Matamales, J., Monserrat, J. F., and López, J., "Localization in Wireless Networks: The Potential of Triangulation Techniques," *Wireless Personal Communications*, vol. 68, no. 4, 2013, pp. 1525–1538. DOI: 10.1007/s11277-012-0537-2

cited on p. 21

132 Le, T.-K. and Ho, K. C., "Joint Source and Sensor Localization by Angles of Arrival," *IEEE Transactions on Signal Processing*, vol. 68, 2020, pp. 6521–6534. DOI: 10.1109/tsp.2020.3037412

cited on p. 22

133 Meng, W., Xie, L., and Xiao, W., "Communication Aware Optimal Sensor Motion Coordination for Source Localization," *IEEE Transactions on Instrumentation and Measurement*, vol. 65, no. 11, 2016, pp. 2505–2514. DOI: 10.1109/tim.2016.2596078

cited on p. 22

134 Dai, Z., Wang, G., and Chen, H., "Sensor Selection for TDOA-Based Source Localization Using Angle and Range Information," *IEEE Transactions on Aerospace and Electronic Systems*, vol. 57, no. 4, 2021, pp. 2597–2604. DOI: 10.1109/taes.2021.3061826

cited on pp. 22, 49

135 Caffery, J. and Stuber, G., "Overview of radiolocation in CDMA cellular systems," *IEEE Communications Magazine*, vol. 36, no. 4, 1998, pp. 38–45. DOI: 10.1109/35.667411

cited on p. 22

136 Ballal, T. and Bleakley, C. J., "3D location and orientation estimation using Angle of Arrival," *2009 IEEE International Symposium on Intelligent Signal Processing*, 2009, pp. 21–26. DOI: 10.1109/wisp.2009.5286580

cited on p. 22

137 Xie, Y., Wang, Y., and You, X., "Closed-form location estimator from TOA/AOA/AOD measurements in MIMO communication systems," *2009 IEEE Sarnoff Symposium*, 2009, pp. 1–6. DOI: 10.1109/sarnof.2009.4850277

cited on p. 23

138 Chang, Y. T., Wu, C. L., and Cheng, H. C., "Integrated Cross-Correlation and Genetic Algorithm to Improve TDOA-Based Locating System in Preventing Radio Interference," *2014 International Symposium on Computer, Consumer and Control*, 2014, pp. 1078–1081. DOI: 10.1109/is3c.2014.281

cited on p. 23

139 Chang, Y.-T., "Simulation and Implementation of an Integrated TDOA/AOA Monitoring System for Preventing Broadcast Interference," *Journal of Applied Research and Technology*, vol. 12, no. 6, 2014, pp. 1051–1062. DOI: 10.1016/s1665-6423(14)71665-7

cited on pp. 23, 27

140 Kakubari, Y., Koga, T., Miyazaki, H., Shimada, H., and Nihei, S., "Enhancement of Passive Surveillance System for Airport Surface Movement," *Electronics & Communications in Japan*, vol. 97, no. 3, 2014, pp. 24–30. DOI: 10.1002/ecj.11525

cited on pp. 23, 27

141 Filip-Dhaubhadel, A., Bellido-Manganell, M. A., Gräupl, T., and Schnell, M., "Feasibility Assessment of LDACS-Based Wide Area Multilateration," *2022 IEEE/AIAA 41st Digital Avionics Systems Conference (DASC)*, 2022, pp. 1–10. DOI: 10.1109/dasc55683.2022.9925808

cited on pp. 23, 25

142 Mandlik, M. and Nemec, Z., "An accurate Time-Difference measurement method for passive radar applications," *2013 23rd International Conference Radioelektronika (RADIOELEKTRONIKA)*, 2013, pp. 406–409. DOI: 10.1109/radioelek.2013.6530953

143 Alia, L., Italiano, A., and Pozzi, F., "Advanced tools to analyze the expected performance of multilateration and wide area multilateration," *2014 Tyrrhenian International Workshop on Digital Communications - Enhanced Surveillance of Aircraft and Vehicles (TIWDC/ESAV)*, 2014, pp. 82–86. DOI: 10.1109/tiwdc-esav.2014.6945453 cited on pp. 23, 27

144 Kwon, S., Choi, Y., Moon, S., You, C., Liu, H., Kim, J.-H., Kim, D. J., Park, H., Kim, J. Y., and Hwang, I., "Performance Enhancement of Hybrid TDOA/AOA Using Multipath Delay Estimation," *Wireless Personal Communications*, vol. 115, 3 2020, pp. 2551–2568. DOI: 10.1007/s11277-020-07696-2 cited on p. 23

145 Kwon, S., Choi, Y., Moon, S., You, C., Liu, H., Kim, J.-H., Kim, D. J., Park, H., Kim, J. Y., and Hwang, I., "Performance Enhancement of Hybrid TDOA/AOA Using Multipath Delay Estimation," *Wireless Personal Communications*, vol. 115, 3 2020, pp. 2551–2568. DOI: 10.1007/s11277-020-07696-2 cited on p. 23

146 Chen, Y. and Kobayashi, H., "System design and analysis of repeating GPS," *ITSC 2001. 2001 IEEE Intelligent Transportation Systems. Proceedings (Cat. No.01TH8585)*, 2001, pp. 2–5. DOI: 10.1109/itsc.2001.948619 cited on p. 23

147 LI, W., CHEN, R., GUO, Y., and FU, C., "Closed form algorithm of double-satellite TDOA + AOA localization based on WGS-84 model," *Chinese Journal of Aeronautics*, vol. 32, no. 10, 2019, pp. 2354–2367. DOI: 10.1016/j.cja.2019.05.016 cited on p. 23

148 Hanh, N. Q., Reju, V. G., and Khong, A. W. H., "Impact Localization on Rigid Surfaces Using Hermitian Angle Distribution for Human–Computer Interface Applications," *IEEE Transactions on Multimedia*, vol. 20, no. 6, 2018, pp. 1448–1461. DOI: 10.1109/tmm.2017.2772441 cited on p. 23

149 Zhou, R., Chen, J., Tan, W., Yuan, H., and Cai, C., "Sensor Selection for Hybrid AOA-TOA Localization with Correlated Measurement Noise in Underwater Wireless Sensor Networks," *Wireless Communications and Mobile Computing*, vol. 2022, Esmaiel, H., Ed., 2022, p. 2 779 760. DOI: 10.1155/2022/2779760 cited on p. 23

150 Wang, G. and Ho, K. C., "Accurate Semidefinite Relaxation Method for 3-D Rigid Body Localization Using AOA," *ICASSP 2020 - 2020 IEEE International Conference on Acoustics, Speech and Signal Processing (ICASSP)*, 2020, pp. 4955–4959. DOI: 10.1109/icassp40776.2020.9054338 cited on p. 24

151 Wang, G., Ho, K. C., and Chen, X., "Bias Reduced Semidefinite Relaxation Method for 3-D Rigid Body Localization Using AOA," *IEEE Transactions on Signal Processing*, vol. 69, 2021, pp. 3415–3430. DOI: 10.1109/tsp.2021.3086360 cited on p. 24

152 Rui, L. and Ho, K. C., "Elliptic Localization: Performance Study and Optimum Receiver Placement," *IEEE Transactions on Signal Processing*, vol. 62, no. 18, 2014, pp. 4673–4688. DOI: 10.1109/tsp.2014.2338835 cited on p. 24

153 Huang, J. H., Barr, M. N., Garry, J. L., and Smith, G. E., "Subarray processing for passive radar localization," *2017 IEEE Radar Conference (RadarConf)*, 2017, pp. 0248–0252. DOI: 10.1109/radar.2017.7944206 cited on pp. 24, 25

cited on p. 24 154 Daun, M., Nickel, U., and Koch, W., "Tracking in multistatic passive radar systems using DAB/DVB-T illumination," *Signal Processing*, vol. 92, no. 6, 2012, pp. 1365–1386. DOI: 10.1016/j.sigpro.2011.09.005

cited on p. 24 155 Lü, M., Yi, J., Wan, X., and Liu, Y., "Experimental research of drone monitoring using multi-static passive radar," *The Journal of Engineering*, vol. 2019, no. 20, 2019, pp. 6795–6798. DOI: 10.1049/joe.2019.0580

cited on p. 25 156 Renzo, M. D., Debbah, M., Phan-Huy, D.-T., Zappone, A., Alouini, M.-S., Yuen, C., Sciancalepore, V., Alexandropoulos, G. C., Hoydis, J., Gacanin, H., Rosny, J. de, Bounceu, A., Lerosey, G., and Fink, M., "Smart Radio Environments Empowered by AI Reconfigurable Meta-Surfaces: An Idea Whose Time Has Come," *EURASIP Journal on Wireless Communications and Networking*, vol. 2019, 2019, pp. 1–20. DOI: 10.48550/arxiv.1903.08925

cited on p. 25 157 Bazzi, A. and Chafii, M., *RIS-Enabled Passive Radar towards Target Localization*, 2022

cited on p. 25 158 Loschmidt, P., Gaderer, G., Simanic, N., Hussain, A., and Moreira, P., "White rabbit - sensor/actuator protocol for the CERN LHC particle accelerator," *SENSORS, 2009 IEEE*, 2009, pp. 781–786. DOI: 10.1109/icsens.2009.5398529

cited on p. 49 159 Mantilla-Gaviria, I. A., Leonardi, M., Balbastre-Tejedor, J. V., and de los Reyes, E., "On the application of singular value decomposition and Tikhonov regularization to ill-posed problems in hyperbolic passive location," *Mathematical and Computer Modelling*, vol. 57, no. 7, 2013, pp. 1999–2008. DOI: 10.1016/j.mcm.2012.03.004

cited on p. 49 160 Pourkhaatoun, M. and (Reza) Zekavat, S. A., "TOA estimation techniques: A comparison," *Handbook of Position Location*. John Wiley & Sons, Ltd, 2018, ch. 7, pp. 237–267. DOI: 10.1002/9781119434610.ch7

cited on p. 57 161 Scharf, L. and Demeure, C., *Statistical Signal Processing: Detection, Estimation, and Time Series Analysis*, ser. Addison-Wesley series in electrical and computer engineering. Addison-Wesley Publishing Company, 1991.

cited on p. 61 162 Chaffee, J. and Abel, J., "GDOP and the Cramer-Rao bound," *Proceedings of 1994 IEEE Position, Location and Navigation Symposium - PLANS'94*, 1994, pp. 663–668. DOI: 10.1109/plans.1994.303374

cited on p. 62 163 Musin, O. R. and Tarasov, A. S., "The Tammes Problem for N = 14," *Experimental Mathematics*, vol. 24, no. 4, 2015, pp. 460–468. DOI: 10.1080/10586458.2015.1022842

cited on p. 62 164 Fontanelli, D., Shamsfakhr, F., and Palopoli, L., "Cramer–Rao Lower Bound Attainment in Range-Only Positioning Using Geometry: The G-WLS," *IEEE Transactions on Instrumentation and Measurement*, vol. 70, 2021, pp. 1–14. DOI: 10.1109/tim.2021.3122521

cited on p. 62 165 Michael Buehrer, R. and Venkatesh, S., "Fundamentals of time-of-arrival-based position location," *Handbook of Position Location*. John Wiley & Sons, Ltd, 2018, ch. 6, pp. 199–236. DOI: 10.1002/9781119434610.ch6

Appendices

The General TOA/TDOA Linear Equation

A

This appendix is from from a paper entitled "A Review of Linear Multilateration Techniques and Applications" that is in review at the journal *IEEE Access* [4]. I hereby confirm that the use of this article is compliant with all publishing agreements.

The two classic linear solutions to TOA [27] and TDOA [22] multilateration problems can both be derived from the same set of linear equations. The key step in [27] is to add a nuisance variable to represent the non-linear terms related to the unknown variable $\mathbf{u}$ in Eq. 2.5, with the assumption that $d_u = 0$. Applying this same approach, but keeping d_u, we get the equation

$$x_i^2 + y_i^2 + z_i^2 - d_i^2 = 2x_i x_u + 2y_i y_u + 2z_i z_u - 2d_i d_u - K \tag{A.1}$$

where $K = x_u^2 + y_u^2 + z_u^2 - d_u^2$. This is a system of equations with five unknowns, which can be written as

$$\mathbf{A}_g \mathbf{x}_g = \mathbf{b}_g \tag{A.2}$$

where

$$\begin{aligned}
\mathbf{A}_g &= \begin{bmatrix} 2x_1 & 2y_1 & 2z_1 & -2d_1 & 1 \\ \vdots & \vdots & \vdots & \vdots & \vdots \\ 2x_n & 2y_n & 2z_n & -2d_n & 1 \end{bmatrix} \\
\mathbf{b}_g &= \begin{bmatrix} x_1^2 + y_1^2 + z_1^2 - d_1^2 \\ \vdots \\ x_n^2 + y_n^2 + z_n^2 - d_n^2 \end{bmatrix} \\
\mathbf{x}_g &= \begin{bmatrix} x_u \\ y_u \\ z_u \\ d_u \\ K \end{bmatrix}.
\end{aligned} \tag{A.3}$$

The linear equations in Sec. 2.2.1 can be obtained from this by the transformation

$$\mathbf{A}_{\text{TOA}} = \mathbf{A}_g \begin{bmatrix} 1 & 0 & 0 & 0 \\ 0 & 1 & 0 & 0 \\ 0 & 0 & 1 & 0 \\ 0 & 0 & 0 & 0 \\ 0 & 0 & 0 & 1 \end{bmatrix} \tag{A.4}$$

and then truncating $\mathbf{x}_g$ by removing the d_u term.

The linear equations in Sec. 2.2.1 are created using the matrix

$$\mathbf{A}_{\text{TDOA}} = \begin{bmatrix} -1 & 1 & 0 & \dots & 0 \\ -1 & 0 & 1 & \dots & 0 \\ \vdots & \vdots & \vdots & \ddots & 0 \\ -1 & 0 & 0 & \dots & 1 \end{bmatrix}. \tag{A.5}$$

This allows for the creation of

$$\mathbf{A}_{\text{TDOA}} = \mathbf{A}_{\text{TDOA}}\mathbf{A}_g \begin{bmatrix} 1 & 0 & 0 & 0 \\ 0 & 1 & 0 & 0 \\ 0 & 0 & 1 & 0 \\ 0 & 0 & 0 & 1 \\ 0 & 0 & 0 & 0 \end{bmatrix} \tag{A.6}$$

and $\mathbf{b}_{\text{TDOA}} = \mathbf{A}_{\text{TDOA}}\mathbf{b}_g$. The TDOA equations also require truncating $\mathbf{x}_g$ by removing the t term. This transformation explains why the TDOA equations in Sec 2.2.1 require at least five measurements even though they only use four unknowns. Matrix $\mathbf{A}_{\text{TDOA}}$ is of rank $n-1$, so an extra set of measurements is required.

There is no benefit to using Eq. A.3. The truncated forms given in Eqs. A.4 or A.6, utilize the same data and only require inverting a 4×4 matrix rather than a 5×5 matrix. Consequently, equations that include both d_u and K nuisance variables are rarely seen in the literature, an example being [55].